



**CHALMERS**  
UNIVERSITY OF TECHNOLOGY



# **Study of the effect of additives on the adsorption and antibacterial properties of cellulose-based composites**

Master's thesis in Biotechnology

JESSIKA MAGNUSSON RUNE

DEPARTMENT OF CHEMISTRY AND CHEMICAL ENGINEERING

---

CHALMERS UNIVERSITY OF TECHNOLOGY  
Gothenburg, Sweden 2025  
[www.chalmers.se](http://www.chalmers.se)



MASTER'S THESIS 2025

Study of the effect of additives on  
the adsorption and antibacterial  
properties of cellulose-based  
composites

JESSIKA MAGNUSSON RUNE



Study of the effect of additives on the adsorption and  
antibacterial properties of cellulose-based composites

JESSIKA MAGNUSSON RUNE

© JESSIKA MAGNUSSON RUNE, 2025.

Supervisor: Kinga Grenda, Adsorbi

Supervisor: Romain Borders, Department of Chemistry and Chemical Engineering, Chalmers

Examiner: Lars Evenäs, Department of Chemistry and Chemical Engineering, Chalmers

Master's thesis 2025.

Department of Chemistry and Chemical Engineering

Chalmers University of Technology

SE-412 96 Göteborg

Sweden

Telephone +46 (0)31-772 1000

Study of the effect of additives on the adsorption and antibacterial properties of cellulose-based composites  
JESSIKA MAGNUSSON RUNE  
Department of Chemistry and Chemical Engineering  
Chalmers University of Technology

## Abstract

Air pollution, especially indoors, presents a need for air cleaning technologies to mitigate hazards of particulate matter, poisonous gases and biological contaminants. For removal of gaseous pollutants, such as VOCs, the most common method is adsorption using adsorbents. The company Adsorbi produces a novel adsorbent which, compared to the current standard adsorbent activated carbon, has a higher adsorption capacity and a more reliable uptake. To improve chemisorption, the material is functionalized with an additive in the form of an amine-based polymer. However, this additive is of fossil origin, which raises environmental concerns and the need for replacements.

In this project, four alternative, more sustainable amine-based additives – chitosan, graphitic nitride, gelatine, and dodecyl dipropylene triamine (henceforth referred to as Y-amine) – were incorporated into Adsorbi's material, separately and in combination with the original additive and using three different methods of addition. The production involved granulation – a method of mixing dry powder with a liquid binder to form granules. The resulting prototypes were subsequently evaluated in terms of size distribution, bulk density, pollution and moisture uptake using a gravimetric study, and microbial properties using disk diffusion and broth dilution assays.

All prototypes adsorbed the VOC acetaldehyde, with variations in adsorption capacity, adsorption rate, and saturation time. These variations are attributed to (i) the diverse chemical reactivity of the additives – mainly to the presence of primary amines – and (ii) the different bulk densities of the granules. Higher reactivity resulted in increased adsorption rates and higher bulk densities resulted in shorter saturation times. Increase in viscosity or volume of the liquid binder produced larger granules and varying compositions resulted in different bulk densities, highlighting the importance of production procedure. Microbial evaluations gave contradicting results. When submerged in growth media, the adsorbents exhibited antibacterial properties, which is attributed to leaching of two material components identified as antibacterial in their raw form. Both Y-amine and the original amine-based additive have antibacterial properties, the effects of which are apparent in the disk diffusion assay. The Y-amine prototypes in the broth dilution, unexpectedly, exhibited growth, which is attributed to the inherent variability of live bacteria, susceptibility testing and contaminated materials.

Although the procedure needs to be optimized, the results suggest all alternative additives evaluated, particularly Y-amine, chitosan, and graphitic nitride, can be successfully incorporated into Adsorbi's material, producing functional adsorbents.

Keywords: Adsorbents, Adsorption, Air cleaning technologies, Air pollution, Physisorption, Chemisorption, VOCs, Granulation, MIC test, Disk diffusion, Microbial properties, amine-based functionalization, Gravimetric study, AC.



# List of Abbreviations and Acronyms

Below are abbreviations and acronyms used repeatedly throughout this master's thesis listed in alphabetic order.

AC	Activated carbon
BET	Brunauer-Emmett-Teller
CO	Carbon monoxide
CO <sub>2</sub>	Carbon dioxide
GC	Growth control
GRAS	Generally regarded as safe
H <sup>+</sup>	Hydrogen ion
HCl	Hydrochloric acid
HEPA	High efficiency particulate air
HO <sub>2</sub>	Hydroperoxyl
HVAC	Heating, ventilation, and air conditioning
IAQ	Indoor air quality
MIC	Minimum inhibitory concentration
MOA	Mode of action
NH <sub>3</sub>	Ammonia
NO	Nitrogen oxide
NO <sub>2</sub>	Nitrogen dioxide
O <sub>2</sub> <sup>-</sup>	Oxide ion
O <sub>3</sub>	Ozone
OD	Optical density
OH	Hydroxide
PAHs	Polycyclic aromatic hydrocarbons
PCO	Photocatalytic oxidation
PM	Particulate matter
PRM	Passive removal material
ROS	Reactive oxygen species
SC	Sterility control
S <sub>N</sub> 2	Nucleophilic substitution
SO <sub>2</sub>	Sulfur dioxide
UV	Ultraviolet
UVGI	Ultraviolet germicidal irradiation
VOCs	Volatile organic compounds
WHO	World Health Organization
QACs	Quaternary ammonium compounds

# Content

<b>LIST OF ABBREVIATIONS AND ACRONYMS.....</b>	<b>VII</b>
<b>CONTENT .....</b>	<b>VIII</b>
<b>LIST OF FIGURES.....</b>	<b>XI</b>
<b>LIST OF TABLES .....</b>	<b>XIII</b>
<b>1. INTRODUCTION.....</b>	<b>1</b>
<b>1.1. Background.....</b>	<b>1</b>
<b>1.2. Purpose and goal of the master’s thesis.....</b>	<b>2</b>
<b>2. THEORY .....</b>	<b>3</b>
<b>2.1. Air pollution.....</b>	<b>3</b>
<b>2.2. Indoor air pollution.....</b>	<b>4</b>
<b>2.3. Air purification technologies for indoor use.....</b>	<b>4</b>
2.3.1. Mechanical filters .....	5
2.3.2. Electronic filters and ionizers .....	6
2.3.3. UV-photocatalytic oxidation .....	6
2.3.4. UV-light disinfection systems .....	7
2.3.5. Biological purification strategies .....	7
2.3.6. Adsorption .....	7
2.3.7. Combining technologies .....	8
<b>2.4. Adsorption and other related phenomena.....</b>	<b>8</b>
2.4.1. Sorption and its distinct forms .....	8
2.4.2. Physisorption and chemisorption .....	9
<b>2.5. Adsorbents – adsorbing materials and their properties.....</b>	<b>10</b>
2.5.1. Surface area .....	10
2.5.2. Porosity and pore types.....	11
2.5.3. Diffusion kinetics – pore and particle size.....	11
2.5.4. Surface activity .....	12
2.5.5. Effects of external conditions .....	12
2.5.5.1. Air flow and residence time .....	13
2.5.5.2. Relative humidity .....	13
2.5.5.3. Temperature.....	13
2.5.5.4. Equilibrium pressure .....	14
2.5.6. Adsorbent regeneration .....	14
2.5.7. Antimicrobial properties .....	15
<b>2.6. Adsorbent materials in use .....</b>	<b>16</b>
2.6.1. Activated carbon – a common adsorbent .....	16

<b>2.7. Modifications to promote chemisorption using amines .....</b>	<b>17</b>
2.7.1. Amines – properties and structure.....	17
2.7.2. Reactivity of amines .....	18
2.7.2.1. Intermolecular interactions .....	18
2.7.2.2. Basicity and nucleophilicity .....	18
2.7.2.3. Relative reactivity.....	19
2.7.3. Amine-based capture of air pollutants .....	20
2.7.4. Antimicrobial properties of amines.....	20
2.7.5. Alternative amine-based additives .....	20
2.7.5.1. Chitosan.....	21
2.7.5.2. Graphitic nitride (g-C <sub>3</sub> N <sub>4</sub> ) .....	22
2.7.5.3. Gelatine .....	23
2.7.5.4. Y-amine.....	24
<b>2.8. Granulation.....</b>	<b>25</b>
2.8.1. Influence of binder properties .....	26
2.8.2. Influence of particle size.....	26
2.8.3. Binder-to-solid ratio and method of application .....	26
2.8.4. Practical implications.....	27
<b>2.9. Adsorbi's material – a cellulose-based adsorbent for gaseous pollutants.....</b>	<b>27</b>
<b>3. MATERIALS AND METHODS.....</b>	<b>28</b>
<b>3.1. Material variations – prototypes, reference sample, and negative control.....</b>	<b>28</b>
<b>3.2. Material production process.....</b>	<b>29</b>
<b>3.3. Materials .....</b>	<b>31</b>
<b>3.4. Material characterization .....</b>	<b>32</b>
3.4.1. Size distribution and bulk density.....	32
<b>3.5. Adsorption performance evaluation – gravimetric studies.....</b>	<b>32</b>
3.5.1. VOC uptake .....	32
3.5.2. Moisture uptake .....	33
<b>3.6. Antimicrobial evaluation .....</b>	<b>33</b>
3.6.1. Minimum inhibitory concentration (MIC) determination .....	34
3.6.2. Disk diffusion .....	35
<b>4. RESULTS AND DISCUSSION.....</b>	<b>36</b>
<b>4.1. Observations .....</b>	<b>36</b>
4.1.1. Production.....	36
4.1.2. Gravimetric study with VOC .....	36
<b>4.2. Size fraction distribution .....</b>	<b>37</b>
4.2.1. The reference sample .....	37
4.2.2. The prototypes .....	37
4.2.2.1. Addition point A .....	38
4.2.2.2. Addition point B .....	39
4.2.2.3. Addition point C .....	39
4.2.2.4. Chitosan.....	40
4.2.2.5. Graphitic nitride .....	40

4.2.2.6. Gelatine .....	41
4.2.2.7. Y-amine.....	41
<b>4.3. Pollution uptake .....</b>	<b>41</b>
4.3.1. Amine-based additives – raw vs incorporated in adsorbents .....	42
4.3.2. Adsorption capacity .....	43
4.3.3. Adsorption kinetics .....	44
<b>4.4. Density, additive composition, saturation time, and adsorption capacity .....</b>	<b>46</b>
<b>4.5. Moisture uptake .....</b>	<b>49</b>
<b>4.6. Microbial evaluation .....</b>	<b>50</b>
4.6.1. MIC using broth dilution .....	50
4.6.1.1. MIC of adsorbents .....	50
4.6.1.2. MIC of adsorbent components .....	51
4.6.1.3. The Y-amine prototypes.....	54
<b>4.7. Disk diffusion.....</b>	<b>55</b>
<b>5. CONCLUSIONS .....</b>	<b>57</b>
<b>6. BIBLIOGRAPHY .....</b>	<b>59</b>
<b>APPENDIX A: ADJUSTED PROTOCOL FOR MIC USING BROTH DILUTION AND FOR AGAR DIFFUSION.....</b>	<b>63</b>
<b>APPENDIX B: ADJUSTED PROTOCOL FOR MIC TEST ON SEPARATE COMPONENTS .....</b>	<b>65</b>

# List of Figures

Figure 1. The different forms of adsorption. In A, a description of adsorbate and free compared to occupied active sites is presented. In B, physisorption (adsorbate bound to surfaces through weak intermolecular forces) compared to chemisorption (adsorbate bound to active sites through covalent bonds) are presented. In C, adsorption into a porous granule is visualized, including a blocked pore (1), a through pore (2), roughness (3), an interconnected pore (4), closed pores (5), an open pore (6), desorption (7), pore filling or capillary condensation (8), and both occupied and free active sites (9a and 9b). Figure adapted with modifications from [16] and [15].	9
Figure 2. Some functional groups relevant to the functionality and reactivity of VOCs and amines: ketones, carboxyl acids, acyls, carbonyls, aryls, aldehydes, and amides. Structures from [25].	17
Figure 3. The classification and chemical structure of amines and the closely related quaternary ammonium ion, showing all lone electron pairs. The structures shown are primary, secondary, and tertiary amines, quaternary ammonium ion or ammonium salt and the cyclic amines pyridine and aniline [25]	17
Figure 4. Acid-base reaction – a primary amine reacting as a base with hydrochloric acid, yielding ammonium chloride salt.	18
Figure 5. Reaction forming imines in (1) and an acid/base reaction yielding an ammonium salt in (2).	20
Figure 6. Chemical structure of YC58325 chitosan from Biosynth, modified through deacetylation and addition of hydroxyl groups to invoke solubility. The active sites or functional groups relevant for adsorption – primary amines, primary and secondary hydroxyl, and glycosilic bonds – are highlighted. Figure made with modifications based on the structure of YC58325 chitosan from Biosynth [32].	21
Figure 7. Chemical structure of graphitic nitride, showing sites of potential interactions in the form of electronic properties ( $\pi$ -conjugated systems), Brønsted and Lewis basicity and hydrogen bonding. Figure made with modifications from [35] and [36].	23
Figure 8. A generalized chemical structure with amino acids commonly appearing to a large extent in gelatine. Notably, other amino acids not depicted will also be present. The amino acids are indicated in light highlights, while the active sites or functional groups relevant for adsorption – carboxyls, secondary amines, and quaternary ammonium ionic groups – are indicated in darker highlights. Figure made from [37].	24
Figure 9. Molecular structure of Y-amine. Figure made based on the structure from [41].	25
Figure 10. The granulation process in detail with wetting of solid particles, nucleation (in detail divided into the pendular, funicular, capillary, and droplet states), the consolidation and growth phase, formation of agglomerates and finally wet granules. Figure made with modification from [59].	26
Figure 11. Production procedure of Adsorbi's material showing main production steps and the three different points of addition (A, B and C). The procedure was repeated for all weight ratios to the extent it was possible. The original amine-based additive was added identically each time, in accordance with the original procedure and same as in the reference samples.	30
Figure 12. Method for measuring volume and weight for calculation of apparent density of the adsorbent granules.	32
Figure 13. Setup for gravimetric study: samples of adsorbents and the VOC pollutant acetaldehyde in a desiccator and weighing of samples. A similar setup was used for moisture uptake as well.	33
Figure 14. Granules discolored from VOC adsorption. Evenly colored granules made using point of addition A (to the left) compared to dappled granules made using point of addition B (middle). Fresh granules (to the right) for comparison.	36
Figure 15. The size fraction distribution of the reference sample, separated by fraction sizes ( $> 2.8$ ; $2.8-1$ ; $1-0.63$ ; $< 0.63$ mm) and expressed in weight percent (wt%). All three repeats are included.	37
Figure 16. Size fraction distribution for all prototypes, structured by amine-based additives vertically and by addition points horizontally. Numbering of graphs indicate additive used (1 chitosan, 2 graphitic nitride, 3 gelatine and 4 Y-amine). Ratios of additives are indicated in legends as (alternative:original) and with distinct color shading, darker shades indicating more alternative and vice versa. Points of addition are indicated with their corresponding letter and a distinct pattern (uniform color for A, spotted for B, and dashed for C). Note that there are no error bars as the measurements were done without repeats.	38
Figure 17. The results of the gravimetric study with a known VOC pollutant of (1) all prototypes with the composition 100:0 of amine-based additives and (2) the alternative additives chitosan, graphitic nitride and gelatine evaluated in their raw form. In (1) Y-amine is not included, as it was not tested due to it being in liquid form. In (2) the points of addition are indicated as A, B and C. Uptake is measured in pollutants captured by	

<i>weight of sample (<math>g_{\text{pollutant}}/g_{\text{adsorbent}}</math>) and presented per hour. Results from the reference sample granules are included for comparison in both inserts.</i>	42
<i>Figure 18. Results of the gravimetric study using the VOC acetaldehyde for all prototypes containing the tested alternative additives, including one of reference samples for comparison. Prototypes containing chitosan are presented in (1), graphitic nitride in (2), gelatine in (3), and Y-amine in (4). The ratio of alternative to original additive (alternative:original) is indicated in the legends along with points of addition A, B and C. The undersaturated samples are marked with a cross, indicating they may not have reached their maximum adsorption capacity. Adsorption is presented as the weight of pollutants captured to the weight of adsorbent (<math>g_{\text{pollutant}}/g_{\text{adsorbent}}</math>).</i>	43
<i>Figure 19. Density (g/ml) plotted to saturation time (h). All prototypes are presented, differentiated by addition points (indicated as A, B, and C). Reference samples are included in all graphs.</i>	46
<i>Figure 20. Density (g/ml) plotted to weight percent of alternative amine-based additives. All prototypes are presented, differentiated by addition points (indicated as A, B, and C). Reference samples are included in all graphs.</i>	47
<i>Figure 21. Saturation time (h) plotted to weight percent of alternative amine-based additives. All prototypes are presented and differentiated by addition points (indicated as A, B, and C). Reference samples are included in all graphs.</i>	47
<i>Figure 22. Final uptake (<math>g_{\text{pollutant}}/g_{\text{adsorbent}}</math>) plotted to density (g/ml). All prototypes are presented, differentiated by addition points (indicated as A, B, and C). Reference samples are included in all graphs.</i>	48
<i>Figure 23. Moisture uptake for prototypes containing chitosan, graphitic nitride, gelatine and Y-amine and the reference sample included for comparison. The prototypes containing chitosan are shown in (1), graphitic nitride in (2), gelatine in (3) and Y-amine in (4) and the point of addition is indicated in the legend as A, B and C. The uptake is measured in weight increase (<math>g_{\text{moisture}}/g_{\text{adsorbent}}</math>).</i>	49
<i>Figure 24. OD measurements from broth dilution assay with additive A, concentrations ranging from lowest (1) to highest (5). A dilution series of purely growth media and the same amounts of additive A is included as a reference sample. The results of the GC and SC are included for comparison.</i>	52
<i>Figure 25. OD measurements from wells containing the carrier particle, concentrations ranging from lowest (1) to highest (5). The results of the GC and SC are included for comparison.</i>	52
<i>Figure 26. OD measurements from wells containing additive B, concentrations ranging from lowest (1) to highest. The results of the GC and SC are included for comparison.</i>	53
<i>Figure 27. OD measurements from both repeats of the broth dilution assay of granules containing Y-amine. Growth control and sterility control are included as reference sample.</i>	54
<i>Figure 28. The average diameter of the zones presenting inhibited growth around the granules, based on the three replicates, are presented for all granules evaluated.</i>	55

## List of Tables

<i>Table 1. All adsorbents produced: the prototypes, the reference sample, and the negative control. For the prototypes, the variations on amine-based additive composition are indicated as weight ratios of alternative to original amine-based additives. The alternative used is indicated in the headers. The different methods of incorporating the amine-based additives are indicated as points of addition A, B, and C. The variations that were not feasible to produce are crossed out. ....</i>	<i>29</i>
<i>Table 2. The amounts of alternative and original amine-based additives added, with a distinction between additions made before and after the large batch was split into four parts. Additionally, the different amounts needed for each prototype weight ratio (alternative:original) are included. For clarity, the final composition for each prototype's weight ratio and the negative control are also included. ....</i>	<i>31</i>
<i>Table 3. The final composition, which is identical across all material variations, expressed as weight percent. .</i>	<i>31</i>
<i>Table 4. Broth dilution assay results of adsorbent prototypes, the negative control, and the reference sample. OD measurements indicating growth are presented as Yes and lack of growth as No. ....</i>	<i>50</i>
<i>Table 5. Broth dilution assay results of separate components, 5 indicates highest amount tested and 1 lowest. Apparent growth indicated as Yes, lack of growth indicated as No, and inconclusive results indicated as Inc. ...</i>	<i>51</i>

# 1. Introduction

## 1.1. Background

The World Health Organization (WHO) defines air pollution as the presence of a “chemical, physical or biological agent that modifies the natural characteristics of the atmosphere” and distinguishes between outdoor (ambient) and indoor air pollution. According to the WHO, nearly 99% of the global population breathes air that exceeds their guidelines for safe long-term exposure. Approximately 2.4 billion people are exposed to elevated levels of household pollutants, which also include microbes such as bacteria, viruses, and fungi. Exposure contributes to various acute and chronic health issues, including stroke, heart disease, lung cancer, diabetes, respiratory distress, and metabolic dysfunctions [1, 2]. Together, exposure to indoor and outdoor pollution is associated with an estimated 7 million premature deaths annually. In response to growing concerns, the United Nations recognized a clean, healthy, and sustainable environment as a human right in July 2022, emphasizing the importance of clean air to address both environmental and health threats [3].

Air pollution represents a major challenge with far-reaching consequences for both the natural environment and human health. It arises from a diverse array of sources, ranging from large-scale industrial activities to everyday household activities. Pollutants such as carbon monoxide (CO), ozone (O<sub>3</sub>), nitrogen dioxide (NO<sub>2</sub>), and sulfur dioxide (SO<sub>2</sub>) are frequently released into the atmosphere, where their behavior and adverse impacts vary depending on their source and environmental conditions. Depending on the site of emission and on weather conditions, pollutants can give rise to a range of problems on local, regional, and global levels and persist for extended periods of time [1].

In recent years, there has been growing recognition of the importance of creating clean and healthy indoor air environments. Many sources of indoor air pollution originate from within our homes, including building materials, furniture, and finishes. These materials can emit harmful pollutants, such as volatile organic compounds (VOCs), making it challenging to remove the source of pollution entirely. Ventilation systems are often inadequate or poorly designed, potentially exacerbating air quality issues by redistributing pollutants rather than removing them effectively. There is therefore an increasing interest in air-cleaning technologies tailored for indoor environments. These technologies aim to address both particulate matter (PM) and gaseous pollutants effectively, with adsorption as one of the standard methods for gas uptake. Additionally, air cleaning technologies preferably capture and neutralize microbes, keeping both the air and the purification material clean [4].

Adsorption works by binding pollutants to a surface through weak molecular forces and – depending on the material – chemical bonding, trapping them and preventing their circulation in the air. The efficiency of this process depends largely on the adsorbent material. Currently, activated carbon (AC) is the most widely used material for this purpose. AC is known to have a high efficiency in pollution removal due to its large surface area and storage capacity [5]. However, its application comes with limitations and environmental challenges. One primary issue is the material’s saturation. Over time, AC becomes saturated with pollutants, requiring either replacement or regeneration of the material in order to recycle it, increasing operational costs and environmental burdens. Moreover, adsorption captures pollutants but does not neutralize them, turning used AC filters into hazardous waste that necessitates proper disposal. Under certain conditions, such as changes in humidity or temperature, the risk of re-emission of previously adsorbed pollutants further diminishes its reliability [6]. Furthermore, AC is primarily made from fossil-based carbons, sourced mainly for the European production from coal mines in China, Poland, and Germany. While renewable materials and organic waste are being researched as alternative feedstocks, these remain underutilized. Regardless of the raw material, both the production and regeneration process require high temperatures, consuming large amounts of

energy and further increasing the environmental footprint [7]. These drawbacks highlight the need for new air-cleaning materials that are more sustainable and efficient. Future developments should focus on improving adsorption efficiency, minimizing waste, incorporating renewable materials and developing low-impact production methods.

Adsorbi is a company centered around a new, sustainable, and high functioning material for adsorption of gaseous air pollutants. Adsorbi is committed to developing materials that combine high performance with sustainability, using cellulose and additives as primary ingredients. Thus, this master's thesis primarily focuses on substituting the fossil-derived amine-based additive currently utilized in the material with more sustainable amine-based alternatives, some of them being of natural origin. The objective of the replacement is to enhance the functional properties of the material while significantly reducing its environmental footprint. By integrating more sustainable additives, Adsorbi strives to align its materials with modern demands for eco-friendly, high-performing solutions that contribute to cleaner air and a healthier environment. Additionally, as the material's microbial properties when using the alternative amine-based additives have not been evaluated, an antimicrobial study will be performed.

## 1.2. Purpose and goal of the master's thesis

The purpose of this master's thesis is to develop novel materials for adsorption (adsorbents) of gaseous air pollution by implementing naturally occurring or more sustainable amine-based additives into one of Adsorbi's current materials, as a replacement to the currently utilized amine-based additive.

The goal of the study is to produce novel adsorbents using four alternative additives and evaluate the resulting prototypes in terms of their adsorption capacity for VOCs, benchmarking their performance against a selected standard material composition. Furthermore, the material's microbial properties will be evaluated, providing valuable insight into its interaction with microbes it may be exposed to. This research aims to contribute to the development of sustainable and high-performing materials for air purification applications.

## 2. Theory

### 2.1. Air pollution

The natural composition of gases in the atmosphere is fairly constant, with the majority being nitrogen, followed by oxygen. Gases like carbon dioxide (CO<sub>2</sub>) and water vapor content fluctuate throughout the day due to photosynthesis and over the year due to seasonal changes. Air pollutants are compounds released into the atmosphere because of human activities that change the naturally occurring atmospheric compositions. Pollutants come in various forms, including solid particles, liquid droplets, and gases, often originating from sources such as fossil fuel combustion and oil-based products. The pollutants are typically, but not always, toxic to human health and the environment. Although natural events such as forest fires and volcanic eruptions contribute to the release of toxic compounds, human activities contribute with the majority. Once released, these pollutants follow complex pathways and can have diverse, adverse effects on both the environment and human health [1].

Once in the atmosphere, pollutants may travel long distances, accumulating in high concentrations or diluting across vast areas, spreading their impact, and potentially causing widespread adverse effects. If dissolved in water droplets, pollutants can reach the ground and compounds such as NO<sub>2</sub> and SO<sub>2</sub> form acids, contributing to acid rains that harm natural ecosystems, especially aquatic environments, and urban areas. The resulting lower pH can leach heavy metals from the soil, contaminating aquatic environments and drinking water supplies. Additionally, nitrogen compounds contribute to eutrophication, further disrupting aquatic ecosystems [1].

To address air pollution's impact on human health and the environment, the WHO established their first air quality guidelines in 1987, with the latest update in 2021. These guidelines prioritize six major pollutants, also known as classic pollutants: PM<sub>10</sub> and PM<sub>2.5</sub> (particles with a diameter of  $\leq 10 \mu\text{m}$  and  $\leq 2.5 \mu\text{m}$  respectively), O<sub>3</sub>, NO<sub>2</sub>, SO<sub>2</sub> and CO, while also noting additional pollutants like ultrafine particles, sand and dust storms [2]. In 2000 WHO published additional guidelines for indoor air quality (IAQ) in Europe, expanding to 35 compounds including organic pollutants (e.g., carbon disulfide, toluene), inorganic pollutants (e.g., asbestos, lead), and specific indoor pollutants (e.g., tobacco smoke). In 2010, further indoor air guidelines were introduced for 9 selected compounds, including benzene, formaldehyde, polycyclic aromatic hydrocarbons (PAHs), and NO<sub>2</sub>. Still, the pollutants included in the guidelines constitute only a fraction of the existing air pollutants [8, 9].

Pollutants in the atmosphere can undergo various fates and engage in numerous chemical reactions. A distinction exists between primary pollutants, which are directly emitted from a source, secondary pollutants, which form through reactions among primary pollutants and atmospheric compounds, and precursors to secondary pollutants. Primary pollutants undergo both chemical and photochemical reactions in the sunlight, often producing multiple secondary pollutants. For instance, formaldehyde is oxidized by photolysis or by reactions with hydroxide (OH), yielding secondary pollutants like CO and hydroperoxyl (HO<sub>2</sub>) radicals. CO is slowly oxidized to form O<sub>3</sub>, while HO<sub>2</sub> oxidizes nitrogen oxide (NO) to NO<sub>2</sub>, and forms hydroxyl radicals. The photolysis of NO<sub>2</sub> also generates O<sub>3</sub>, meaning each formaldehyde molecule can potentially produce two O<sub>3</sub> molecules. O<sub>3</sub> is a key photochemical oxidant and plays a major role in atmospheric oxidation processes. Additionally, gaseous pollutants can aggregate to form PM, which may further interact with gases, increasing both toxicity and local pollutant concentrations [10]. Notably, the WHO highlights that their guidelines, though comprehensive, assess each chemical individually. The combined exposure to multiple pollutants, and the complex chemical reactions and interactions occurring between them are not included in their current guidelines [2].

Formaldehyde, along with other significant pollutants such as benzene, naphthalene, and PAHs, are classified as VOCs. Although the definitions of VOCs vary, they generally refer to organic compounds with a high volatility and low boiling points (typically 50–260 °C) that exist in gas form at ambient conditions. Compounds with lower boiling points (around 50–100 °C) are classified as very volatile, while those with higher boiling points (240–400 °C) are semi-volatile [11]. VOCs commonly include alkanes, alkenes, aromatic compounds, and aldehydes, and often function as precursors to O<sub>3</sub> and contribute to the formation of PM. Several VOCs, such as benzene and formaldehyde, are known carcinogens. Although their final degradation product is CO<sub>2</sub>, this process can be slow, causing various environmental and health issues along the way. VOCs primarily originate from combustion and the evaporation of liquid fuels but also occur in many common household materials and products, including paints, solvents, and cleaning agents [10].

## 2.2. Indoor air pollution

Indoor air quality (IAQ) often differs from outdoor air quality, with certain pollutants reaching much higher concentrations indoors—sometimes up to 10 times higher [6]. Indoor pollution commonly originates from within buildings with sources including building material and household activities such as cooking or heating, making the removal of the source difficult. High concentrations of these hazardous substances can significantly degrade air quality and affect all regions, impacting low-, middle- and high-income countries alike. Indoor air pollution is particularly concerning given that people spend a substantial and increasing amount of time indoors, with vulnerable groups – such as those in day-care centers and retirement homes – at high risk of exposure [9].

The WHO has developed guidelines specifically for IAQ, identifying eleven key pollutants based on their indoor sources and health impacts, including CO, NO<sub>2</sub>, PAHs, radon, PM<sub>2.5</sub>, PM<sub>10</sub> and VOCs such as benzene, formaldehyde, naphthalene, and tetrachloroethylene. A second list with twelve additional pollutants, including asbestos, O<sub>3</sub> and other VOCs such as acetaldehyde, hexane and toluene were noted as significant but lacking sufficient data for guideline formation [9]. In total, over four hundred organic and inorganic compounds, along with biological contaminants like mold, bacteria, fungi, dust, and pollen, have been identified as problematic [6].

To further illustrate indoor pollutants, formaldehyde can be taken as an example. Formaldehyde is a VOC, with indoor air being the primary source of human exposure, often at levels significantly higher than those outdoors. Indoor concentrations may be distressingly elevated, raising health concerns about irritation of the upper airways, lung effects such as asthma, and an increased risk of cancer. Key sources include building materials, furniture, insulation (particularly from the 1980s), textiles, varnishes, paints, wallpaper, and wood products with formaldehyde-containing resins like plywood. Additionally, formaldehyde is emitted from common household products such as cleaning agents (e.g., detergents, disinfectants, fabric softeners), cosmetics (e.g., liquid soap, shampoo, nail polish) and electronic equipment. Formaldehyde can also be emitted from smoking, heating, cooking, candles, and yield from oxidation of other VOCs or reactions between alkenes and O<sub>3</sub>. Exposure is typically heightened in older buildings and in conditions of high temperature and humidity [9]. Due to its various health risks, the presence of formaldehyde underscored the urgent need for measures to improve IAQ.

## 2.3. Air purification technologies for indoor use

The most common strategy to improve IAQ is ventilation, which is simply a dilution of the indoor pollutants with the generally cleaner outdoor air. However, this method has limitations. Ventilation may not be feasible in certain indoor spaces, and it can be energy-intensive, particularly in climates requiring heating or cooling. In urban environments with elevated levels of outdoor air pollution,

introducing ambient air can exacerbate IAQ issues rather than resolve them. An alternative approach is source control, which involves limiting or eliminating pollution sources indoors. While effective in some cases, this strategy is not always practical, as many pollutants originate from essential aspects of buildings or occupant activities, such as emissions from building materials, cooking, or cleaning products [12, 6].

Given these challenges, a third strategy becomes essential: pollution extraction. This involves actively removing pollutants from indoor air using air cleaning technologies. These systems can target specific contaminants and operate effectively in enclosed spaces, regardless of external air quality. Various forms of air purification are increasingly recognized as a critical solution for maintaining healthy indoor environments, particularly in situations where ventilation and source control are insufficient or impractical [12, 6].

Air cleaning technologies are designed to address various indoor pollutants, which, for the purpose of air purification, are typically classified into three categories: suspended particles (e.g. dust, pollen), VOCs, and microorganisms (e.g., bacteria and viruses). Logically, the technologies are typically categorized based on their target pollutant: dust removal, gas purification, and sterilization, each corresponding to the one of the three categories of indoor pollutants. Filters, such as High efficiency particulate air (HEPA) filters, are commonly used for particle removal and can also capture larger microorganisms. For gaseous pollutants, adsorption remains the most efficient method with AC as the standard material. Additionally, photocatalytic cleaning technology and adsorption shows promise for VOCs degradation. Microbial sterilization is typically achieved through ultraviolet (UV) light [4]. However, conventional technologies often face limitations such as incomplete pollutant removal, emission of harmful byproducts, toxic waste generation, high energy consumption and costly installations and maintenance [6]. Addressing these challenges is crucial for developing sustainable, effective, and accessible air purification solutions.

### 2.3.1. Mechanical filters

Mechanical filters are among the oldest and most widely used technologies for removing PM from air. These filters are made from materials with porous structures, such as fibers of varying sizes and densities or stretched membranes. The primary purpose is the capture of pollutants from active air streams passing through the filters. Filters are classified based on their efficiency in retaining PM of different size ranges, ranging from capture of coarse particles to capture of very fine particles such as bacteria or even viruses [6].

A variety of filters are available, including AC filters, which have been used for decades and are still considered among the most effective options. Advances in nanotechnology, such as the use of nanofibers, are also commonly integrated into filter designs. Filters are widely employed in applications such as breathing apparatus, household dust filters, air purifiers, and HVAC systems (Heating, Ventilation, and Air Conditioning) for buildings [4]. However, it is important to note that filters are generally not effective in removing gases or inactivating captured microbes [6].

Regular filters made with traditional fibrous materials offer several advantages, including high removal efficiency, low initial cost, and a relatively simple structure. However, they also come with notable drawbacks. The filtration efficiency is directly proportional to the pressure drop of the airflow, caused by the increased resistance in the flow. A high pressure drop – defined by Hussein (2022) as “a decrease in fluid pressure during flow between two points” [13] – causes higher energy consumption and elevated maintenance costs [6].

Over time, filters become saturated with captured pollutants. To maintain functionality regular maintenance is required, commonly in the form of cleaning or replacement. If neglected, a saturated filter risks releasing trapped pollutants back into the air stream, compromising air quality.

Additionally, the cleaning or replacement process creates the challenge of managing the toxic waste generated by the pollution capture [6].

Another drawback of filters is the issue of filter colonization. Trapped bacteria and fungi are not eliminated and can begin to grow on the filter's surface, which is typically highly biocompatible. As filters trap energy-rich organic compounds that can serve as a food source, they provide an ideal environment for growth. Colonization disrupts the filter's capacity to capture pollutants and presents an additional problem as the colonies can be a source of secondary pollutants. This is particularly concerning in sensitive environments – such as hospitals – where compromised air quality can have profound consequences [4].

### 2.3.2. Electronic filters and ionizers

Some filters incorporate a static electrical charge to enhance particle removal, such as electrostatic precipitators. The removal process involves electrically charging particles and collecting them on oppositely charged deposition plates (precipitators). However, these electronic filters may produce hazardous byproducts, such as charged particles, secondary pollutants such as O<sub>3</sub>, and ultra fine particles. Under certain conditions, these emissions may offset any improvements in IAQ. Over time, these filters can also become clogged and require regular cleaning. Similar to air filters, neglecting maintenance can compromise their performance and effectiveness [6].

Air ionization technology, another approach to air purification, generates ions to remove pathogens, VOCs, and PM. Devices employing this technology include unipolar ionizers (producing only negative ions) and bipolar ionizers (generating both positive and negative ions). Bipolar ionization occurs when an alternating voltage source is applied to a tube with two electrodes, generating hydrogen ions (H<sup>+</sup>) and oxide ions (O<sub>2</sub><sup>-</sup>) ions from water vapor. These ions cluster around microorganisms, creating hydroxyl radicals that disrupt microbial cells, resulting in water formation and microbial inactivation. Ionizing technology has demonstrated the ability to improve IAQ by reducing bacteria, viruses, fungi, PM, and VOCs. However, it also produces secondary pollutants, such as O<sub>3</sub>, and often has relatively low total removal efficiency. Additionally, the cost of these systems can be high [6].

### 2.3.3. UV-photocatalytic oxidation

Photocatalytic oxidation (PCO) is a light-mediated redox reaction involving gases and biological particles adsorbed on the surface of a solid metal oxide semiconductor material, known as a photocatalyst. Titanium dioxide is the most common photocatalyst. When exposed to light at specific UV wavelengths, the photocatalyst generates reactive oxygen species (ROS) that remain bound to its surface. These highly reactive compounds effectively degrade adsorbed organic and inorganic gases, as well as microorganisms. PCO offers several advantages: it features a fast reaction rate, a relatively low pressure drop, and versatility in handling a wide range of compounds. Some designs can utilize sunlight as a light source, reducing energy consumption. Additionally, the photocatalyst theoretically has a long lifecycle due to its self-cleaning or regenerating properties. The primary drawback of PCO is the potential generation of harmful byproducts. Ideally, pollutants react on the catalyst's surface to produce harmless end products, such as water vapor and CO<sub>2</sub>, i.e. mineralization. However, incomplete oxidation can lead to the formation of toxic byproducts, which may be more hazardous than the original pollutants—such as alcohols converting to aldehyde. To mitigate this issue, additional filters or hybrid systems can be integrated to capture or neutralize these byproducts [6].

### 2.3.4. UV-light disinfection systems

Wavelengths in the UVC range (200–280 nm), particularly those around 254 nm, are absorbed by proteins, RNA, and DNA in microorganisms and can be used for ultraviolet germicidal irradiation (UVGI). The light causes irreversible damage and, although the required dose varies depending on the target species, effectively inactivates all types of microorganisms. This makes UVC light a powerful disinfectant, and UVGI disinfection systems are commonly used for air purification, especially in healthcare settings where the removal of bacteria, viruses, fungi, and other pathogens is critical [6].

While not always straightforward, UVGI lamps can be integrated into ventilation systems through various installation methods. The main disadvantages of this technology include the production of O<sub>3</sub> as a byproduct and the potential harm UV light poses to humans. As a result, maintenance must be performed carefully to ensure safety. Additionally, UVGI systems are limited to targeting microbial pollutants and are not effective for removal of other types of contaminants [6].

### 2.3.5. Biological purification strategies

The use of plants to remove pollutants is known as phytoremediation. It can be applied to air as well as other media and the approach is generally cost-effective, with low implementation and maintenance costs. Plants have been shown to remove VOCs, making them a viable solution for improving IAQ. They can function passively in simple forms, such as potted plants, or as components of active filtration systems, including HVAC systems or “green walls”. Researchers are also exploring the use of microalgae and biofilters, which employ immobilized bacteria or fungi to degrade pollutants. Beyond pollutant removal, indoor greenery provides additional benefits such as oxygen generation, increased humidity, and passive acoustic insulation. Furthermore, plants enhance indoor aesthetics and offer positive psychological benefits, including reduced stress, increased comfort and improved overall health [4, 6].

The primary limitation of phytoremediation is the current lack of comprehensive research. Additionally, depending on the plant species used, there is a risk of releasing other organic compounds, such as pollen which could potentially affect IAQ [4, 6].

### 2.3.6. Adsorption

Adsorption is the most efficient technique for capturing gases, enabling the successful removal of VOCs and inorganic gaseous pollutants. Commonly used adsorbent materials include AC, zeolites, silica gel, activated alumina, mineral clay, and certain polymers, with AC being the most widely used. Adsorbents function as passive removal materials (PRMs), which, unlike active filtration systems, operate without requiring additional energy input or forced airflow. This energy efficiency is a major advantage, and the process produces minimal byproducts [6].

However, adsorption has its limitations. Typically, it is sensitive to high humidity, which can significantly reduce removal efficiency. This occurs due to capillary condensation of water vapor, which coats the adsorbent material and blocks adsorption sites, leading to an inhibition effect. This issue is pronounced in the use of AC [6].

While adsorption can capture bioaerosols (such as bacteria and fungi), the material must possess antibacterial properties to prevent colonization. As with filtration, adsorption does not neutralize hazardous substances but merely collects them. This results in a concentration of toxic compounds that must be managed and disposed of properly to prevent environmental and health risks [6].

### 2.3.7. Combining technologies

Achieving full air purification often requires multiple technologies. When combined strategically, these technologies can produce synergistic effects that enhance their overall efficiency [4].

One example is the combination of PCO with adsorption. The photocatalytic reaction rate tends to be slow when pollutant concentrations are low. However, incorporating an adsorbent material can locally concentrate pollutants by trapping them on its surface, thereby increasing the reaction rate. The pollutants are then effectively degraded through the photocatalytic process, which simultaneously regenerates the adsorbent. This synergy improves the performance of both methods [4].

Similar benefits can be achieved by integrating PCO with traditional filters. Adding adsorbents to technologies that generate byproducts, such as electronic filters, can help capture and mitigate the impact of those byproducts. Likewise, combining plants with air-cleaning technologies like AC or nanotechnology can optimize air purification [6, 4]. The issue of colonization on filters can also be addressed through combination approaches as filters can be treated with antimicrobial surfaces. Examples include filters infused with silver or paired with sterilizing UV light, which inhibit microbial growth. An ideal surface prevents adhesion of microbes and, if adhesion does occur, prevents growth, preferably through killing [14, 6].

## 2.4. Adsorption and other related phenomena

The ability of some materials to take up undesirable compounds has been known and utilized since ancient times. Materials such as clay, sands and wood charcoal were used as early as in Ancient Egypt, Greece, and Rome for purposes like desalination of water, clarification of oils and for medicinal purposes. Modern times have brought an improved understanding of the phenomenon and an expanded range of available materials with increased functionality. Today it is used in a wide variety of applications such as desiccants (removing moisture to retain dryness), catalysts, separation of gases, purifications, drug delivery, pollution control and respiratory protection. Additionally, it is utilized for material characterization, such as determination of surface area, pore size, and texture for powders and other porous materials, including pigments, cements, and membranes [15].

### 2.4.1. Sorption and its distinct forms

The broadest term, *sorption*, covers both *adsorption* and *absorption*. Adsorption is the phenomena of a compound coating a surface, while absorption is the penetration of a compound past the surface into the bulk. The processes differ in kinetics, with adsorption being quicker than absorption. As adsorption happens in increasingly small pores, the exact difference between absorption into a solid interphase and adsorption into pores of molecular dimensions become hard to define, but the distinction is still practical. Additionally, adsorption is further divided into *physisorption* and *chemisorption*. The opposite process is *desorption* for physisorption and *dissociation* for chemisorption. If conditions change after an equilibrium is reached, the system moves towards a new equilibrium either through adsorption or desorption/dissociation. Adsorption happens at the interface between two bulk phases: one solid and one fluid (liquid or gaseous). A compound is termed *adsorptive* when in the bulk fluid phase and *adsorbate* when bound to a surface and the material to which it binds is termed *adsorbent* [15]. Out of these phenomena, this master's thesis will discuss the uptake of *gases* into a *solid* through *adsorption*.

Any solid surface exposed to a gas will result to some extent in adsorption, often defined as the enrichment of one or several components in the interfacial layer (the region between the bulk phases) through diffusion. Adsorption and its distinct forms are shown in Figure 1 using a porous granule as adsorbent. From the perspective of the adsorptive, it will diffuse from the bulk phase into a film nearer

the surface, locally increasing concentrations and finally adsorbing onto the surface of the material. The adsorptive diffuse into all accessible spaces and if the material is porous it will result in pore filling (see 8 in Figure 1). The extent of adsorption depends on a range of factors, including size of the available surface area in the material, the relative pressure of each compound, temperature, humidity, and the physical and chemical nature of the surface. Diffusive transportation is also of importance, especially in determining the rate of adsorption. A high diffusion rate may be necessary as several areas of implementation require efficient air purification within a limited timeframe. Once an equilibrium is reached, the material is at its maximum adsorption capacity, measured as the mass of adsorbate per mass of adsorbent ( $g_{\text{adsorbate}}/g_{\text{adsorbent}}$ ) [15, 16].

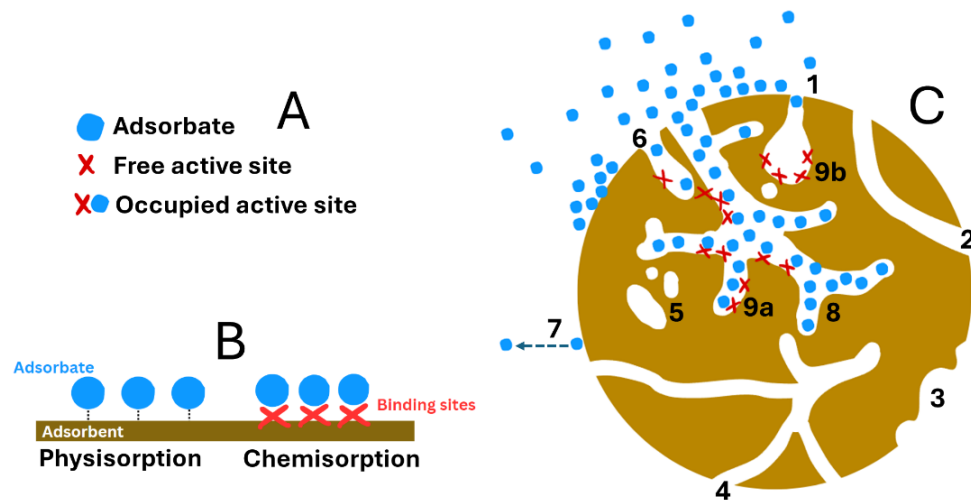


Figure 1. The different forms of adsorption. In A, a description of adsorbate and free compared to occupied active sites is presented. In B, physisorption (adsorbate bound to surfaces through weak intermolecular forces) compared to chemisorption (adsorbate bound to active sites through covalent bonds) are presented. In C, adsorption into a porous granule is visualized, including a blocked pore (1), a through pore (2), roughness (3), an interconnected pore (4), closed pores (5), an open pore (6), desorption (7), pore filling or capillary condensation (8), and both occupied and free active sites (9a and 9b). Figure adapted with modifications from [16] and [15].

## 2.4.2. Physisorption and chemisorption

Adsorption is classified as either chemisorption or physisorption, two processes which although often happening simultaneously retain distinct properties [15]. A visual representation of both forms of adsorption into a porous granule is shown in Figure 1.

*Chemisorption* occurs when a reaction between the surface of the adsorbent and the adsorbate takes place, resulting in covalent bonds. Depending on the adsorbent-adsorbate system, the bonds can form through electron transfer or pairing, ion/ligand exchange, Lewis acid-base interactions or reduction/oxidation reactions. Chemisorption is limited to a monolayer, meaning the surface can at most be covered in a layer of the compound with the thickness of one molecule. The binding is highly specific in that active groups on the surface of the material – active sites – react with a part of the adsorbate, changing the chemical identity of the adsorbate. However, compounds with properties similar to the target pollutant can bind to the same active sites, resulting in competitive adsorption. This decreases the pollution removal efficiency and presents the need for high specificity in adsorbent materials [15, 16].

Chemisorption is considered irreversible as the bonding is strong, often of covalent nature, compared to the bonds in physisorption, and the reverse reaction (dissociation) is rare compared to the reverse reaction of physisorption (desorption, see number 7 in Figure 1). The thermodynamics in these reactions are the same as those of the chemical reactions. They are usually endothermic and require an

activation energy that is typically high compared to physisorption. Because of this, chemisorption is generally favored by higher temperatures and by gases that react readily with the surface. At too low temperatures the extent of chemisorption decreases and may be negligible [15].

*Physisorption* is a physical phenomenon where compounds settle on a surface and bind without chemical reactions, but through weak intermolecular forces with smaller energy requirements. These include van der Waals forces, hydrophobic interactions, electrostatic interaction, hydrogen bonding, and  $\pi$ - $\pi$ -interactions of double bonds between carbon atoms, neither of which change the electronic structure or chemical identity of the adsorbate. Physisorption is typically more common than chemisorption, it has a significantly lower specificity but is commonly seen with organic molecules. The weak intermolecular forces are reversible, and desorption occurs to a further extent than disassociation. Since there is no change of chemical composition in the adsorptive, adsorbates desorb with a retained chemical identity. Unlike chemisorption, the enrichment on the surface can happen in multiple layers, especially if the relative pressure of a compound is high. The adsorbate will bind to both surface and other adsorbate, a monolayer closest to the material is in contact with the surface while outside layers may only have contact with other adsorbates. Multiple layered physisorption may also be added onto a monolayer of chemisorbed molecules. For gaseous molecules this means a condensation to liquid form and the changing energy in physisorption is generally close to the energy of this phase change. If a multilayer adsorption of gases occurs in small pores to the extent that the entire pore space is filled with a liquid separate from the gas phase, it is termed capillary condensation [15, 16, 17].

Physisorption is an exothermic process, typically requiring significantly less activation energy compared to chemisorption. Although transport limitations such as slower diffusion or inaccessible surfaces affect the rate, physisorption generally reaches an equilibrium quickly. The process is favored by gases that easily condense (liquefiable gases) and higher partial pressures. However, as with all exothermic processes, its efficiency decreases with rising temperature. Notably, the physisorption equilibrium is in general more sensitive to environmental conditions than chemisorption, making it less dependable for binding pollutants. If the partial pressure of a compound decreases or the temperature increases, physisorption can weaken or reverse, leading to desorption and potential re-emission of pollutants [15].

## 2.5. Adsorbents – adsorbing materials and their properties

With certain materials, adsorption can be substantial and highly effective. The extent of adsorption is influenced by external factors such as relative pressure, humidity, airflow, temperature, pH, and the chemical properties of the gases involved. Additionally, the intrinsic properties of the adsorbent material – especially surface area and porosity – are fundamental in determining its adsorption capacity, as they directly affect surface accessibility and interaction potential. A good adsorbent has a large adsorption capacity, fast adsorption rate, is cost effective, non-toxic, easy to reuse and robust throughout varying conditions. Although each adsorption system is unique, certain general factors consistently enhance adsorption efficiency [15, 16], as will be discussed below.

### 2.5.1. Surface area

As adsorption occurs on surfaces, defining and distinguishing a surface area inevitably becomes essential for accurately characterizing a material's adsorptive properties, laying a foundation for understanding its performance in various applications. In general, a larger surface area provides increased adsorption capacity, and it is of great importance when designing an adsorbent. This is especially true for physisorption [15, 16].

A material's surface area includes both external and internal areas and correlates to porosity. However, voids in the material that are not connected to the surface (see 5 in Figure 1), become closed off from the surrounding and inaccessible to adsorbates. This highlights the need for distinguishing true specific surface area and the accessible surface area, where the former is a material's entire surface area and the latter is only the areas accessible from outside, contributing to adsorption capacity (see 2–4 and 6 in Figure 1 for accessible surface areas) [15, 16].

Notably, the measuring of surface area is never precise as non-accessible areas are difficult to measure with conventional methods and all the measurements vary depending on the scale used (similar to the measurement of a coastline on a map). Furthermore, assessing the surface area of powders or mixes of larger particles depends on the shape and size of the particles. Fine powders are often clustered together into secondary structures – looser aggregates or harder agglomerates – that within them contain most of the surface area, providing additional difficulties in finding a precise surface area. To simplify, less complex models or methods are often utilized to attain an approximate experimental surface area. One such method is the Brunauer-Emmett-Teller (BET) nitrogen sorption method. Based on the theory of the formation of an initial monolayer, it measures the amount of nitrogen adsorbed at 77 K and using the BET equation calculates the corresponding surface area. Although the theory has later evolved, the method still prevails as an empirical procedure [15].

### 2.5.2. Porosity and pore types

Defined as the ratio of total void volume to apparent volume of a particle or solid, porosity is an essential property of an adsorbent. A porous material contains voids in the form of cavities, channels, and pores, the presence of which significantly increases surface area and adsorption capacity [15, 16].

Pores are split into categories depending on either size or characteristics. Pore size is specified as pore width, usually meaning the shortest distance between walls in unevenly shaped pores. The categories micropores (< 2 nm), mesopores (2–50 nm) and macropore (> 50 nm) are generally used, although not well defined. Notably, the smallest pores can be of molecular dimensions. This distinction by size is relevant as compounds diffuse and bind differently depending on the size of the pore and the pore size distribution [15].

When it comes to pore characteristics the number of categories is larger; as shown in Figure 1 there are closed pores (no access to the surface), open pores (with access to the surface), blind pores (pores that end in blind alleys), interconnected pores (pores connecting to other pores), through pores (pores forming tunnels with at least two surface openings) and roughness (surface irregularities where the depth is less than the breadth). Notably, precise distinctions between the categories are difficult and most porous materials consist of complex networks with a wide range of pore sizes, shapes, and characteristics. Simplifications are therefore common, often by assuming a common shape for all pores [15, 16].

Adsorption into pore spaces can consist of layered physisorption and chemisorption onto active sites representing reactive functional groups (see 9a and 9b in Figure 1). If adsorbates occupy all surface areas, active sites, and voids in a pore it is considered filled, causing capillary condensation (see 8 in Figure 1) [15, 16].

### 2.5.3. Diffusion kinetics – pore and particle size

For efficient adsorption of gases, the rate and extent of the diffusion of the adsorbate is critical. A fast adsorption means an equilibrium is reached quickly and the material's properties can have a major impact on these kinetics. Adsorbent materials come in various forms adapted to different applications and for gas adsorption, it is generally preferred to use granules – usually consisting of irregularly

shaped particles of around 0.2–5 mm – to facilitate rapid diffusion rates. The distribution of pore sizes also has a significant impact on diffusion rates and together with granule sizes contribute substantially to the overall adsorption performance both regarding kinetics and total capacity [5].

The adsorption process can roughly be divided into bulk diffusion (movements in the fluid bulk phase), film diffusion (transport from bulk phase to adsorbent surface), pore diffusion (diffusion from external surfaces into pores) and lastly physical interactions and chemical reactions on surfaces (physisorption and chemisorption). In this context, the physicochemical reactions with the surface occur rapidly, making the kinetics depend on either film or pore diffusion, depending on which is rate limiting at the time. While film diffusion is proportional to external concentrations, mainly partial pressure, the rate of pore diffusion is primarily limited by the fluidity of the adsorbates within the pores, which depends on the pore structure and distribution in the material, rather than on external conditions. At times, the pore diffusion process dominates adsorption and for porous adsorbents, pore filling is the most common mechanism of adsorption (see 8 in Figure 1) [15, 16].

When testing adsorption, the process is at first rapid due to high driving forces of mass transfer and significant amounts of available, vacant binding sites. The uptake then plateaus due to increasing saturation of available surface area and during this time the pore filling is generally rate limiting. The effect of pore size is notable, with the macro- and mesopores becoming filled and saturated first. Additionally, these larger pores facilitate diffusion inside the material, increasing the overall speed of the transport process. Micropores notably saturate slower due to a higher diffusion resistance and this can be the dominating and rate limiting process after a plateau is reached. Once filled, smaller pores can bind a molecule from several sides, making the binding stronger [15, 16].

The size of the adsorbate is also important, with smaller compounds having faster diffusion rates and thereby quicker adsorption. Additionally, pore size and to some extent pore shape influences what is adsorbed, causing size-selective adsorption. Generally, adsorbates of a certain size will be favored by pores that are well-matched to its size and shape. Although the presence of too large molecules can result in pore blocking (see 1 in Figure 1), this size selection is useful for removing smaller compounds from a mixture, decreasing competitive adsorption. Consequently, materials with microporous structure are generally considered more effective for ions and small molecules [15, 16].

#### 2.5.4. Surface activity

The physicochemical properties of the surface significantly impact adsorption performance, mainly by influencing chemisorption properties. Tailoring an adsorbent to certain applications or target pollutants is commonly done through surface functionalization or modification, changing surface properties, and improving adsorption performance. Generally, the functionalization is targeted towards improving either affinity towards a target pollutant and/or preventing aggregation which otherwise can pose a problem when utilizing nanosized adsorbents. Adding compounds containing reactive functional groups increases desirable interactions, adds to the number of active sites (see 9a and 9b in Figure 1) and mitigates competitive adsorption. Examples of commonly used functional groups include amines, imines, carboxyl acid, phosphoric acid, and hydroxyl along with different forms of surfactants [16].

#### 2.5.5. Effects of external conditions

The performance of an adsorbent depends on the unique system in which it is implemented. In addition to material properties, external conditions significantly affect the outcome. Primary physical parameters influencing adsorption performance include temperature, relative humidity, partial pressures, and air velocity. The latter is particularly relevant for filter systems with active air flow but can translate to air circulation or diffusivity in passive adsorbent materials as these factors influence exposure time. Relative humidity also plays a role as it is a common competitive species for

adsorption. The primary chemical parameters include the adsorbate's molecular size, equilibrium and saturation pressure, and polarity, the latter of which is particularly important at high relative humidity [12, 15].

#### 2.5.5.1. Air flow and residence time

The extent of adsorption is impacted by the time a pollutant is in the vicinity of the adsorbent. As opposed to filtering systems, PRMs require no additional energy input to create airflow, making air velocity irrelevant. However, the residence time is still impacted by the extent of air circulation in the surrounding air. Increased circulation and thereby increased airflow reduces residence time and – depending on the diffusion and reaction rates – may not provide sufficient exposure time for adsorption to occur, reducing pollution removal. However, increased air flow also improves adsorption rates as it facilitates mass transfer. Additionally, increased airflow enhances the mixing of surrounding air, which is critical for indoor environments. These spaces often contain poorly mixed air with localized areas of high concentrations near pollution sources and low concentrations near adsorbents due to their removal properties, overall reducing pollution removal efficiency. The required exposure time depends primarily on the material. Highly reactive materials are generally transport-limited and favored by increased airflow, while less reactive materials are generally reaction-limited and require slower airflow. Consequently, there is not one optimal airflow, but a desirable airflow must balance providing adequate residence time with maintaining proper mixing of the surrounding air and will be different for each unique case [12].

#### 2.5.5.2. Relative humidity

High relative humidity can substantially impair a material's adsorption capacity, a limitation observed in many adsorbents including the commonly used AC. As chemisorption is limited by a finite number of active sites, competitive adsorption from water molecules will substantially decrease adsorption capacity. Additionally, high relative humidity can cause capillary condensation of water in micropores and clustering of water on the surface, preventing pore diffusion and forming a hydrophilic layer on the surface. For non-polar target pollutants, this has adverse effects as water effectively blocks surfaces and micropores, lessening both chemisorption and physisorption. For polar VOCs though, this may facilitate adsorption, and water-soluble compounds, such as formaldehyde, can experience an increased removal efficiency at higher relative humidities. This is due to condensed water acting as “water bridges” and an added absorption capacity as pollutants dissolve in the condensed water. However, these improvements are not entirely reliable, as interactions with water molecules compete with and attenuate interactions between the adsorbate and the material surface, reducing uptake permanence [18, 12].

Notably, despite its established significance, several studies indicate that the effects of relative humidity below 50% are often negligible. However, as a well-functioning material should maintain performance under varying conditions, a low moisture uptake is still regarded as an essential characteristic in adsorbents [18, 12].

#### 2.5.5.3. Temperature

Temperature influences adsorption characteristics and capacity by altering diffusivity properties, reaction rates and molecular kinetic energy. For indoor environments, increasing temperatures commonly result in increased emissions – especially of VOCs – from indoor sources and result in changes in relative humidity [12].

With higher temperatures, desorption is favored as the weak intermolecular forces associated with physisorption are disrupted, reducing the binding energy between adsorbate and adsorbent.

Conversely, a higher molecular kinetic energy facilitates diffusion which increases adsorption and especially adsorption rates. For chemisorption, a higher temperature provides the necessary reaction energies, thus increasing reaction rates [12].

The interaction between temperature and humidity is also relevant. A study of beads of AC in a fluidized bed highlights this interaction using a non-polar VOC. Substantial, adverse effects on pollution removal from increased relative humidity were seen at and above 70%. When testing increasing temperatures in dry air, the overall effect on pollution removal efficiency was adverse but minor, while temperature increases in high relative humidity had an overall large positive effect. This was attributed to an increasing temperature decreasing the relative humidity, highlighting the importance of the complex interactions governing adsorption capacity [19].

Although not always straightforward, with the outcome depending on the unique system characteristics, it can generally be surmised that higher temperatures increase the typically endothermal chemisorption but decrease the typically exothermal physisorption, often resulting in an overall reduction in adsorption capacity [12, 16].

#### 2.5.5.4. Equilibrium pressure

The equilibrium pressure and saturation pressure of an adsorptive at a constant temperature (below the compound's critical temperature) significantly influence the extent to which it is adsorbed. The relationship between the amount adsorbed (mol per mass unit of adsorbent) and the relative pressure (the equilibrium pressure divided by the saturation pressure) at a constant temperature can be described through the *adsorption isotherm*. Distinct relationships exist between a material's properties and its adsorption characteristics. Consequently, a material's unknown characteristics can be determined by studying its adsorption properties. The adsorption isotherm is one such way to determine a material's characteristics, when shown graphically, the material isotherm reflects the material structure [15].

Although some adsorbents function differ for varying partial pressures, an increase in partial pressure of a compound (giving higher concentrations of the adsorptive) generally increases the adsorption efficiency for that adsorptive [15].

#### 2.5.6. Adsorbent regeneration

Once an equilibrium is reached, an adsorbent is at its maximum adsorption capacity and fully saturated. Saturated adsorbents can be recycled or regenerated through enforced desorption. Regeneration can be accomplished through various methods, ranging from simple rinsing with water to complex procedures involving multiple treatment steps. Generally, regeneration takes two forms: thermal and chemical, with the latter being the most common due to its relative simplicity. These processes typically require substantial energy input and often result in permanent changes to the material's structural, chemical, and physical attributes. Regenerated adsorbents frequently experience a significantly reduced adsorption capacity. Still, regeneration increases the material's lifespan and substantially reduces its environmental footprint compared to its newly produced counterpart. For an adsorbent to be commercially successful, reusability through regeneration is considered essential [20].

Thermal regeneration involves heating the saturated material – often to very high temperatures – using inert gases, steam, or electric currents. It can function through desorption only, or via a combination of desorption and decomposition. The latter can be facilitated by hot inert gases and further enhanced by the presence of metals, microwaves, or ultrasounds. For pollutants with high affinity to the adsorbent, particularly harsh conditions may be necessary. This will ultimately harm the material, resulting in collapsing micropores and other chemical changes. The extent of the surface damage varies and while

some AC can retain close to 100% of their original capacity over several regenerations, the typical outcome is substantially decreased functionality [20].

Chemical methods include solvent extraction and treatments with acid-base solutions that alter the adsorbate-adsorbent interactions, favoring desorption. For instance, polar solvents such as methanol reduce and break up hydrophobic interactions. The success of this regeneration and how much of the initial adsorption capacity is maintained varies greatly [20].

Consequently, having a high desorption efficiency that is energy efficient and economically viable in the standard regeneration processes is a desirable adsorbent characteristic. This poses an issue, as the ability to adsorb efficiently generally counteracts the ability to desorb efficiently. The presence of micropores is central to this contradiction, as they facilitate efficient adsorption while significantly impeding desorption. As a result, combining the two properties is difficult and considering trade-offs is required [20].

### 2.5.7. Antimicrobial properties

Removing microorganisms from indoor air is critical for maintaining high IAQ, protecting peoples' health by reducing exposure to pathogenic bioaerosols such as bacteria, viruses, fungi, and spores. These are known to cause a variety of diseases and health effects such as infectious respiratory diseases and allergies and their presence indoors is of particular concern with people spending an increasing amount of time indoors [21, 22].

Bioaerosols can be captured through common air purification technologies such as filtration, electrostatic precipitation, and impaction. However, these methods and materials have a limited capacity for inactivating microbials, causing risks of re-emission and colonization. Microbials growing on air purification materials poses the risk of releasing secondary pollutants, decreasing IAQ and creating undesirable odors. This is especially problematic for particularly sensitive areas of application, such as hospitals, and presents a need for antimicrobial adsorbent materials. The ability to inactivate or kill bacteria and viruses would essentially render a material immune to colonization [21, 22].

An antimicrobial agent is a substance that either inhibits growth or kills microbes, mainly bacteria, viruses, and fungi. The umbrella term is *biocide*, which describes a chemical agent that inactivates microorganisms. More specific terms include the target microorganism such as *antibacterial*, *antiviral*, and *antifungal* and suffixes "cidal" and "static" differentiate between killing agents and inhibition of growth. Other terms indicate use, such as *antiseptics* for application in and on the body, *disinfectants* for surfaces and materials, and *preservatives* for preventing growth in products like food. Only *sterilization* kills all microorganisms, including spores, and although useful it is a drastic measure that is only necessary in sensitive cases [23, 14].

Antimicrobial agents have a mechanism or mode of action (MOA) through which an organism is killed or its growth inhibited. A generalized, typical series of events is (i) interaction with the surface of a cell, (ii) penetration into the intracellular space and (iii) finding the target site where specific damage is caused. Interaction with only the surface is less common but can be equally efficient. In contrast to antibiotics, biocides typically have a broad spectrum and multiple targets [23, 14].

A surface can have antibacterial properties, either on its own or through the addition or coating of an active agent. The surface acts either as passive through repulsion or repelling of microbials or active through killing. Repelling is mainly from hydrophilic/hydrophobic interactions, electrostatic forces, and steric repulsion. Killing mechanisms can also occur through electrostatic repulsion in addition to biocidal interactions. The biocidal interactions can function through surface-bound agents causing contact-killing materials, or through the release of solution-bound agents. Incorporating an

antimicrobial agent in filters and other air purification technologies helps improve antimicrobial performance and filters coated in antimicrobial agents such as chitosan or quaternary ammonium compounds (QACs) are currently implemented commercially [21].

## 2.6. Adsorbent materials in use

Many adsorbents are currently on the market, including zeolites, silica gel, activated alumina, mineral clays, and metal-organic-frameworks, with the most common material being various forms of AC [6].

### 2.6.1. Activated carbon – a common adsorbent

AC is an amorphous carbonaceous material known for its high adsorption capacity. Its efficient adsorption and storage capacity are mainly due to its exceptionally large surface area and high porosity – including a range of pore sizes. Presently, it is one of the finest materials for pollution removal from both liquids and gases and used as a standard in multiple industries (e.g., food, cosmetics, automotive applications, precious metal recovery). It is a general adsorbent that in theory adsorbs anything, though in practicality compounds with high molecular weight, high polarizability, and the presence of certain functional groups (such as halogens or double bonds) are favored. Organic compounds and heavier inorganic compounds generally adsorb to the largest extent. When saturated, AC can be re-activated using both thermal and chemical regeneration. It is relatively resistant to the damages from the processes and its structure is often preserved, allowing the material to be reused several times [5].

As a common standard adsorbent, AC has vastly different application areas requiring a range of different properties in terms of surface characteristics, physical form, and functionalization through surface modification. Consequently, AC is produced in a variety of forms ranging from carefully tailored for specific implementations to broad, generalized adsorbent functioning on a variety of pollutants. Options for physical form include powdered, extruded, and granular AC. The latter is the most common form for gas adsorption, typically consisting of heterogeneous particles ranging from 0.2 to 0.5 mm in diameter, a form well suited for the high diffusivity required for gas adsorption [5].

Achieving the desired final AC material in terms of surface characteristics and physical form involves careful combination of raw material and production process design, both of which significantly influence the final structure and functionality. In theory, any carbonaceous material can serve as raw material, with common sources including waste materials such as coconut husks, wood, and paper mill waste and fossil sources such as coal and coal-tar pitch. Granular AC is predominantly produced from coconut husks and the fossil materials coal and peat [5]. In the European production, the most common raw material is fossil coal, primarily mined in China [7]. Increasing awareness of problems related to using fossil materials, improving methods, and expanding production with renewable sources rather than coal has been a popular topic of research. Replacing the dominating fossil sources with biomaterial wastes provide marked improvements to production both in terms of environmental footprint and economic viability [7, 5].

Regardless of the raw material though, the refining process required is in broad terms similar and involves either a chemical or physical process of carbonization, crushing and activation. Raw material is burned to charcoal, crushed, and then exposed to an activation process which greatly increases the surface area (from around 2–5 m<sup>2</sup>/g to 1 000 m<sup>2</sup>/g or more). The physical process involves carbonization in an atmosphere of inert gases (typically nitrogen or argon) and activation through heating in an oxidizing atmosphere (typically with oxygen or steam). Chemical activation, which is generally the preferred method, utilizes acids or bases to achieve the same goal. Both processing options require the charcoal be kept at very high temperatures (450–1 200 °C), substantially increasing energy consumption [5].

Both the acquisition of fossil raw materials and the production has an extensive environmental footprint in ecological consequences at the coal mines and in high energy usage. Using regenerated AC or biomaterial waste as raw material only partly mitigates the environmental drawbacks compared to fossil-sourced, new AC. The issue of high energy consumption in both new production and regeneration remain [7, 5]. This presents a challenge and necessitates the development of alternative, more sustainable adsorbents.

## 2.7. Modifications to promote chemisorption using amines

Chemisorption is generally favored by the presence of electron-donor functional groups – such as amines – which are commonly utilized to add functionality to adsorbents and increase pollution capture. Amine-based functionality is particularly well-suited for chemisorption due to its strong reactivity with a wide range of pollutants, including  $\text{NO}_x$  gases and VOCs. VOCs typically contain multiple functional groups, such as aldehydes, carboxylic acids, alcohols, and aromatic rings, which can be taken advantage of for chemisorption. Some relevant functional groups for the reactivity of amines and VOCs are shown in Figure 2. The resulting irreversible bonds significantly reduce the risk of re-emission, ensuring stable and reliable pollutant capture. Amine-based materials also maintain their chemisorption capacity under varying environmental conditions, such as fluctuations in temperature and humidity, and exhibit high selectivity for specific pollutants. Additionally, amines typically provide some antibacterial and/or antimicrobial effects, which is advantageous for potential use in microbial removal and mitigating risks of colonization [24, 20].

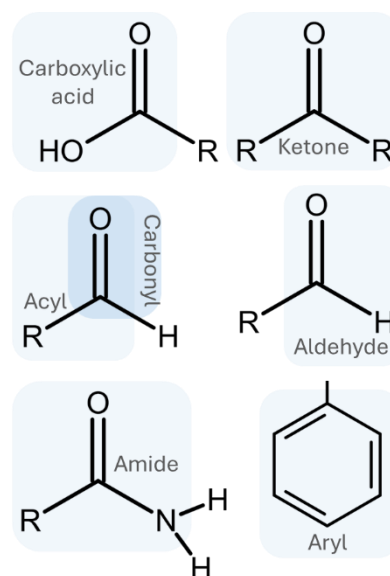


Figure 2. Some functional groups relevant to the functionality and reactivity of VOCs and amines: ketones, carboxyl acids, acyls, carbonyls, aryls, aldehydes, and amides. Structures from [25].

### 2.7.1. Amines – properties and structure

Amines are a principal functional group in organic chemistry, closely related to ammonium ( $\text{NH}_3$ ). With the ability to react as bases, nucleophiles, and ligands, they have a versatile reactivity. Amines are categorized based on the number of carbon atoms bonded to the nitrogen atom. As shown in Figure 3, amines with nitrogen binding to (i) one carbon are called primary ( $1^\circ$ ), (ii) two carbons are called secondary ( $2^\circ$ ) and (iii) three carbons are called tertiary ( $3^\circ$ ). Tertiary amines can also bind to a fourth carbon, yielding a quaternary ammonium ion or salt. While not technically an amine, these structures are closely related and share some chemical properties. Additionally, amines where the carbon atom incorporates an aromatic ring are known as cyclic amines (e.g., pyridine and aniline as shown in Figure 3) and exhibit different properties from linear amines [25].

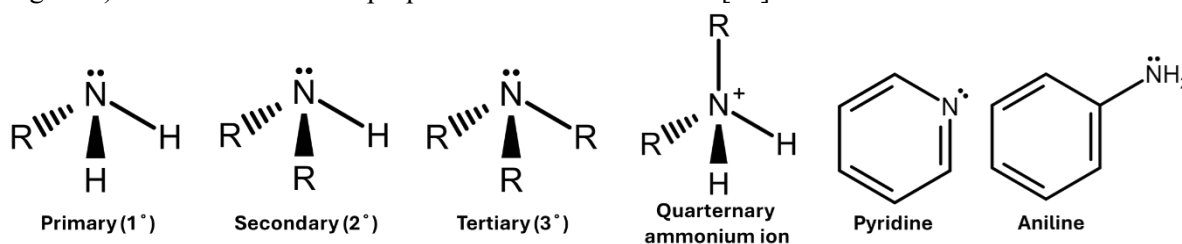


Figure 3. The classification and chemical structure of amines and the closely related quaternary ammonium ion, showing all lone electron pairs. The structures shown are primary, secondary, and tertiary amines, quaternary ammonium ion or ammonium salt and the cyclic amines pyridine and aniline [25]

As shown in Figure 3, the structural geometry varies across amines and substantially influences chemical properties – for primary, secondary and tertiary amines the nitrogen has a tetrahedral geometry, with one of the four substituents being a lone pair of electrons. This lone electron pair is central to its reactivity and allows inversion at the nitrogen center, unlike quaternary ammonium ions which have four substituents and therefore a fixed stereochemistry [25].

## 2.7.2. Reactivity of amines

This section covers amines and their versatile reactivity, which is especially due to their lone electron pair. Although different in composition,  $\text{NH}_3$ , primary, secondary, and tertiary amines all exhibit similar reactivity [25].

### 2.7.2.1. Intermolecular interactions

The N-H bonds in the primary and secondary amines allow for both donating and accepting *hydrogen bonds*, making most amines water soluble. Tertiary amines, although lacking the N-H bond, can still accept hydrogen bonds to a lesser extent, making them less water soluble [25, 26].

The high electronegativity of nitrogen creates a dipole moment, which is stronger in primary and secondary amines than in tertiary. This enables *dipole-dipole interactions*, adding to its intermolecular bonding capacity [25, 26].

The presence of hydrocarbons enables interactions through *van der Waals forces*, which increase in strength with the number and size of substituent hydrocarbons, at the expense of the dipole moment. The loss of dipole moment is especially apparent in tertiary amines where the nitrogen and its lone electron pair are increasingly sterically hindered with added, larger hydrocarbon substituents [26].

The quaternary ammonium ions interact predominantly through ionic forces. The ionic amines are mostly water soluble, but in the presence of anions salts can form and precipitate [25, 26].

### 2.7.2.2. Basicity and nucleophilicity

The lone electron pair in the primary, secondary, tertiary amines and  $\text{NH}_3$  make the compounds basic and enable nucleophilic activity. Amines are sufficiently basic to completely protonate in dilute acid solutions, forming ammonium ions. In the presence of anions, they can form ammonium salts, although these are typically water-soluble [25].

The protonation allows amines to partake in acid-base reactions, for example with hydrochloric acid (HCl), as shown in Figure 4, where the amine acts as a base and accepts a proton from HCl, yielding ammonium chloride salt. Primary and secondary amines can also act as weak acids, giving hydrogen and creating anions, making amines amphoteric compounds (both acids and bases) [25].

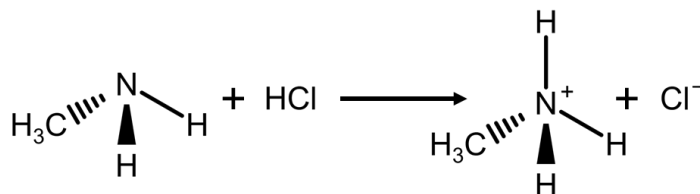


Figure 4. Acid-base reaction – a primary amine reacting as a base with hydrochloric acid, yielding ammonium chloride salt.

The basicity is substantially influenced by the stability of both the lone electron pair and the resulting cation, consequently the basicity of amines depends largely on molecular structure through substitution, steric hindrance, polar effect, and resonance effect. Substituent alkyl groups (a hydrocarbon with the formula  $\text{C}_n\text{H}_{2n-1}$ ) act to stabilize the charge of the ammonium ion through

polarization, typically increasing basicity. However, the third alkyl group typically reverses this trend and decreases basicity, mainly due to increased steric hindrance from the bulky substituents [25, 26].

Basicity is also affected by polar or electron-withdrawing effects of substituents. Nearby electronegative groups – such as halogens or aromatic rings – destabilize the ammonium ion, weakening the base. Resonance effects from substituents, such as from the aromatic ring in aniline (see Figure 3), act to stabilize the lone electron pair and thereby also decrease basicity. Water can also act to stabilize charges and consequently, the basicity of amines differs when in the gaseous or liquid phase [25, 26].

Acid-base reactions are characterized by a reaction with a hydrogen atom, with the amine acting as a base and the reaction partner acting as an acid, as shown in Figure 4. However, as nitrogen is highly electronegative, amines can also function as nucleophiles and partake in reactions such as nucleophilic substitution ( $S_N2$ ) and additional reactions. In nucleophilic reactions, the reaction occurs with any atom other than hydrogen and the reaction partner is called an electrophile. Nucleophilicity is closely related to basicity, mainly due to both depending on the stability of the lone electron pair. However, there is not necessarily a clear correlation, and nucleophilic reactions include significantly larger variations than acid-base reactions. Notably, the nucleophilicity of amines is largely independent of the electrophile in the reaction and the amine seldom acts as a leaving group [26, 27, 28, 29].

Like basicity, nucleophilicity is generally increased by electron-donating groups and charges that destabilize the lone pair and decreased by electron withdrawing groups and resonance that stabilize the resulting ion, again highlighting the importance of substituents. However, nucleophilicity is generally more sensitive to steric hindrances as it impedes access to electrophilic centers, making bulky amines less reactive. When reacting with hydrogen, the lone electron pair need only reach the spherical s-orbital of the hydrogen. Nucleophilic reactions can be much more varied and require more specific points of contact, including the right angle. If the necessary angle is blocked, the reaction is substantially slowed or does not occur at all. Consequently, bulky substituents generally influence nucleophilicity more than they do basicity. Additionally, acid-base reactions are generally quick compared to nucleophilic reactions and reversible, unlike nucleophilic reactions which are typically irreversible [26, 27, 28, 29].

### 2.7.2.3. Relative reactivity

There is no one rule by which to scale the reactivity of all amines, as the combined effects of substituents, surrounding conditions and the non-correlating nucleophilicity and basicity give a combined reactivity. However, assuming the substituents are simple methyl groups, the reactivity of amines can be roughly described as follows. For tertiary amines, electron donating groups are available to a larger extent which increases nucleophilicity and basicity, while the presence of larger substituents also sterically hinders and decreases reactivity, typically resulting in a comparatively low reactivity. Secondary amines have less steric hindrance, with two electron-donating groups, making it a strong nucleophile and base and often more reactive than both primary and tertiary amines. Primary amines have only one electron donating group, weakening nucleophilicity and basicity. However, the small hydrogen substituents provide little steric hindrance, typically increasing reactivity substantially. Additionally, a primary amine can have hydrogen substituted with a hydrocarbon, yielding a secondary amine. Consequently, a primary amine can cycle through several reactions [25, 29].

Regarding intermolecular interactions, the primary and secondary amines can interact through strong hydrogen bonds and dipole-dipole interactions compared to tertiary amines, which exhibit weaker accepting of hydrogen bonds, weaker dipole-dipole interactions and van der Waals forces. Additionally, as they can all form ammonium ions, there is potential for stronger ionic interactions [25, 29].

### 2.7.3. Amine-based capture of air pollutants

Campbell McKenzie et.al (2015) have assessed the chemisorptive abilities of a nanomaterial with a surface-functionalization with an amine-rich polymer coating containing primary, secondary, and tertiary amines. The resulting material showed selective reactivity, capturing compounds containing aldehyde- and carboxylic acid functionality from gases. Aldehydes were captured through a condensation reaction, yielding

imines (see 1 in Figure 5) and carboxylic acids through an acid/base reaction yielding ammonium carboxylate salts (see 2 in Figure 5).

These classes of pollutants are relevant for capture due to their toxicity and presence in urban and indoor areas, originating from for example vehicles, oxidation of other precursor pollutants, and cooking [24].

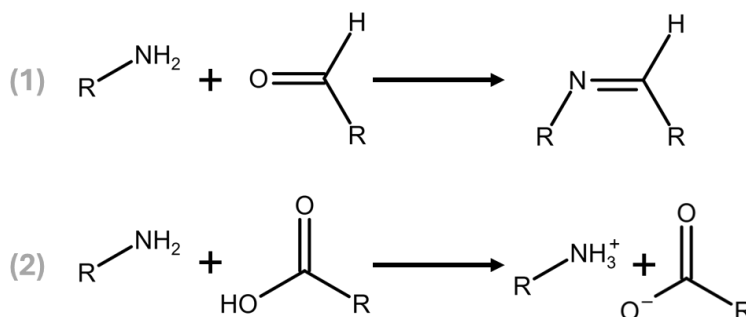


Figure 5. Reaction forming imines in (1) and an acid/base reaction yielding an ammonium salt in (2).

In the evaluation, several compounds with aldehyde- and carboxylic acid functionality but different carbon chains were assessed in order to show broader functionality. The material was shown to adsorb substantial amounts of pollutants despite steric hindrances from branched carbon chains and high volatility from short chains. To evaluate selectivity, the material was exposed to compounds presumably lacking compatible reactivity such as alkenes and alcohols. These were adsorbed to a significantly lesser extent than the aldehydes and carboxylic acids. The adsorption that did occur was presumed to be due to non-reactive adsorption mediated by electrostatic interactions. Exposure to gaseous mixes also showed selective adsorption of mainly aldehydes and carboxylic acids, demonstrating the avoiding of off-target binding. The material outperformed conventional AC in capture of the target pollutants, highlighting the effectiveness of amine functionalization [24].

### 2.7.4. Antimicrobial properties of amines

Generally, QACs possess antimicrobial properties and are widely used as disinfectants and in some instances as coatings on air filters, inducing biocidal features. QACs are often surface active (surfactants), containing a hydrophobic hydrocarbon chain and a hydrophilic amine-based head. Depending on the pH, they are either cationic, anionic, or nonionic, with the first having the strongest biocidal effects. The precise mechanism is unknown, but strong electrostatic interactions between the positively charged QACs and anionic cell wall compounds – mainly the inner wall or cytoplasmic membrane – is generally accepted as the main MOA, making QACs membrane-active. A proposed detailed series of events consists of (i) adsorption and penetration into the cell wall, (ii) reactions with lipids or proteins in the inner wall, causing membrane disorganization, (iii) leakage of intracellular material, (iv) degradation of proteins and nucleic acids, and (v) wall lysis induced by autolytic enzymes. The result of this is cell death through loss of structural organization and integrity, leakage of intracellular compounds and disturbed uptake abilities. As initial interactions partly occur with hydrophobic lipids in the cell wall, the presence of an alkyl chain can increase interaction and increase antibacterial capacity [21, 23].

### 2.7.5. Alternative amine-based additives

Adsorbi is continuously exploring possibilities for material improvements in terms of both performance and lowering the environment footprint. The amine-based additive currently employed is

derived from fossil sources and exhibits some elevated toxicity. Substituting it entirely or partially with a renewable, less toxic compound, while maintaining functionality, is a key focus area. Hence, any alternative amine-based compound explored should preferably be of natural or otherwise more sustainable origin with similar adsorption characteristics as the original. In this section, the four alternatives used to make adsorbent prototypes – chitosan, graphitic nitride, gelatine, and dodecyl dipropylene triamine (henceforth referred to as Y-amine) – are outlined.

### 2.7.5.1. Chitosan

Chitosan is a family of linear polysaccharides with varying composition, size, and monomer distribution, resulting in different properties. The chemical structure of the chitosan used in this study is presented in Figure 6. Chitosan is of natural origin, although it is not abundantly found in natural ecosystems. Consequently, it is typically derived through deacetylation from chitin, a compound found to a significantly larger extent in several biological systems such as in exoskeletons in crustaceans, insects, algae and in fungi cell walls. Historically, chitin was sourced primarily from crustaceans, but due to rising interests in more ethical production, the use of fungi and insects as a source is increasing. A notable advantage is that both production and subsequent modifications can be performed cheaply and under mild conditions, lowering the environmental impact and costs. As of 2019, the global chitosan market was valued at 6.8 billion USD and is expected to expand [30].

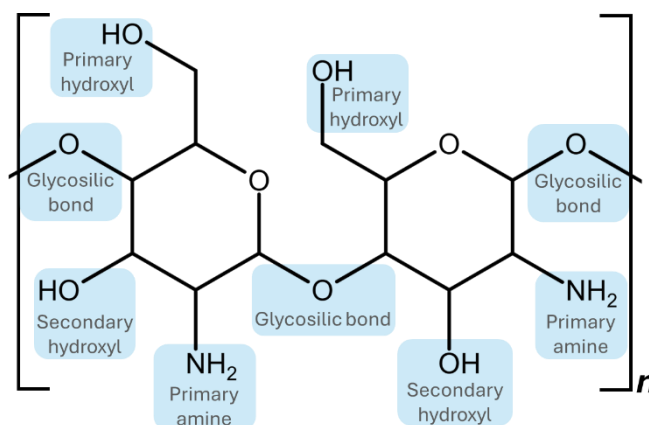


Figure 6. Chemical structure of YC58325 chitosan from Biosynth, modified through deacetylation and addition of hydroxyl groups to invoke solubility. The active sites or functional groups relevant for adsorption – primary amines, primary and secondary hydroxyl, and glycosidic bonds – are highlighted. Figure made with modifications based on the structure of YC58325 chitosan from Biosynth [32].

Due to its inherent variety in composition, chitosan is a multifunctional compound, currently utilized for a multitude of application areas. Its specific properties depend largely on the structure, resulting in varied physicochemical characteristics. Known properties include anti-inflammatory, antioxidant, antimicrobial, antitumoral, biodegradability, and wound healing activities. Notably, chitosan is biocompatible, making it of interest to pharmaceutical applications. Current uses include as a biocatalyst in production, and several high-value industries such as cosmetics and foods. Chitosan has also previously been used to successfully functionalize adsorbent material and is currently used for water treatment [30, 31].

A considerable limitation with chitosan is solubility, which is typically poor in neutral and basic aqueous media but improves slightly in acidic conditions. As solubility is of importance for many application areas, derivatives of chitosan are commonly produced with the purpose of enhancing solubility. Chitosan's solubility in aqueous media depends on the combined effects of pH, degree of acetylation, molecular weight, temperature and polymer crystallinity. The solubility in acidic conditions is due to protonation of its primary amines, making chitosan cationic. Higher acetylation, or greater presence of acetyl groups (acetyl defined as a carbohydrate with the formula  $C_nH_{2n+1}$ ),

decreases solubility as it contributes to hydrophobicity. Lower molecular weight generally enhances solubility, and at a point a lower molecular weight inevitably means the chitosan consists of oligomers rather than polymers, which are soluble at a wider range of pH. Once dissolved, the solution generally exhibits a high viscosity, a characteristic known to be difficult to incorporate in many application areas. Similar to solubility, viscosity is also amplified by higher molecular weight and acetylation degrees. The antimicrobial properties of chitosan include antibacterial and antifungal activity. The mechanism is still debated, but it is widely accepted that it works mainly through inhibition of growth, as experiments have shown growth in bacteria where chitosan was removed [30]. A proposed mechanism is similar to that of QACs, wherein the primary amines become protonated at lower pH. The resulting polycationic characteristics induce electrostatic interactions with the cell membrane, causing changes in permeability and cell integrity. Additionally, if chitosan enters the cell, mechanisms are thought to include inhibition of synthesis of RNA and DNA, resulting in cell death [14, 21].

The chitosan used in this study is YC58325 from Biosynth, which has been modified for increased solubility through substituting acetyl groups with hydroxyl groups. In Figure 6, its chemical structure is provided, with functional groups relevant for adsorption indicated. The principal chemical reactivity is due to the primary amines and the primary and secondary hydroxyl groups. Notably, both amines and hydroxyls can form intermolecular hydrogen bonds. The glycosidic bonds and acetamide groups also contribute, but to a lesser extent. The multiple functional groups enable a number of possible modifications to the polymer. Additionally, they potentially enable chemisorption through interactions with gaseous VOCs, suggesting adsorption potential [30, 32, 14].

As chitosan has already been successfully applied as an adsorptive agent in water treatment and possesses inherent antimicrobial activity, it stands as a promising candidate and will therefore be assessed for incorporation in Adsorbi's material.

#### 2.7.5.2. Graphitic nitride (g-C<sub>3</sub>N<sub>4</sub>)

Graphitic nitride is a conjugated polymer, its chemical structure presented in Figure 7. Although it is not of natural origin, it is among the oldest artificial polymers reported in scientific literature. It is produced comparatively simply through polymerization of nitrogen-rich precursors such as melamine, dicyandiamide, and ammonium, making the raw material used to produce it varied but often natural in origin. The synthesis can take several forms, utilizing both chemical and thermal methods. However, drawbacks include high temperatures used in the production and, in some production forms, the need for high vacuum atmosphere and costly, toxic, or explosive precursors that increase costs and environmental burden [33].

Known for its high physicochemical stability, graphitic nitride is thermally stable up to 600°C and is largely insoluble in both acidic and basic conditions. Its characteristic electron band structure is suitable for use as a metal-free conductor and visible-light-responsive photocatalyst, making it a currently appealing material for sustainable energy production. Although the material itself is stable and has a low toxicity, the surface properties allow for efficient surface engineering and anchored surface compounds or nanoparticles are used to introduce a wide range of functionalities. Common applications of modified graphitic nitride include water splitting, reduction of CO<sub>2</sub>, degrading of organic pollutants, and bacterial disinfection [34, 33].

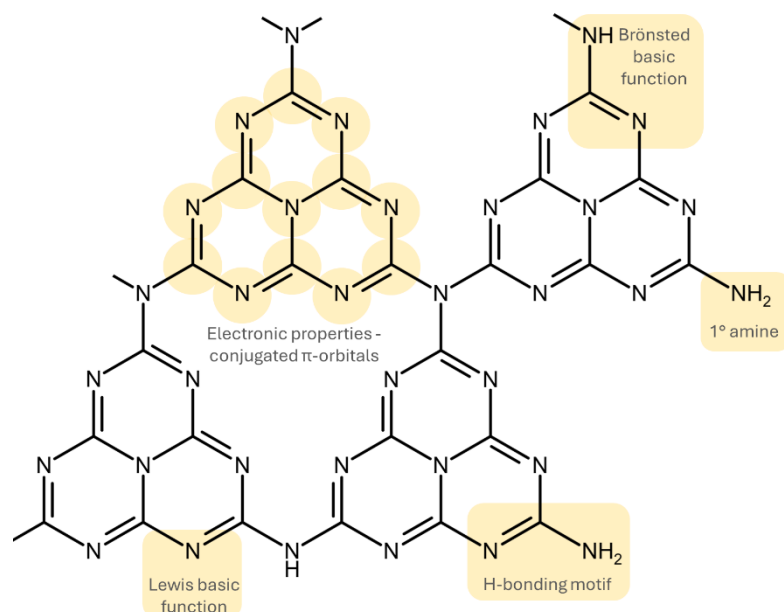


Figure 7. Chemical structure of graphitic nitride, showing sites of potential interactions in the form of electronic properties ( $\pi$ -conjugated systems), Brønsted and Lewis basicity and hydrogen bonding. Figure made with modifications from [35] and [36].

As shown in Figure 7, graphitic nitride contains several functional groups that make it a suitable option for adsorption functionalization. Although in the shape of a sheet, the ends typically present amines and nitrogen in the rings present Lewis base functions. Additionally, the  $\pi$ -conjugated systems allow for  $\pi$ -interactions [35, 36].

### 2.7.5.3. Gelatine

Gelatine is a natural biopolymer showing biocompatibility, biodegradability, it is classified as GRAS (Generally Regarded As Safe) and is in some forms approved for human food. The polymer is typically derived from collagen, a prevalent protein found in abundance in the extracellular matrix of animals in tissues such as cartilage, skin, bones, and tendons. Notably, as a protein collagen contains the standard molecular structure of amino acids on a polypeptide chain. Although newer methods enable synthesis, collagen is primarily sourced from porcine, bovine, avian, and aquatic sources or from slaughterhouse by-products. Deriving gelatine involves rupture of the collagen structure and hydrolysis, which can be achieved chemically or thermally. With an abundant source and simple processing, gelatine is a cheap, easily available and commonly used as a thickener, clarification agent, emulsifier, stabilizer, texturizer, gelling agent, binder and film former used in the food sector, for biomedical and pharmaceutical purposes, in cosmetics etcetera [37].

Gelatine is characterized by a repetition of the triplet Gly-X-Y where Gly is the amino acid glycine and X and Y are other amino acids (commonly proline for X and hydroxyproline for Y). Additionally, variations often occur due to posttranslational modifications and effects from treatments. Gelatine is a diverse polymer, typically consisting of a mixture of positively charged, negatively charged, and hydrophobic amino acid residues with varying molecular weights. Hence, the quality of gelatine is not decided based on chemical formula but its resulting properties such as gel strength, viscosity, thermal stability, and solubility. Despite the processing, the properties of gelatine are largely influenced by the source of collagen, specifically what animal it was harvested from. A generalized chemical structure of gelatine is presented in Figure 8 [38, 37].

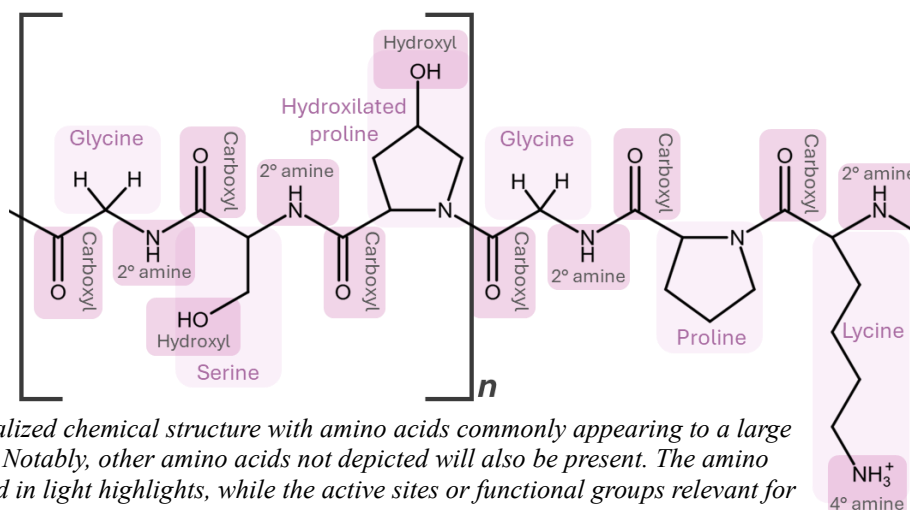


Figure 8. A generalized chemical structure with amino acids commonly appearing to a large extent in gelatine. Notably, other amino acids not depicted will also be present. The amino acids are indicated in light highlights, while the active sites or functional groups relevant for adsorption – carboxyls, secondary amines, and quaternary ammonium ionic groups – are indicated in darker highlights. Figure made from [37].

The gelatine used in this study was from Kremer. It is marked as deionized and intended for use as wood glue and varnishing. It is derived from porcine skin, soluble in warm water, has an average molecular weight of 50 000–100 000 Da, a high gel strength, and consists of grains sized  $\leq 3$  mm [39, 40].

As the precise structure of the gelatine used is unknown, a generalized chemical structure, featuring commonly occurring amino acid residues, is used to predict potential adsorption abilities. The structure is presented in Figure 8, with amino acid residues and potentially relevant active groups highlighted in lighter and darker shades, respectively. Notably, the tertiary amine in proline is not highlighted, as steric hindrance likely renders it non-reactive. In addition to chemical reactions, hydroxyl can form hydrogen bonds and the amine can, depending on the pH, form ionic bonds. The multiple functional groups and possible intermolecular interactions suggest potential adsorption capacity, making gelatine a promising candidate for a new amine-based additive in Adsorbi's material.

#### 2.7.5.4. Y-amine

Y-amine is a fatty polyamine; the chemical structure of the Y-amine used – Triameen Y12D-30 – is presented in Figure 9, with its active groups highlighted. Triameen is produced as a biocide for disinfection and preservation and is regulated by biocidal products regulations from the EU. It is known to effectively kill both gram positive bacteria and enveloped (lipophilic) viruses, and, although to a lesser extent, gram negative bacteria. Selective activity has been shown for fungi and algae, indicating a broad spectrum of activity towards microbes. Y-amine in itself is not of natural origin, but typically naturally sourced to a large extent and as far as is known not carcinogenic, making it a suitable compound for a wide range of applications. Notably, as can be surmised from its structure, it also displays surfactant properties [41, 42].

The MOA, as described previously for QACs, is destruction of the cell wall. For Y-amine in particular, it involves entering the outer cell wall and interacting with the phospholipids in the inner cell wall. As the inner wall disintegrates, the membrane-bound ion-transportation is disrupted. The changed permeability causes unregulated uptake of external compounds, increasing susceptibility to other toxic

compounds present. For the target organisms and with high enough quantities, this results in cell death [41].

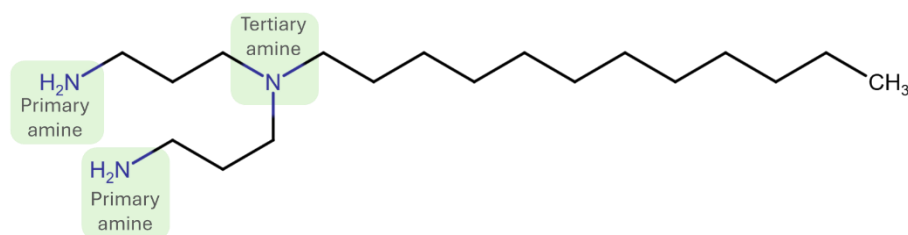


Figure 9. Molecular structure of Y-amine. Figure made based on the structure from [41].

The manufacturer of Triameen describes that its biocidal activity decreases at too low or too high pH levels, with an optimum of somewhat basic conditions. For example, tests have shown that the biocidal effects on the gram-negative bacteria *Pseudomonas aeruginosa* rapidly decreases at and above pH 9. At pH above this, the lack of positive charge decreases adherence to and penetration of the outer membrane, lowering the biocidal activity. It should also be noted that higher water hardness – especially the presence of Ca<sup>2+</sup> and Mg<sup>2+</sup> ions – stabilize bacterial membranes, thus rendering the Y-amine biocide less efficient [41].

As shown in Figure 9, the tertiary amine is partly accessible, although the hydrocarbon chains may be a steric hindrance. Its main reactivity can be attributed to the primary amines, which are well exposed and thus more prone to react. These easily accessible amine groups indicate Y-amine potentially possess efficient adsorption properties, thus making it a promising candidate to replace the current amine-based additive.

## 2.8. Granulation

One of the key steps in the production of Adsorbi's material is granulation, a process widely used across various industries. Characterized by agglomeration, the process essentially turns fine, dry powders into larger, uniform agglomerates known as granules. Granulation involves the enlargement of small particles through agglomeration, resulting in larger, more uniform agglomerates called granules. Compared to fine powders, granules offer several advantages, including improved uniformity, increased bulk density, enhanced hardness, greater physical and chemical stability, and a dust-free product [43, 44].

Granulation is typically performed using one of two primary methods: dry granulation or wet granulation. Wet granulation involves the use of a liquid binder to induce agglomeration, while dry granulation relies on mechanical compression. In wet granulation, the process begins with mixing dry powders, followed by wetting with a liquid binder. This combination of the liquid binder and particle motion – such as tumbling or shear mixing – initiates agglomeration, leading to the formation of granules, which are subsequently solidified through drying [43, 44].

At the particle level, the wet granulation process consists of three key phases: wetting & nucleation, consolidation & growth, and attrition & breakage as shown in Figure 10. During nucleation, the liquid binder creates liquid bridges between particles, promoting the formation of initial aggregates through surface tension and capillary forces. This is followed by the consolidation & growth phase, where smaller aggregates collide, merge, and grow into larger granules through continued agglomeration. Once granules have formed, the process enters the attrition & breakage phase, where granules may rupture or fragment into smaller pieces due to mechanical stress. Notably, growth and breakage often occur simultaneously, contributing to the granules' final properties [43, 44].

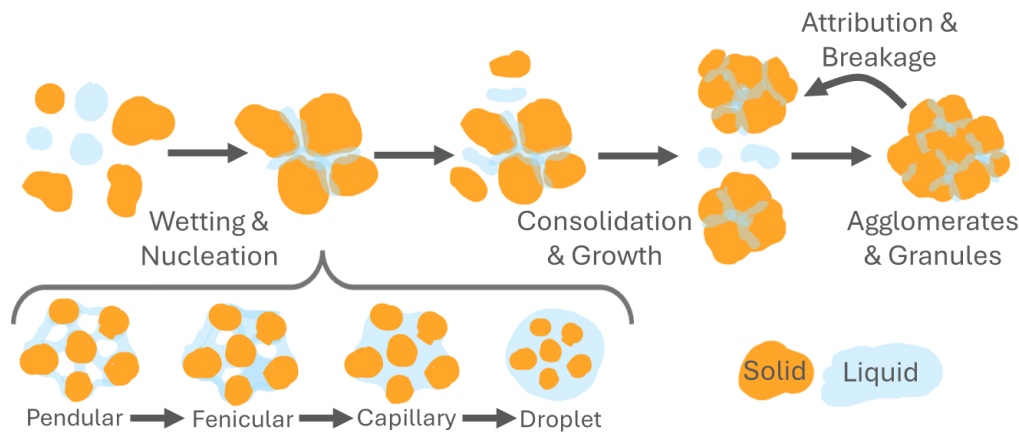


Figure 10. The granulation process in detail with wetting of solid particles, nucleation (in detail divided into the pendular, funicular, capillary, and droplet states), the consolidation and growth phase, formation of agglomerates and finally wet granules. Figure made with modification from [59].

### 2.8.1. Influence of binder properties

The properties of the liquid binder – mainly its viscosity and surface tension – and the method of application significantly influence the granulation process in terms of resulting granule strength, size and uniformity [43, 44].

Binder viscosity directly influences the granule size. Higher viscosity results in larger granules, as greater energy is required to break the liquid droplets. The resulting larger droplets spread less effectively, leading to the formation of larger nuclei and ultimately larger granules. However, as excessively high viscosity inhibits droplet spreading, reduce particle collisions, and inhibit granule growth, an optimal viscosity is essential to balance the process [43, 44].

Surface tension also has a significant impact on granulation, mainly in terms of determining the strength of capillary forces and liquid bridges that bind together particles. A reduction in surface tension weakens the capillary forces and liquid bridges that bind particles together, potentially hindering agglomeration [43, 44].

### 2.8.2. Influence of particle size

The size of the powder particles used in the granulation also influences the process and the amount of binder required. Smaller particles have a larger surface area, requiring more binder to form liquid bridges effectively. This increased surface area creates more contact points between particles, generally resulting in stronger granules. However, granules formed from smaller particles tend to have a more porous structure, which may influence both physical and chemical properties of the resulting granules [44]. Understanding these factors is crucial for optimizing granulation processes to achieve desired granule properties.

### 2.8.3. Binder-to-solid ratio and method of application

The ratio of solid powder to liquid binder is another factor significantly impacting the final properties of the granules. A higher binder ratio promotes nucleation, increasing granule size. However, excessive amounts of liquids can result in overwetting, where the mixture transitions into a slurry, hindering granule formation. Conversely, insufficient liquid prevents agglomeration, leading to poor

granule formation. The proportion of the granular volume occupied by the wet phase also influences the final porosity, as voids are left when the liquid binder evaporates during the drying of the granules.

The method of binder addition is equally important in the granulation process. Common techniques include pouring, melting, and spraying. Among these, spraying is particularly advantageous as it ensures uniform distribution of the binder across the powder particles. This uniformity minimizes the risk of local overwetting, thereby supporting consistent granule growth and quality [44].

#### 2.8.4. Practical implications

With these factors – binder properties, powder size, binder-to-solid ratio, and method of distribution – the granulation process can be adjusted to influence both kinetics of agglomeration and the final size distribution of the granules. Despite extensive knowledge of the factors influencing granulation and substantial research aimed at predicting outcomes, granulation remains a complex process. Its behavior is often challenging to model accurately, and process designs still rely heavily on practical experience and iterative refinement rather than purely theoretical predictions. This highlights the intricate and multifaceted nature of granulation as a manufacturing technique [44].

### 2.9. Adsorbi's material – a cellulose-based adsorbent for gaseous pollutants

Adsorbi is actively developing innovative cellulose-based adsorbents for the effective and secure adsorption of harmful airborne pollutants, particularly VOCs, as a sustainable alternative to AC. The main component of the material is wood-based cellulose, a renewable material traditionally used in paper production. Unlike AC, this material captures pollutants irreversibly, ensuring more stable adsorption performance across varying pollutants and temperatures, while significantly reducing the risk of re-emission. This makes the adsorbent more efficient when compared to AC, with additional benefits such as a longer lifespan, a more sustainable raw material source, and a production process that is less energy intense. Furthermore, the adsorbent undergoes a visible color change as it binds pollutants, providing a clear and user-friendly indication of saturation and replacement needs.

The adsorbent consists of porous granules – mainly composed of a fibrous cellulose-matrix – and its performance is derived mainly from a selection of additives dispersed within the matrix. The complex design ensures enhanced performance and stability in the adsorption. The size of the adsorbent granules can be adjusted to suit intended purposes and are in practicality similar to conventional AC products, making a replacement simple without having to replace existing systems and apparatuses.

Adsorbi is continuously working on exploring possibilities to improve material performance, while lowering the overall material and production environment footprint. The material's microbial properties have not yet been fully evaluated and gaining some understanding of this would yield useful information for future applications and potential challenges with microbial growth. Consequently, this master's thesis focuses on evaluating different naturally sourced or more sustainable amine-based additives to improve the adsorbents' performance while reducing their overall environmental footprint, along with making an initial assessment of the material's microbial properties.

### 3. Materials and methods

This master's thesis is centered around material development. The primary objective is testing alternative amine-based additives by incorporating them into Adsorbi's adsorbent material, creating prototypes. The prototypes were made with variations on (i) amine-based additive composition and (ii) different methods of incorporating the alternative additives into production. The prototypes were subsequently characterized and evaluated in terms of performance and antimicrobial properties in comparison to one of Adsorbi's material compositions.

#### 3.1. Material variations – prototypes, reference sample, and negative control

In total four amine-based additives with a lower environmental footprint were evaluated – chitosan, graphitic nitride, gelatine, and Y-amine – all of which present characteristics promising for the functionalization of adsorbents. Variations in amine-based composition included the alternative additives separately, and in combination with an increasing percentage of the original additive. The compositions are henceforth indicated as weight ratios of alternatives to original amine-based additives – 100:0, 75:25, 50:50, 25:75. All ratios amount to the same total weight and hence all material variations contain the same total amount of amine-based additive. Material containing any of the four alternatives are henceforth called prototypes.

Prototypes were produced using Adsorbi's lab-scale production procedure, an overview of which is presented in the procedure section below. To assess the effects of different methods of incorporating the alternative amine-based additives into the production procedure, three points of addition were introduced. These points of addition – henceforth referred to as points A, B, and C – are also expanded upon in the procedure section.

Additionally, a reference sample was produced according to Adsorbi's original production procedure and composition. Hence, the reference sample's weight ratio is 0:100 and no point of addition is indicated, as only the original procedure was used. Furthermore, a negative control was necessary for the subsequent microbial evaluation. Thus, material containing no amine-based additive was produced. The weight ratio of the negative control is thus 0:0 and the points of addition are irrelevant.

All material variations produced are presented in Table 1, including (i) prototype variations with weight ratios and addition points, (ii) the reference sample, and (iii) the negative control. Notably, some prototypes were unfeasible to produce and are therefore crossed out in Table 1. The prototypes made and the reference sample were subsequently characterized in terms of adsorbent size distribution and bulk density. Performance evaluation in terms of adsorption capacity and moisture uptake was monitored using gravimetric studies. Additionally, microbial properties of the prototypes, the reference sample, and the negative control were assessed using broth dilution and disk diffusion assays.

Table 1. All adsorbents produced: the prototypes, the reference sample, and the negative control. For the prototypes, the variations on amine-based additive composition are indicated as weight ratios of alternative to original amine-based additives. The alternative used is indicated in the headers. The different methods of incorporating the amine-based additives are indicated as points of addition A, B, and C. The variations that were not feasible to produce are crossed out.

Chitosan												
<b>Weight ratio</b>	100:0			75:25			50:50			25:75		
<b>Point of addition</b>	A	B	C	<del>A</del>	B	C	<del>A</del>	B	C	<del>A</del>	B	C
Graphitic nitride												
<b>Weight ratio</b>	100:0			75:25			50:50			25:75		
<b>Point of addition</b>	A	B	C	A	B	C	A	B	C	A	B	C
Gelatine												
<b>Weight ratio</b>	100:0			75:25			50:50			25:75		
<b>Point of addition</b>	A	B	C	A	B	C	A	B	C	A	B	C
Y-amine												
<b>Weight ratio</b>	100:0			75:25			50:50			25:75		
<b>Point of addition</b>	A	<del>B</del>	C	A	<del>B</del>	C	A	<del>B</del>	C	A	<del>B</del>	C
Reference sample – Original composition												
<b>Weight ratio</b>	0:100											
<b>Point of addition</b>	–											
Negative control – No amine-based additives												
<b>Weight ratio</b>	0:0											
<b>Point of addition</b>	–											

### 3.2. Material production process

The prototypes were produced using Adsorbi's established lab-scale production procedure, an overview of which is presented in Figure 11. The procedure consists of three main parts: making of a liquid binder, granulation, and post processing. An aqueous liquid binder is produced where several additives are mixed in liquid form. The liquid binder is mixed with cellulose fibers in the granulation step, forming granules, which are subsequently dried and sieved to sort into different size fractions. The final product is in the form of hard granules distributed into four size fractions: > 2.8 mm; 2.8–1 mm; 1–0.63 mm; < 0.63 mm. Notably, the production procedure could not realistically be done under sterile conditions. Consequently, all materials must be considered contaminated.

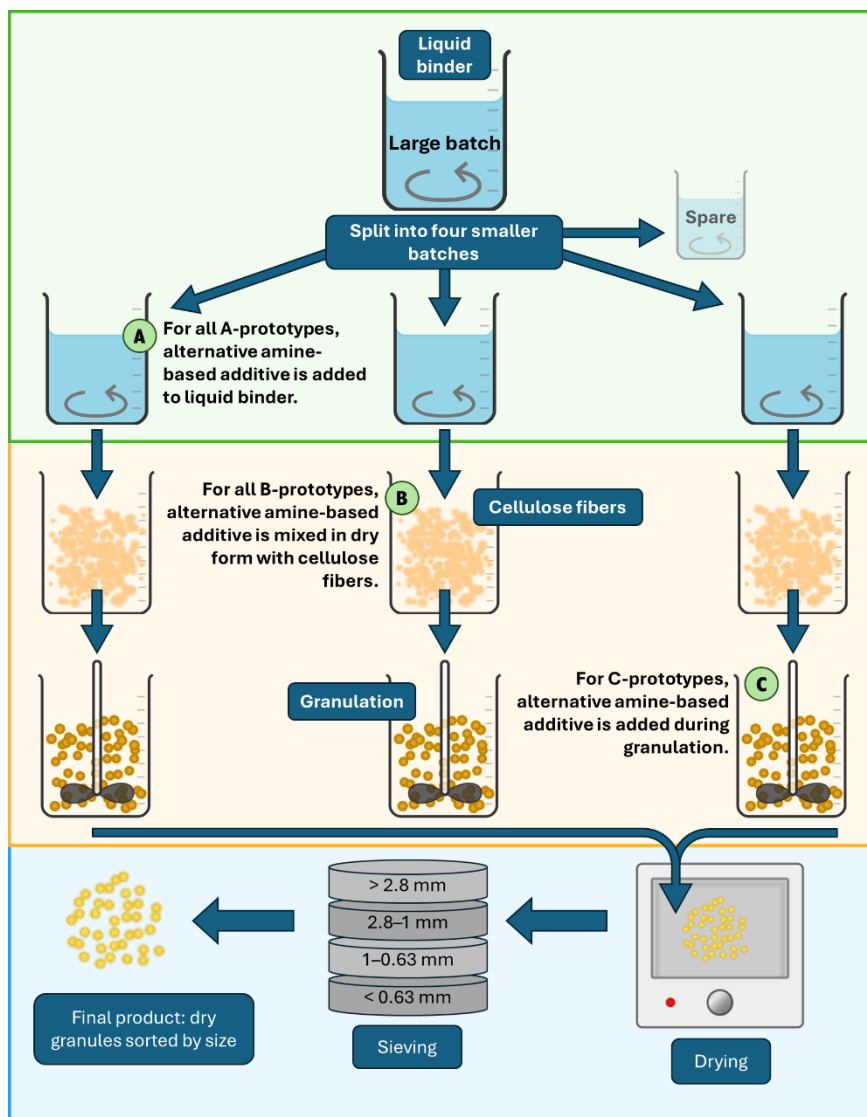


Figure 11. Production procedure of Adsorbi's material showing main production steps and the three different points of addition (A, B and C). The procedure was repeated for all weight ratios to the extent it was possible. The original amine-based additive was added identically each time, in accordance with the original procedure and same as in the reference samples.

Three distinct points of addition for incorporating the alternative additives into the production process were evaluated. These methods are outlined below and illustrated in Figure 11.

**Addition point A:** The alternative additive was mixed with water and added to the liquid binder, ensuring initial dispersion in a liquid phase.

**Addition point B:** The alternative additive was combined with cellulose fibers in dry form prior to granulation, simulating a dry-blending approach.

**Addition point C:** The alternative additive was mixed with a small amount of water, then directly introduced during the granulation process, enabling incorporation at a later stage.

For efficient production, a large batch of liquid binder was produced for each weight ratio of each alternative additive, as shown in Figure 11. The large batch was split into four parts which were further processed separately: the first was made to produce adsorbents using addition point A, the second using addition point B, and the third using addition point C, hence yielding three prototypes from each large batch. The fourth part was kept as a spare and, if not needed, discarded. The reference sample,

although having no variations in points of addition, was made to mimic this production procedure, resulting in identical triplicates.

As the alternative additives had varying properties their respective incorporation differed. Some prototypes could not be produced due to material compatibility issues: Chitosan and the original additives did not mix well in aqueous phase despite attempts to modify conditions such as pH and temperature. Similarly, Y-amine, being in liquid form, could not be mixed in dry form. All non-feasible prototypes are indicated in Table 1.

### 3.3. Materials

All alternative additives – chitosan (YC58325, water soluble chitosan, CAS No: 9012-76-4, Biosynth), graphitic nitride, gelatine (Gelatine Restoration 1, CAS No: 9000-70-8, Kremer pigmente), and Y-amine (Triameen, Y12D-30, CAS No: 2372-82-9) – were used as received or diluted with water prior to addition.

The amine-based additives are presented in Table 2. As outlined in Table 1, prototypes were made with varying weight ratios of alternative to original amine-based additives (100:0, 75:25, 50:50, 25:75) in addition to a reference sample containing only original amine-based additive (0:100) and a negative control containing neither (0:0). Hence, Table 2 presents the various amounts required for the different weight ratios. Notably, the production process involved an initial large batch of liquid binder, subsequently split into four parts, as visualized in Figure 11. Hence, the amounts detailed in Table 2 also distinguish between additions made before and after the splitting of the initial large batch. For clarity, the final compositions in the resulting material variations are included as well.

*Table 2. The amounts of alternative and original amine-based additives added, with a distinction between additions made before and after the large batch was split into four parts. Additionally, the different amounts needed for each prototype weight ratio (alternative:original) are included. For clarity, the final composition for each prototype's weight ratio and the negative control are also included.*

	Amounts added before splitting of large batch, for the weight ratios 100:0, 75:25, 50:50, 25:75, and 0:100	Amounts added after splitting, for the weight ratios 100:0, 75:25, 50:50, 25:75, and 0:100	Final composition (alternative:original) [g]				
			100:0	75:25	50:50	25:75	0:0
<b>Original additive [g]</b>	0; 2.5; 5.0; 7.5; 10	–	0	0.625	1.25	1.875	0
<b>Alternative additive [g]</b>	–	2.5; 1.875; 1.25; 0.625; 0	2.5	1.875	1.25	0.625	0

Apart from the amine-based additive, the final material composition was consistent across all adsorbents produced. The detailed final composition is presented in Table 3.

*Table 3. The final composition, which is identical across all material variations, expressed as weight percent.*

	Final composition [wt%]
<b>Water</b>	33.6
<b>Additive A</b>	5.2
<b>Carrier particle</b>	17.2
<b>Additive B</b>	18.7
<b>Cellulose fibers</b>	22.4

### 3.4. Material characterization

The size distribution and bulk density were measured and calculated to compare prototypes with the reference sample. This provides indications of whether the new compositions affect these properties and characteristics, which could have consequences for future production and uses. The 2.8–1 mm size fraction was selected for subsequent characterization.

#### 3.4.1. Size distribution and bulk density

The size distribution was measured by weighing all size fractions separately after sieving, calculating the total mass and the weight percentage of each size fraction.

To measure the bulk density of the adsorbents, a 10 ml graduated cylinder was filled with adsorbent to simultaneously assess both weight and volume. Figure 12 illustrates the setup and the procedure was repeated three times to ensure consistency. The bulk density (g/ml) was calculated by dividing the weight measured (g) by the volume measured (ml) and an average was calculated using the three repeats.

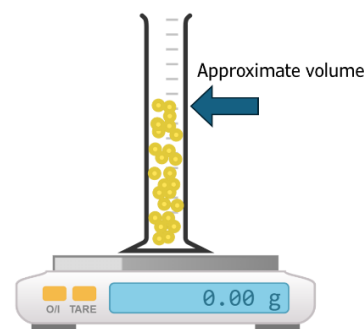


Figure 12. Method for measuring volume and weight for calculation of apparent density of the adsorbent granules.

### 3.5. Adsorption performance evaluation – gravimetric studies

A gravimetric study is a method used to quantify the amount of adsorbate adsorbed in a material, providing insight into both the kinetics of adsorption and the maximum adsorption capacity. The maximum adsorption capacity is measured in mass of adsorbate per mass of adsorbent at the material's saturation point ( $\frac{g_{\text{adsorbate}}}{g_{\text{adsorbent}}}$ ) [45, 16]. To evaluate uptake of both a VOC ( $\frac{g_{\text{pollutant}}}{g_{\text{adsorbent}}}$ ) and moisture ( $\frac{g_{\text{moisture}}}{g_{\text{adsorbent}}}$ ), two gravimetric studies were performed. The 2.8–1 mm size fraction was selected for evaluation and due to time restraints only one repeat of each gravimetric study was performed.

#### 3.5.1. VOC uptake

To evaluate the material's pollution uptake, a known weight of the adsorbent was exposed to a VOC pollutant – acetaldehyde – and the mass increase of the material was measured at various time points. This process provides insights into both the adsorption kinetics and the material's adsorption capacity. All prototypes (see Table 1), the reference sample, and the alternative amine-based additives in their raw form (excluding Y-amine as it is a liquid) were evaluated.

Between 0.1–0.15 g of adsorbents or raw alternative amine-based additive were placed in 4 ml glass bottles inside a desiccator at room temperature. The bottles were positioned alongside an open flask containing the VOC acetaldehyde. When necessary, more acetaldehyde was added to the flask to maintain a consistent exposure concentration. The samples were removed for weighing at specific time intervals: 5 min, 1 h, 24 h and then daily, as feasible. Due to operational constraints, such as weekends, the measurements were occasionally paused. During pauses, the acetaldehyde flask was removed from the desiccator and then returned as the test resumed. Prior to and after all pauses, the weight of each sample was recorded. The experimental setup for this procedure is illustrated in Figure 13.

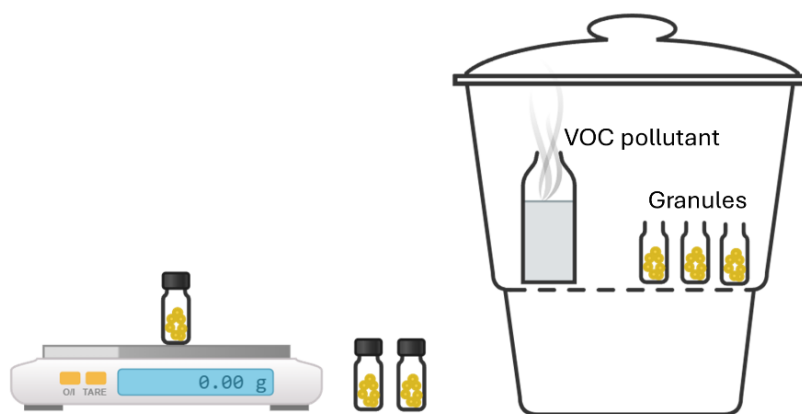


Figure 13. Setup for gravimetric study: samples of adsorbents and the VOC pollutant acetaldehyde in a desiccator and weighing of samples. A similar setup was used for moisture uptake as well.

When “sweating” on the adsorbent surface appeared, the sample was considered saturated, and the test stopped. If condensation was observed at the bottom of the vial with the tested adsorbents, the sample was considered oversaturated. The maximum adsorption capacity was calculated using Equation (1) at the saturation point.

$$M_{uptake} = \frac{m_{f+s+voc} - m_{f+s}}{m_{f+s} - m_f} = \frac{m_{voc}}{m_s} \left[ \frac{g}{g} \right] \quad (1)$$

Where  $m_f$  is the weight of the flask,  $m_{f+s}$  the weight of flask and sample, and  $m_{f+s+voc}$  is the weight of the flask, sample and adsorbed VOC as measured throughout the test. Subtraction gives the weight of adsorbed pollutant as  $m_{voc}$  and weight of sample as  $m_s$ . The resulting  $M_{uptake}$  is the uptake of VOC per mass of adsorbent ( $g_{pollutant}/g_{adsorbent}$ ).

As oversaturated adsorbents were beyond their maximum adsorption capacity, their final weight was not included in subsequent evaluations. Weights recorded after pauses caused significant noise in the data and were consequently removed. The remaining datapoints were plotted to show a weight increase over time. Notably, the over-saturated adsorbents require further evaluation to obtain the right saturation point and for more reliable results the gravimetric study should be performed with at least triplicates for each developed prototype. However, this was not done due to the limited time and scope of the project.

### 3.5.2. Moisture uptake

A moisture adsorption assessment was conducted to evaluate the material’s response to humidity. The procedure followed the setup detailed in Figure 13, substituting the VOC acetaldehyde with establishing an environment with 55% relative humidity within the desiccator, maintained at room temperature. Due to the slower nature of moisture adsorption compared to that of pollutants, measurements were taken less frequently and over an extended period of time (first once a day, then once a week and lastly after several weeks). The data was processed using Equation 1, replacing VOC with moisture ( $g_{moisture}/g_{adsorbent}$ ). No pauses were made and all data points were used in subsequent analyses.

## 3.6. Antimicrobial evaluation

Antimicrobial susceptibility testing is a standard laboratory procedure typically used to assess a pathogen’s susceptibility to different antibiotics. Common methods include determination of the minimum inhibitory concentration (MIC) such as broth dilution and disk diffusion assays [46].

Notably, this assessment will focus on the reverse relationship – evaluating the antimicrobial properties of different materials. The same procedures can effectively be applied for both purposes.

In this study, antimicrobial properties were evaluated using a broth dilution and disk diffusion bioassay. Broth dilution bioassay involves growing a known concentration of bacteria in multiple wells, each containing an increasing concentration of the antimicrobial agent being evaluated. The observed difference in bacterial growth with increasing agent concentration indicates the MIC, which serves as a standard measurement of the agent's antimicrobial properties [47]. The disk diffusion bioassay involves inoculating an agar plate with bacteria, placing a small amount of the agent on the surface and incubating to let the bacteria grow in contact with it. If an area around the material shows signs of inhibited growth, the diameter of this zone gives an indication of the material's antimicrobial properties [48].

When evaluating antibacterial properties, a suitable bacterial strain should be selected as a standard, as it is assumed to represent the behavior of other bacteria with similar characteristics, primarily based on Gram-positive or Gram-negative classifications [46]. Here, the bacteria used in both assays was *Staphylococcus epidermidis*, a gram-positive bacteria occurring naturally on human skin. It is classified as RG-1 and BSL-1, the lowest categories of risk groups and biosafety levels, meaning it is non-pathogenic in healthy adults [49].

A total of two broth dilution assays – one evaluating the adsorbents and the other assessing their individual components – along with one disk diffusion assay, were conducted. The modified protocols for the broth dilution assay involving the adsorbent prototypes and the disk diffusion assay are provided in Appendix A. The modified protocol for the broth dilution assay evaluating the individual components of the adsorbents is included in Appendix B. The adsorbents evaluated in all assays included the reference sample, the negative control, and prototypes with the weight ratio 100:0, to assess the effect of the tested alternative additives on microbial growth independently of the original additive. The 2.8–1 mm size fraction was again selected. Furthermore, addition point A was chosen due to its apparently most homogeneous adsorbent granules, as determined from visual observations.

### 3.6.1. Minimum inhibitory concentration (MIC) determination

Measuring MIC using a broth dilution assay is a standard procedure and the protocol *Agar and broth dilution methods to determine the minimal inhibitory concentration (MIC) of antimicrobial substances* by Irith Wiegand, Kai Hilpert and Robert E.W Hancock was used as a reference [50]. However, as this protocol is meant mainly for liquid penicillin and not for solid material, adjustments were necessary. Additionally, it should be noted that no adsorbents or components tested could be considered sterile, reducing the reliability of the results.

The first assay included the adsorbents: the reference sample, prototypes, and the negative control. A series with increasing amounts of adsorbents was created using cell culture plates of 12 wells. Each concentration series consisted of 0.4 g; 0.2 g; 0.1 g; 0.05 g; 0.025 g of adsorbents. Additionally, a growth control (GC) and a sterility control (SC) were added to each plate, as indicated in the original protocol. Bacterial media and growth media were added to all wells and after an overnight incubation the optical density (OD) was measured. As OD measures turbidity, it is a standard method to evaluate bacterial growth, although it inevitably includes dead bacteria, debris and potential other turbid components.

A second assay was motivated by unexpected results in the first. The wells containing prototypes made with Y-amine exhibited unexpected growth, prompting a repeat of the assay. The repeat was identical to the initial assay, except for an addition of a lower concentration of 0.0125 g, extending the concentration series. Additionally, an unexpected lack of growth in the negative control prompted testing of the components in the adsorbents individually.

For the assessment of the individual components, it was desired to assess the same amounts as had been present in each well in the initial test. This was complicated by the adsorbents drying in the production process and consequently, a conversion had to be made from dry weight to wet weight for all components initially containing water. The conversion included (i) determining the dry fraction of each component present in the adsorbents, (ii) when necessary, converting this dry weight to wet weight, (iii) repeating for each weight in the concentration series. The resulting weights subsequently evaluated are detailed in Appendix B. Notably, this necessitated testing the components in their raw form with no treatments, rather than as a part of a complex matrix and following a heat treatment.

Assessing the components separately required additional changes to the original protocol. With some of the components being liquids, this came with the addition of a dilution series. The cellulose fibers tested filled the wells, turning the content turbid and viscous and making OD measurements difficult. Measuring growth in the wells was not feasible, but investigations were made to demonstrate if live bacteria were present. A small amount of liquid was extracted from the wells after incubation, placed in fresh culture media, and incubated again for 4 hours. OD measurements from these incubated samples were used to indicate if live bacteria were present in the wells containing cellulose fibers.

Notably, two of the components (additive A and the carrier particle) are on the nanoscale, making OD measurements to estimate bacterial growth less dependable. Pan, Zhang, He, Katagori, and Chen (2014) have studied the effects of nanoparticles in concentrations of 0.1–1.0 mg/ml on quantification of both gram positive and gram negative bacteria. Their conclusion was that the nanoparticles did interfere and made the quantification less dependable [51]. This is necessarily taken into account when the results are interpreted.

### 3.6.2. Disk diffusion

A standard disk diffusion protocol, *Kirby-Bauer Disk Diffusion Susceptibility Test Protocol* by Jan Hudzicki [52] was utilized and adjusted. The fully modified protocol is included in Appendix A.

Three agar plates were prepared and streaked with the bacteria *S. epidermidis*. Six adsorbent granules were put on each plate: the reference sample, a negative control, and the prototypes. Once on the agar plate, the granules were wetted with a drop of growth media in order to attach them and increase contact with the surface. The plates were kept at 37 °C overnight to induce growth. The diameter of the zones around the adsorbents exhibiting inhibited growth were measured using a ruler and rounded up to the nearest millimeter, as indicated in the protocol.

## 4. Results and discussion

This section presents the results from the characterization, the performance evaluation, and the microbial assessment of the adsorbent prototypes developed within the project. The characterization focuses on both (i) the composition of amine-based additives and (ii) the different methods of incorporation. The performance evaluations and assessment of microbial properties focus mainly on the composition, as the methods of incorporation were not observed to have any substantial influence.

### 4.1. Observations

As the alternative additives had varying properties, their respective incorporation and observable influence on the production process differed. Noteworthy observations made during the production process were as follows. For addition points A, B, and C see Figure 11.

#### 4.1.1. Production

- For chitosan, a water-soluble form was used, enabling the otherwise poorly soluble chitosan to be added at point A and C. As its original form was a fine powder, addition to point B was straightforward. Notably, the dissolved chitosan had an exceedingly high viscosity, especially at higher concentrations.
- Graphitic nitride came in the form of a fine powder, making addition to point B straightforward. When mixed with water, dispersed with continuous mixing. Mixing was done immediately before the addition to points A and C.
- The gelatine came as rough, small, grains which, after heating, dissolved in both liquid binder at point A and in water at point C. Notably, the dissolved gelatine had a high viscosity. For point B, the rough grains were sheared to the extent it was possible, creating finer grains. Still, the sheared gelatine was rougher than the chitosan and graphitic nitride powders.
- Y-amine came in liquid form and was added as is to point A. Point B was skipped and for point C it was diluted in water similar to the other components to ensure a similar production process and a consistent final water content across all samples. However, as it added to the total liquid content, the volume of liquid binder was larger for all samples containing Y-amine.

#### 4.1.2. Gravimetric study with VOC

During the gravimetric study using the VOC acetaldehyde, the adsorbents went through the expected color change. As the reference samples turned a dark brown, most prototypes reached a somewhat lighter, brown color. Importantly, the adsorbents made using points of addition A presented an even color throughout. However, the adsorbents made using points of addition B and C exhibited dappled coloring, suggesting a less homogeneous composition. Assuming the amine-based additive is responsible for the color change, this suggests the alternative additives were poorly distributed and that points of addition B and C are not suitable for producing homogeneous adsorbents. The different color changes seen in adsorbents made using addition point A and B are shown in Figure 14, with fresh adsorbents for comparison.



Figure 14. Granules discolored from VOC adsorption. Evenly colored granules made using point of addition A (to the left) compared to dappled granules made using point of addition B (middle). Fresh granules (to the right) for comparison.

## 4.2. Size fraction distribution

In this section, the influence on size arising from both material composition and points of addition are discussed. All adsorbents were separated by size into four fractions ( $> 2.8$ ;  $2.8-1$ ;  $1-0.63$ ;  $< 0.63$  mm), as illustrated in Figure 11. The original adsorbent composition and procedure was optimized to maximize the  $2.8-1$  mm size fraction. However, with the addition of new compounds and strategies of incorporation, the size fraction distribution changed.

### 4.2.1. The reference sample

The size distribution of the reference sample, including all three replicates, is presented in Figure 15. This composition and production procedure is optimized to maximize the  $2.8-1$  mm size fraction. This can be seen in the size distribution for the reference samples presented in Figure 15, where this size fraction is dominating. The variation among the repeats is likely due to human error and inherent variations in granulation and production. Multiple addition steps can lead to composition inconsistencies, and some dry components are lost in the form of dust during granulation, resulting in differences in the final adsorbents. The three repeats were identical and designed to replicate the production procedure used for prototypes, as explained in Figure 11.

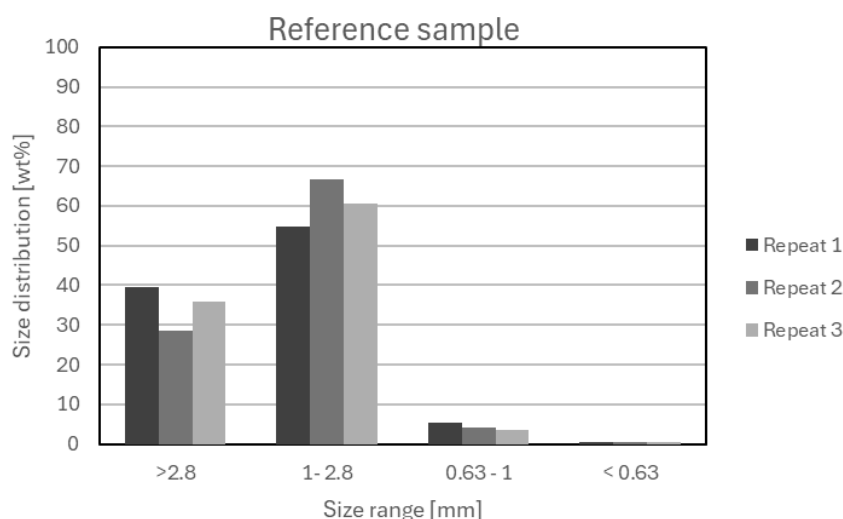


Figure 15. The size fraction distribution of the reference sample, separated by fraction sizes ( $> 2.8$ ;  $2.8-1$ ;  $1-0.63$ ;  $< 0.63$  mm) and expressed in weight percent (wt%). All three repeats are included.

### 4.2.2. The prototypes

In this section, the influence on the size distribution arising from the varying amine-based additives and the different points of addition are discussed in detail. The size distributions of all prototypes are presented in Figure 16, structured by alternative amine-based additives and by points of addition, highlighting their respective influence. For details on their compositions and production see Table 1 and Figure 11.

## Size fraction distributions for additive and addition points

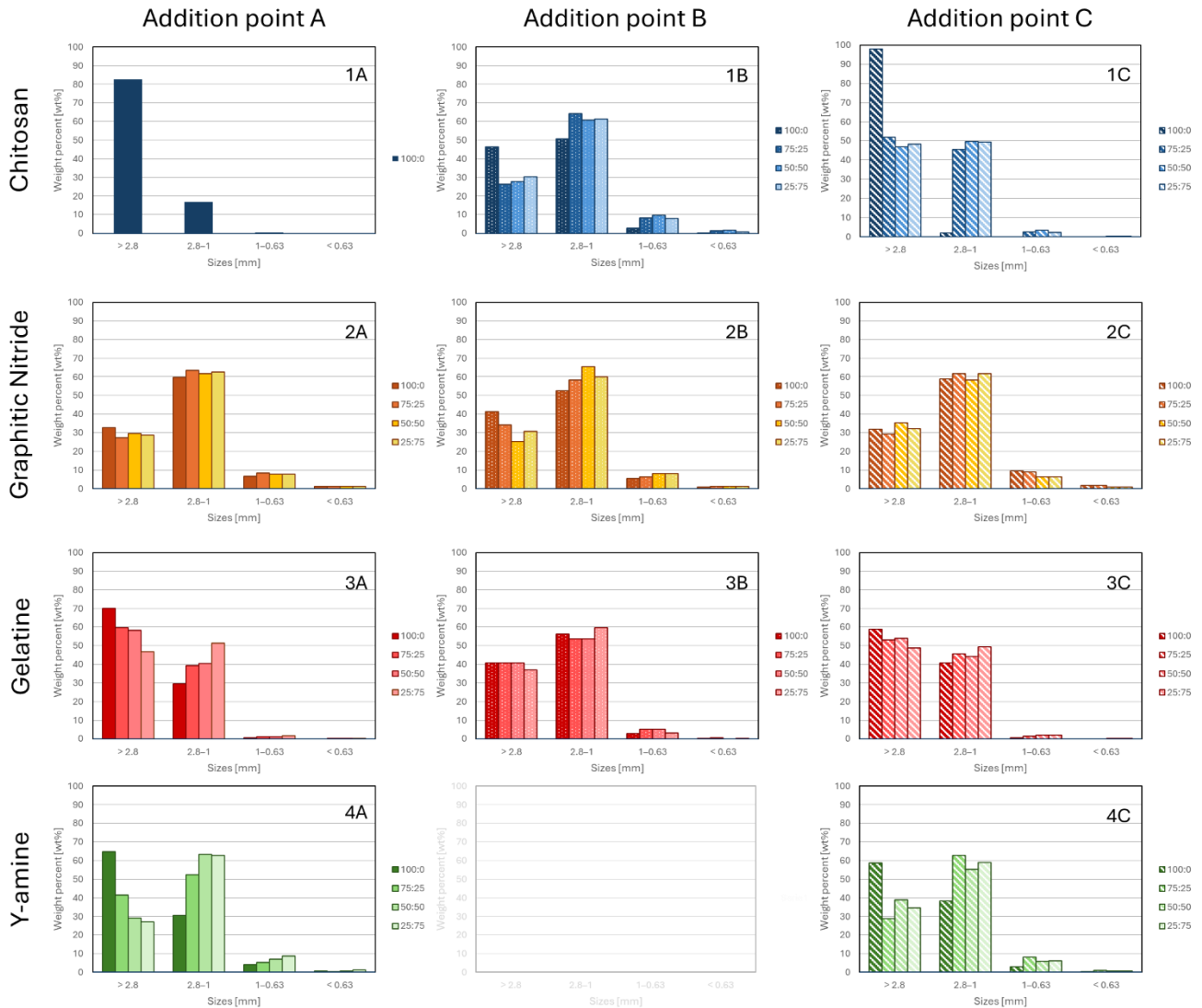


Figure 16. Size fraction distribution for all prototypes, structured by amine-based additives vertically and by addition points horizontally. Numbering of graphs indicate additive used (1 chitosan, 2 graphitic nitride, 3 gelatine and 4 Y-amine). Ratios of additives are indicated in legends as (alternative:original) and with distinct color shading, darker shades indicating more alternative and vice versa. Points of addition are indicated with their corresponding letter and a distinct pattern (uniform color for A, spotted for B, and dashed for C). Note that there are no error bars as the measurements were done without repeats.

### 4.2.2.1. Addition point A

In column A (see 1-4A in Figure 16), all prototypes produced using addition point A – adding the tested alternative additives to the aqueous binder – are presented. Notably, 1A in Figure 16 has only the 100:0 ratio as it was not feasible to mix chitosan with the original additive.

As the alternative additives were dissolved or mixed in the liquid binder, varying viscosities were observed, a factor known to influence particle size in granulation. The highest viscosity was seen with chitosan, accounting for markedly large amounts of adsorbents in the largest size fraction (> 2.8 mm) in 1A in Figure 16.

A marked increase in viscosity was also observed with gelatine, accounting for the increase seen in the largest size fraction (> 2.8 mm) seen in the 100:0 ratio prototype in 3A in Figure 16. As the ratio of gelatine decreased and was replaced by the original material composition, the effect on the viscosity became less apparent. This is also reflected in 3A in Figure 16, as the > 2.8 size fraction decreases and is replaced by the 2.8–1 mm size fraction. The 25:75 prototype presents a size distribution similar to that of the reference sample.

Graphitic nitride was dispersed in the liquid binder and had no visible effect on the viscosity compared to the reference sample, which is consistent with the fraction distribution in 2A in Figure 16, which bears strong resemblance to the distribution of the reference sample presented in Figure 15.

The Y-amine was observed to slightly decrease the viscosity of the liquid binder, which is inconsistent with the substantial portion in the largest size fraction (> 2.8 mm) seen in the 100:0 ratio prototype in 4A in Figure 16. However, Y-amine was the only amine-based additive tested in liquid form, increasing the total volume of the liquid binder compared to the other prototypes (unlike water content, which is consistent across all samples as detailed in Table 3). This presents a plausible explanation for the larger adsorbents, as particle size in granulation is also increased by a larger relative amount of liquid binder to solid fraction. The size fraction distribution moves towards smaller adsorbents – dominated by the 2.8–1 mm fraction – when the tested additive is increasingly replaced by the original material composition.

The observed size increases among the prototypes suggest an increase in viscosity or amount of liquid binder substantially influence granulation and result in larger adsorbents. The 25:75 ratio samples all display a size distribution comparable to the reference sample, suggesting lower levels of any alternative additives do not significantly affect the size fraction distribution, or that potential effects are overshadowed by the dominant influence of the original additive.

#### 4.2.2.2. Addition point B

In column B (1-3B in Figure 16), all prototypes produced using addition point B – mixing the tested alternative additives in dry form with cellulose fibers prior to granulation – are presented. Notably, no prototypes made with Y-amine and addition point B exist, as Y-amine is a liquid.

As the tested amine-based additives were added in dry form, it had no effect on the viscosity or amount of the liquid binder but contributed to the dry content. However, compared to the consistent amount of cellulose fibers used for the granulations (see Table 2 and 3), this increase was minor. Consequently, the size fraction distribution across the column (1-3B) is similar to that of the reference sample presented in Figure 15.

#### 4.2.2.3. Addition point C

In column C (1-4C in Figure 16), all prototypes produced using addition point C – adding the tested alternative additive during the granulation process – are presented. The additives were mixed with a small amount of water prior to addition, with adjustments made to preserve consistent final water content across all prototypes.

In 1C in Figure 16, the 100:0 ratio prototype exhibits exceptionally large adsorbents, with nearly all distributed within the > 2.8 mm size fraction. Given that chitosan was dissolved in a limited amount of water prior to its addition, the resulting increase in viscosity was substantial and visibly more pronounced compared to when it was added to the liquid binder (see 1A in Figure 16). The predominance of large adsorbents aligns with the marked viscosity increase of the liquid binder.

As the amount of chitosan added was reduced, substituted by the original additive, the effect of the viscosity increase was diminished, explaining the 75:25, 50:50, and 25:75 ratio prototypes exhibiting

markedly smaller adsorbents in comparison. Notably, the 25:75 prototype still presented a larger portion in the > 2.8 mm size fraction than most other 25:75 prototypes, suggesting that the influence is not entirely negated. Oddly, the 75:25, 50:50, and 25:75 prototypes present similar size distributions, potentially owing to the inherent variability of granulation.

Although gelatine also resulted in a viscosity increase, its effect was markedly less than that of chitosan and not drastically different from when it was added to the liquid binder (see 3A in Figure 16). Although the 50:50 prototype slightly diverges, the size distribution presented in 3C in Figure 16 otherwise closely resembles that in 3A, with higher amounts of gelatine producing larger adsorbents and vice versa.

Graphitic nitride, recurrently, was not observed to influence the viscosity and consequently 2C in Figure 16 exhibits a size distribution similar to that of the reference sample in Figure 15.

For consistency, the liquid Y-amine was mixed with the same amount of water as the other prototypes. The addition of Y-amine recurrently increases the amount of liquid binder added, in theory resulting in larger adsorbents. However, as seen in 4C, this was only observed in the 100:0 prototype, with the other ratios presenting a larger variability and no consistent size decrease.

The size distributions can partly be explained similarly to that of addition point A, considering viscosity and the total amount of liquid binder used in granulation. However, there is less consistency in the trends, particularly in 4C. Importantly, addition point C involved an extra addition of liquid binder in the granulation process, potentially introducing more inherent variability in the granulation step, which may explain the observed inconsistencies.

#### 4.2.2.4. Chitosan

In row 1 (1A, B and C in Figure 16), all prototypes containing chitosan are presented. The size distributions in 1A and 1C – where chitosan was dissolved in the aqueous liquid binder or water prior to addition – show significantly larger adsorbents compared to the reference sample while 1B – where chitosan was added in dry form – show a size distribution similar to the reference sample. This is hypothesized to be due to the increase in viscosity of dissolved chitosan.

Chitosan is generally poorly water soluble and its high molecular weight and polymeric structure (see Figure 6) causes the solution to be highly viscous, especially at higher concentrations. Additionally, the abundant hydroxyl groups interact with and bind water molecules, further increasing viscosity.

The increased viscosity of dissolved chitosan, caused by its high molecular weight, polymeric structure, and hydroxyl groups result in larger adsorbents (1A and 1C in Figure 16) compared to both the reference sample and the adsorbents where chitosan was added in dry form (1B in Figure 16).

#### 4.2.2.5. Graphitic nitride

In row 2 (2A, B and C in Figure 16), all prototypes with graphitic nitride as the functional additive are presented, all of which markedly resemble the reference sample. This similarity is likely due to graphitic nitride not influencing either the viscosity when dissolved or the liquid content in the granulation.

Graphitic nitride is a flat molecule arranged in layered sheets (see Figure 7). Due to the lack of rotating bonds and the structure's high stability, it is generally insoluble in water, although it can interact with water molecules through its polar groups. Consequently, the graphitic nitride dispersed but did not dissolve and caused no noticeable change in viscosity, explaining why all addition points presented equivalent size distributions.

Assuming graphitic nitride did not significantly influence the size distribution, the influence from the varying amounts of alternative additive should be dominating. However, there is not much difference across the ratios of alternative to original additive, suggesting either that original additive and graphitic nitride have similar influences, or that the influence of both is negligible compared to that of the other components in the adsorbents (see Table 3).

The size distributions are remarkably similar across both addition points and the ratios of graphitic nitride to original additive, indicating graphitic nitride does not significantly influence the size distribution. This is likely due to the lack of changes in viscosity, or that the potential effects of both original additive and graphitic nitride are overshadowed by dominating influence from other components in the material.

#### 4.2.2.6. Gelatine

In row 3 (3A, B and C in Figure 16), all prototypes with gelatine used as the amine-based additive are presented. The prototypes in 3A and 3C in Figure 16 – where gelatine was dissolved in the aqueous liquid binder or water – present larger adsorbents while 3B – where gelatine was added in dry form – presents a size distribution similar to the reference sample.

Similar to chitosan, gelatine has a high molecular weight, a polymeric structure, and several functional groups that can interact with water (see Figure 8), causing viscosity increase in aqueous solutions.

The increased viscosity of dissolved gelatine, caused by its high molecular weight, polymeric structure, and polar groups interacting with water, result in larger adsorbents (3A and 3C in Figure 16) compared to the reference sample and the adsorbents where gelatine was not dissolved in aqueous media (3B in Figure 16).

#### 4.2.2.7. Y-amine

In row 4 (4A and 4C in Figure 16), all prototypes with Y-amine as the alternative additive are presented. The prototypes present varied size distributions, with higher amounts of Y-amine resulting in larger adsorbents and lower amounts resulting in a distribution similar to the reference sample.

Y-amine (see Figure 9) is a small molecule with two amino groups, causing it to be in liquid form at standard conditions and making it readily water soluble. Consequently, it did not increase the viscosity of the liquid binder or water when it was dissolved, which should result in smaller adsorbents.

However, as it is a liquid, the total amount of liquid binder was increased, resulting in increased adsorbent granule sizes. Therefore, the prototypes containing only Y-amine (100:0) in both 4A and 4C present larger adsorbents. As the amount of Y-amine decreases, so does the influence on size distribution, resulting in smaller adsorbents that are more similar to the reference sample.

### 4.3. Pollution uptake

This section presents the results from the gravimetric studies using the VOC acetaldehyde for the adsorbent prototypes, the reference sample and the alternative amine-based additives in their raw form, discussing their performance in terms of pollution uptake. The gravimetric study involved exposure to acetaldehyde for an extended time period (the setup is shown in Figure 13). The weight increases were measured recurrently throughout, and the adsorption performance was evaluated as weight of adsorbed VOC by weight of the material sample ( $g_{\text{pollutant}}/g_{\text{adsorbent}}$ , as detailed in Equation 1) per hour. This provides information on both adsorption kinetics and maximum adsorption capacity.

### 4.3.1. Amine-based additives – raw vs incorporated in adsorbents

This section discusses potential inherent adsorption capacity of the amine-based additives in their raw form and the synergistic effects of prototype development. To evaluate the effects of incorporating the amine-based additives into the adsorbents, the pollution uptake of the raw amine-based additives are compared to the same additives incorporated into adsorbents, as presented in Figure 17.

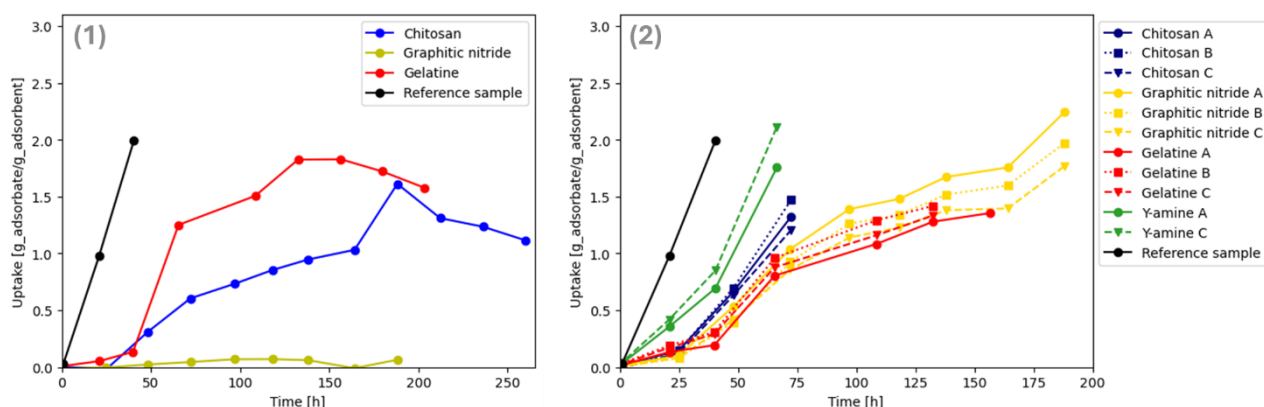


Figure 17. The results of the gravimetric study with a known VOC pollutant of (1) all prototypes with the composition 100:0 of amine-based additives and (2) the alternative additives chitosan, graphitic nitride and gelatine evaluated in their raw form. In (1) Y-amine is not included, as it was not tested due to it being in liquid form. In (2) the points of addition are indicated as A, B and C. Uptake is measured in pollutants captured by weight of sample ( $g_{\text{pollutant}}/g_{\text{adsorbent}}$ ) and presented per hour. Results from the reference sample granules are included for comparison in both inserts.

Presented above are the results from the gravimetric study of the tested alternative amine-based additives chitosan, graphitic nitride, and gelatine in their raw form (see 1 in Figure 17) and the results of all adsorbent prototypes with the 100:0 ratio (see 2 in Figure 17). The results from the reference sample are included for further comparison. The uptake of the raw additives indicates inherent adsorption abilities, while the uptake in the prototypes show the combined effects of the compound incorporated into the material matrix of the prototypes. Comparing these results facilitates an understanding of the extent functionality is added from incorporating the amine-based compounds into the cellulose-matrix of the prototypes. The incorporation should induce synergistic effects of combining physisorption and chemisorption.

As seen when comparing 1 to 2 in Figure 17, the difference between raw and incorporated additives is most apparent with graphitic nitride. This compound on its own displays little to no inherent adsorption capacity, while incorporation into adsorbents results in a substantial adsorption capacity, indicating the synergistic effects of combining physisorption and chemisorption. However, the same marked improvement is not observed when comparing raw and incorporated chitosan and gelatine. Both raw compounds display some inherent adsorption ability, although it is followed by a weight decrease, likely due to experimental errors. Adsorbents incorporating chitosan and gelatine also exhibit adsorption abilities, although no significant improvement compared to the raw compounds is observed. Consequently, no synergistic effects are observed, although a comparison is made difficult due to the weight decrease in 1 in Figure 17.

The synergistic effects of combining physisorption and chemisorption in the developed prototypes are apparent in the graphitic nitride prototypes, but not in the chitosan or gelatine prototypes. This may be due to experimental errors or variations from the weight decrease in 1 in Figure 17, or it might indicate that incorporating chitosan and gelatine into the adsorbent is a poor way to maximize their adsorption capacity.

### 4.3.2. Adsorption capacity

In this section, the effects of the amine-based additive compositions on adsorption capacity are discussed. The results from the gravimetric study with the VOC acetaldehyde for all prototypes are presented in Figure 18 – measured in  $g_{\text{pollutant}}/g_{\text{adsorbent}}$  – indicating the prototypes' maximum adsorption capacity measured in this experiment.

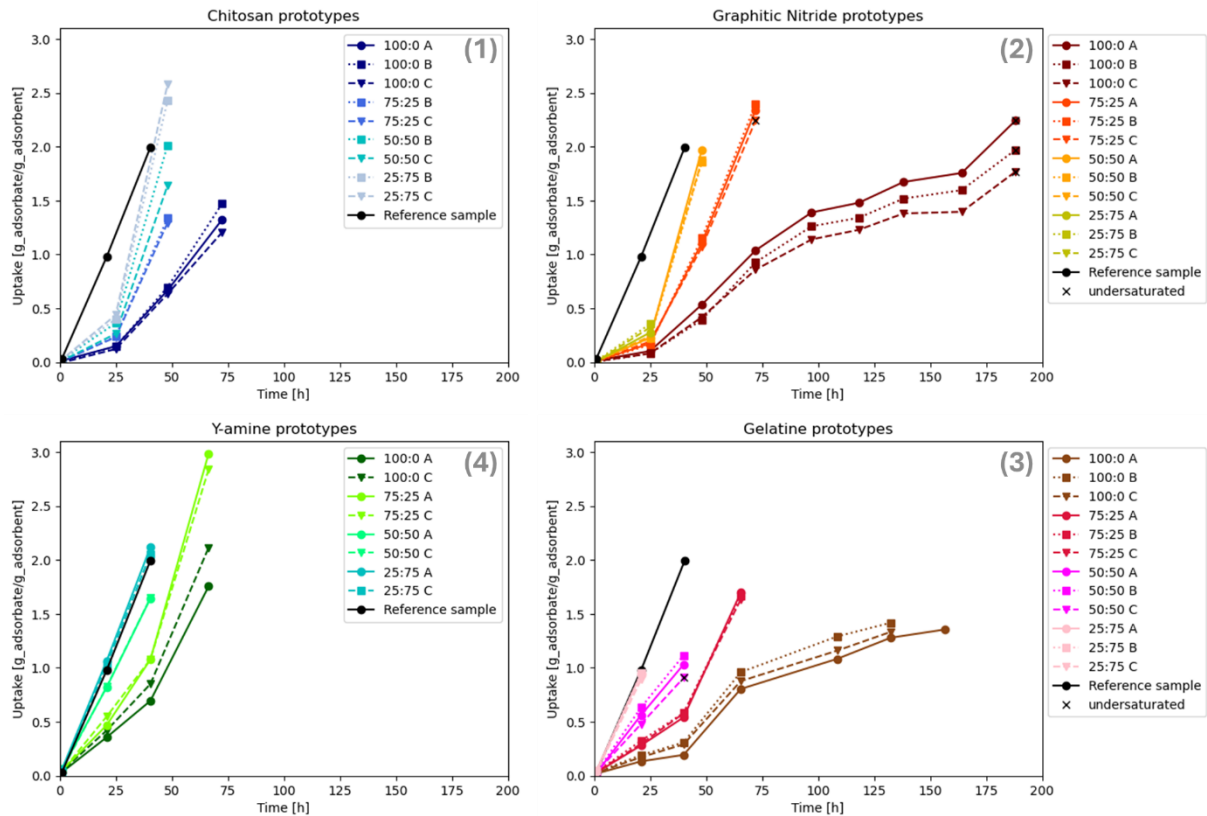


Figure 18. Results of the gravimetric study using the VOC acetaldehyde for all prototypes containing the tested alternative additives, including one of reference samples for comparison. Prototypes containing chitosan are presented in (1), graphitic nitride in (2), gelatine in (3), and Y-amine in (4). The ratio of alternative to original additive (alternative:original) is indicated in the legends along with points of addition A, B and C. The undersaturated samples are marked with a cross, indicating they may not have reached their maximum adsorption capacity. Adsorption is presented as the weight of pollutants captured to the weight of adsorbent ( $g_{\text{pollutant}}/g_{\text{adsorbent}}$ ).

In Figure 18, the results from the prototypes are included, with the results from the reference sample for comparison. Note that some may have been undersaturated, i.e. could still adsorb further, when the study ended and that the final weights of oversaturated samples were removed. The undersaturated samples are marked with a cross, indicating they may not have reached their maximum adsorption capacity.

The adsorption capacity measured for the reference sample presented above was just below 2.0  $g_{\text{pollutant}}/g_{\text{adsorbent}}$ , which is consistent with previous experiments with the material. In this experiment, the reference sample was exceeded by several of the prototypes, with the 75:25 ratio Y-amine prototype presenting the highest adsorption capacity at around 3  $g_{\text{pollutant}}/g_{\text{adsorbent}}$  (see 4 in Figure 18). However, as the 75:25 ratio diverges from the other Y-amine prototypes, this may be attributed to experimental error or inherent variation. Still, the Y-amine prototypes generally exhibit a high adsorption capacity, close to the reference. This is likely due to a combination of the high reactivity of the primary amines present in Y-amine (see Figure 9) and their incorporation into the adsorbent's porous matrix, making them readily accessible. Additionally, primary amines can cycle through reactions and bind more than one pollutant.

The 25:75 ratio chitosan prototypes present the second highest adsorption capacity in this experiment, at around  $2.5 \text{ g}_{\text{pollutant}}/\text{g}_{\text{adsorbent}}$  (see 1 in Figure 18). As this prototype is followed by the 50:50 ratio, chitosan seems to perform best in combination with the original additive, although all chitosan prototypes perform tolerably well. This uptake is attributed to the various functional groups (mainly primary amines and hydroxyl groups) present in chitosan (see Figure 6).

With the graphitic nitride prototypes there is great variation in the measured adsorption capacities (see 2 in Figure 18). While the 100:0, 75:25, and 50:50 ratio prototypes present considerable adsorption, the 25:75 ratio prototype presents the lowest adsorption capacity out of all prototypes. The poor performance of the 25:75 ratio prototype may be attributed to experimental errors. As graphitic nitride is also a larger molecule, it may aggregate and act to block pores and thereby decrease mass transport. The adsorption seen among the prototypes is attributed to mainly the primary amines and acid-base interactions of graphitic nitride (see Figure 7).

The gelatine prototypes also present great variations in the measured adsorption capacities (see 4 in Figure 18) and it is the only alternative additive where no prototype exceeds the reference sample. Although gelatine contains an abundance of reactive groups, it is a large molecule and steric hindrance of the reactive sites and fewer available primary amines may explain the poorer adsorption capacity measured (see Figure 8)

As seen in 2 and 3 in Figure 18, the graphitic nitride and gelatine prototypes both display variations in their final adsorption capacity, with the highest capacities in both prototypes exhibited by the 75:25 ratios, followed by the 100:0 ratios. Although no trend can be observed, it suggests that both gelatine and graphitic nitride have some adsorption properties.

Regarding the different methods of incorporating the additives, the different points of addition seems to have little effect on the maximum adsorption capacity across all prototypes. This is surprising considering the heterogeneity seen in the adsorbents produced using point of addition A and C (see Figure 14). The composition, instead, seems to have a greater influence. The heterogeneity of the adsorbent seems therefore to have little effect on adsorption capacity.

Looking at the 100:0 prototypes, both the Y-amine and graphitic nitride prototypes perform similar to the reference and some combination of original and alternative additives are shown to outperform the reference sample with all alternatives but gelatine. To summarize, this suggests all alternatives tested induce some functionalization of the adsorbent, although gelatine to the least extent. These adsorption properties are primarily attributed to the chemical activity from the functional groups previously discussed. However, there seems to be no discernable pattern relating the final adsorption capacities to composition and there is substantial variation, likely due to inconsistencies during production and from human errors. Additionally, the undersaturated samples may not have reached their maximum adsorption capacity.

### 4.3.3. Adsorption kinetics

In this section, the effects of the different amine-based additives on adsorption kinetics – the adsorption rate and saturation time – are discussed, using the results from the gravimetric study presented in Figure 18. As the adsorption is plotted over time, adsorption kinetics can be assessed from curve slopes and saturation timepoints.

Figure 18 shows that the steepness of the slopes follows the ratio of alternative to original additive across all graphs, with the 25:75 prototypes presenting the steepest curve, followed by the 50:50, the 75:25, and lastly the 100:0 ratio prototypes. The reference sample is generally quick to saturate compared to the prototypes and presents the steepest curve across all prototypes (with the exception of the 25:75 ratio Y-amine prototype which is slightly steeper, see 3 in Figure 18). As the ordering is

consistent for all tested alternative additives, this suggests the original adsorbent composition with original additives has a substantial impact on the kinetics of adsorption. This quicker adsorption rate can be attributed to the complexity and optimization of the original adsorbent composition.

Among the prototypes, those containing Y-amine consistently present steep curves (see 4 in Figure 18). In previously tested amine-based additives, it is known that primary amines are highly reactive and potentially rate limiting in the adsorption studied. This can explain the fast kinetics exhibited by the Y-amine prototypes, which contain an abundance of available primary amines (see Figure 9).

The chitosan prototypes also present steep curves and thus fast kinetics. Chitosan also contains primary amines (see Figure 6), again underscoring that this functional group is potentially rate determining for the adsorption studied. However, chitosan, like Y-amine, contains two primary amines, but the molecule itself is substantially larger, resulting in less primary amines present per gram of prototype. If only primary amines are rate limiting, this difference should be more noticeable. Unlike Y-amine though, chitosan contains several hydroxyl groups that can react or bind through hydrogen bonding. The substantial number of hydroxyl groups may increase the adsorption rate of the chitosan prototypes, resulting in only slightly slower kinetics compared to the reference sample and Y-amine prototypes.

The graphitic nitride and gelatine prototypes both generally exhibit flatter curves and thereby slower kinetics. The slower adsorption kinetics is particularly seen in the 100:0 prototypes, all of which saturate after 125 hours. For gelatine, there is a mixture of active groups including some primary amines, although much fewer than in the Y-amine and chitosan prototypes and with substantially more steric hindrance. Furthermore, the 2D nature of g-C<sub>3</sub>N<sub>4</sub> can limit the mass transport of the pollutant. There are other, less reactive functional groups such as carboxyl and hydroxyl groups (see Figure 8), potentially explaining the prolonged adsorption time. The number of primary amines in graphitic nitride depends on how broken up the structure is (see Figure 7). Other active sites include hydrogen bonding, Lewis base interactions and  $\pi$ - $\pi$  interactions, providing a range of binding sites, although not all as reactive as the primary amines, explaining the slower kinetics.

Depending on the material, physisorption can be dominating during the first hours of adsorption. Looking at the initial 25 hours in Figure 18, the reference sample and Y-amine prototypes seemingly present the quickest adsorption, followed by gelatine, chitosan, and lastly graphitic nitride. If it is assumed that the first 25 hours are dominated by physisorption, this provides information on the material's physical structure rather than its chemical properties. The presence of larger pores (macro- and mesopores) generally gives faster adsorption, while micropores fill slower. Thus, the results indicate that the Y-amine prototypes contain larger pores, similar to the reference sample. The gelatine and chitosan prototypes are slower and graphitic nitride significantly slower, indicating they generally contain smaller pores. A potential conclusion from the first 25 hours is that the original amine-based additive and the Y-amine increase adsorption kinetics by increasing pore sizes in the material, in addition to their chemical properties. More studies on the internal composition and apparent density of the adsorbents would be required to support this hypothesis.

Notably, the variation between the different addition points – A, B, and C – is again small, indicating the composition has a greater influence on adsorption than its production procedure, despite the visible differences seen in Figure 14.

The adsorption kinetics are largely attributed to the presence of active groups and their reactivity. The faster adsorption exhibited in the Y-amine prototypes is attributed to its available primary amines. Similarly, the fast adsorption exhibited by the chitosan prototypes is attributed to both primary amines and a substantial amount of hydroxyl groups. For the gelatine and graphitic nitride prototypes, their slower adsorption is explained by their abundant but less reactive functional groups. However, if the first 25 hours are dominated by physisorption, the initial adsorption rates can be attributed to pore

structure rather than chemical properties. The reference sample and Y-amine prototypes present the highest uptake rate in the first 25 hours, indicating that the reference sample and the Y-amine prototypes contain larger pores.

## 4.4. Density, additive composition, saturation time, and adsorption capacity

The adsorption properties exhibited by the adsorbents cannot exclusively be explained by their composition, as they are influenced by a complex interaction of factors. Different densities influence adsorption in terms of pore size and available surface area. Higher densities result in smaller pores, slowing adsorption rate, and a smaller available surface area results in a shorter saturation time and diminished adsorption capacity. Therefore, this section explores the interactions between bulk density, additive composition, saturation times, and the final pollution uptake to further evaluate and explain material characteristics and functionality.

Figure 19 presents bulk densities plotted to saturation timepoints for each addition point. The results indicate a negative correlation – a decreasing granular bulk density results in longer saturation times.

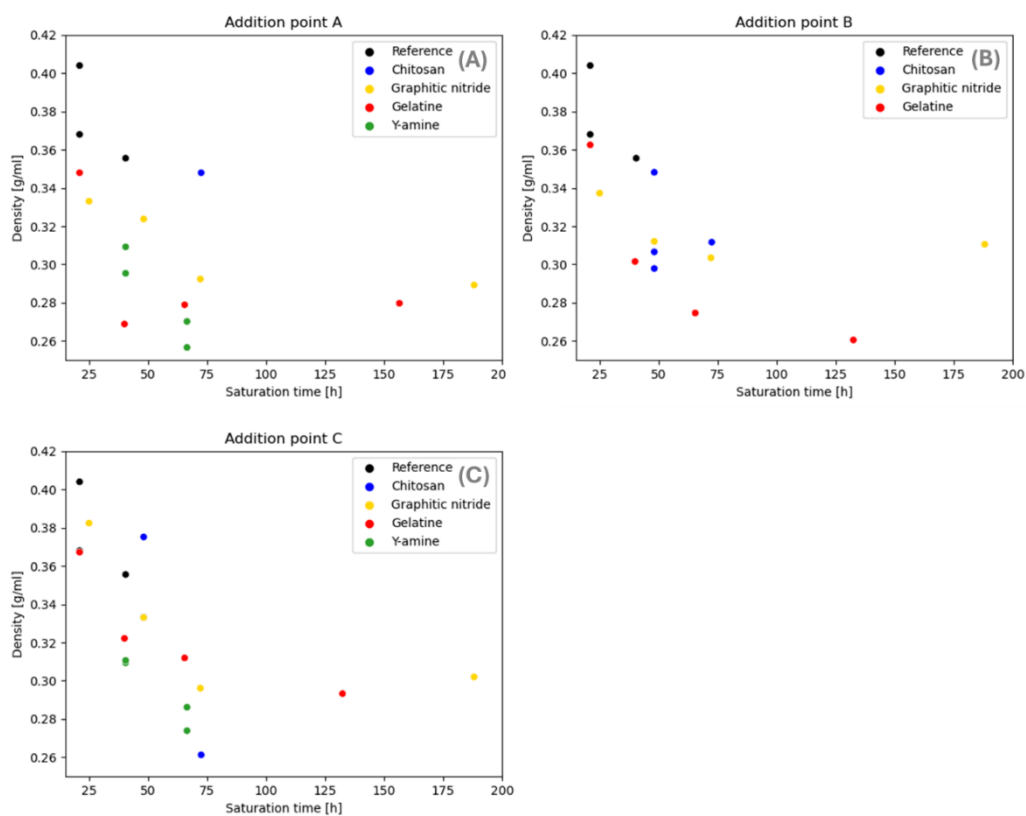


Figure 19. Density (g/ml) plotted to saturation time (h). All prototypes are presented, differentiated by addition points (indicated as A, B, and C). Reference samples are included in all graphs.

A higher bulk density suggests the internal voids in the adsorbents are smaller and the number of closed pores (see 5 in Figure 1) increases, limiting available surface area. In Figure 19, it is shown that higher densities correlate with shorter saturation times, possibly due to a decreased available surface area. Consequently, the influence from the alternative amine-based additives may be due both to changes in chemisorption capacity and changes in density.

To further examine the correlations, bulk density plotted to the amount of alternative amine-based additive is presented in Figure 20 and the amount of alternative amine-based additive plotted to saturation times are presented in Figure 21.

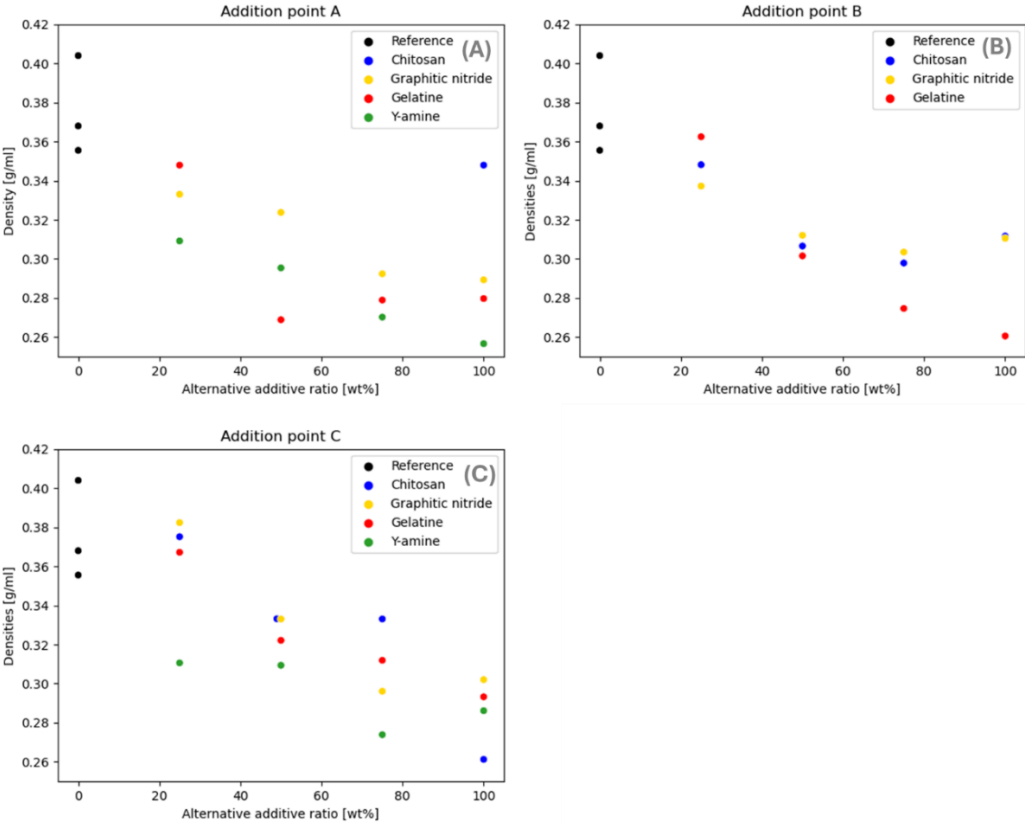


Figure 20. Density (g/ml) plotted to weight percent of alternative amine-based additives. All prototypes are presented, differentiated by addition points (indicated as A, B, and C). Reference samples are included in all graphs.

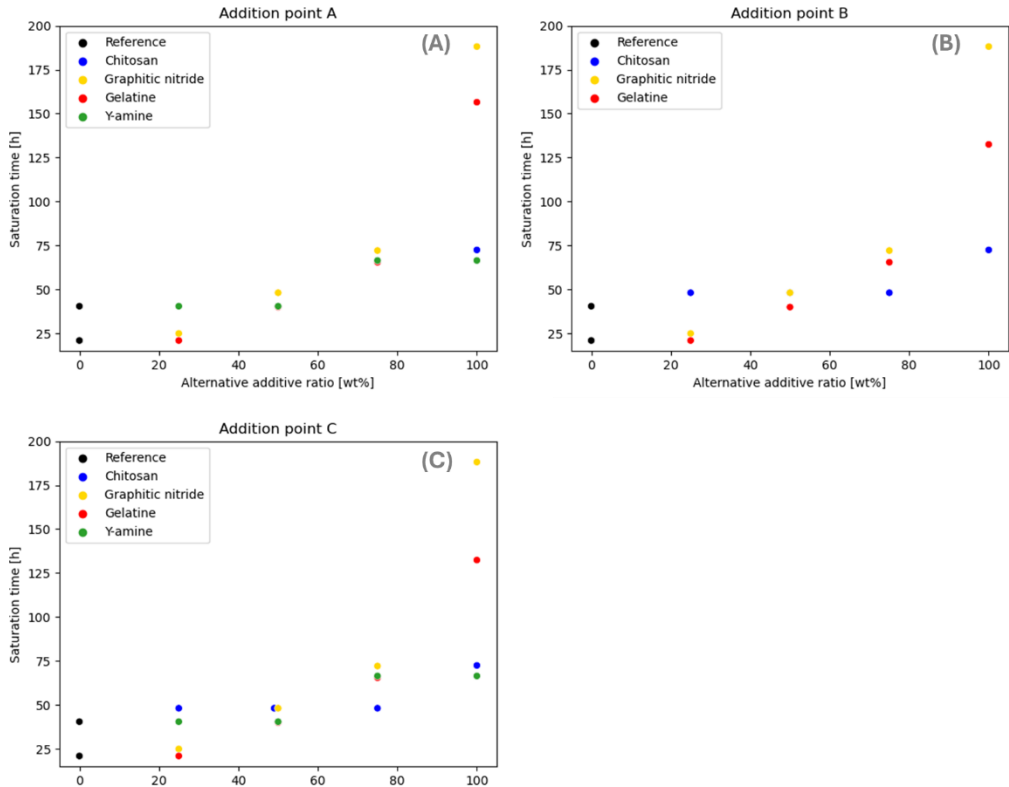


Figure 21. Saturation time (h) plotted to weight percent of alternative amine-based additives. All prototypes are presented and differentiated by addition points (indicated as A, B, and C). Reference samples are included in all graphs.

Figure 20 shows that the original composition has a higher density than prototypes containing increasing amounts of alternatives. Figure 21 shows that increasing amounts of alternatives extend the saturation times. As the alternatives vary, this suggests that the original amine-based additive causes both a substantial increase in the final bulk density and decrease in the saturation time. Additionally, in both Figure 20 and Figure 21, the 100:0 prototypes present greater variations than all other compositions tested, supporting that the presence of even small amounts of the original amine-based additive is enough to substantially influence bulk density and saturation times. The original amine-based additive having a substantial influence on the final adsorbent form is also consistent with the results from size distribution presented in Figure 16.

To evaluate different densities and their correlation to VOC uptake, bulk densities are plotted to the measured final uptake ( $\frac{g_{\text{pollutant}}}{g_{\text{adsorbent}}}$ ) in Figure 22.

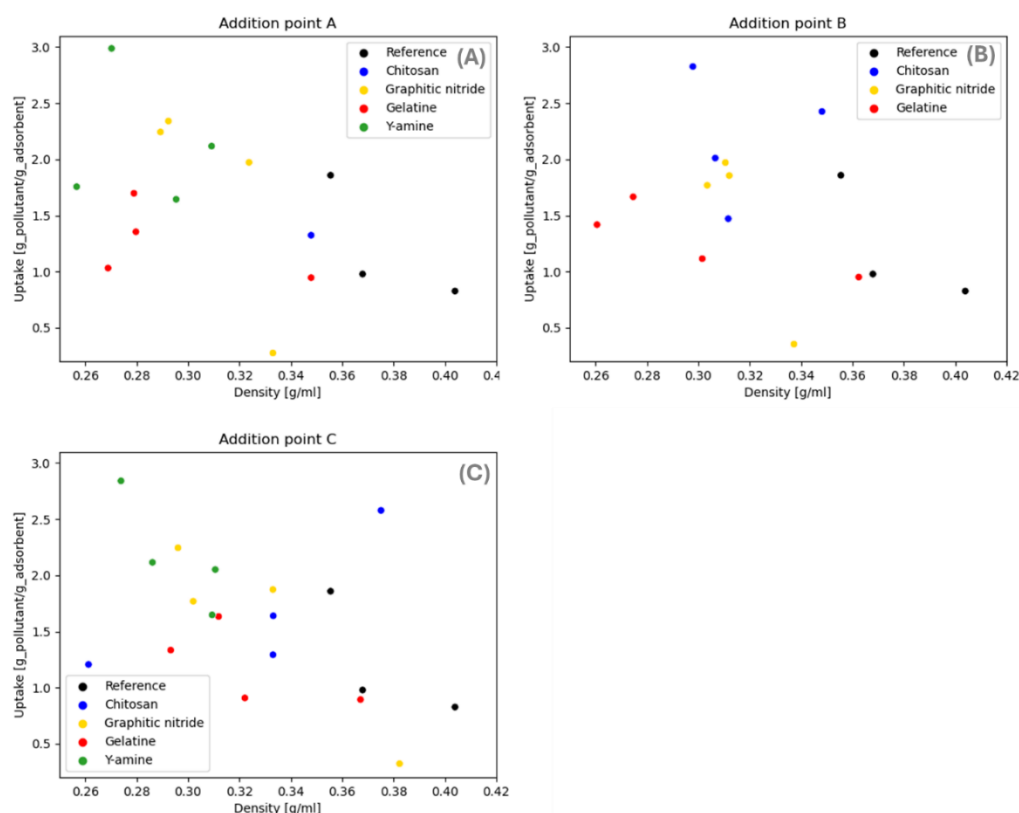


Figure 22. Final uptake ( $\frac{g_{\text{pollutant}}}{g_{\text{adsorbent}}}$ ) plotted to density (g/ml). All prototypes are presented, differentiated by addition points (indicated as A, B, and C). Reference samples are included in all graphs.

Although a higher density generally means a decreased adsorption capacity, there is no clear correlation, indicating the adsorption capacity depends more on other factors, such as the composition, than the density.

The relationship between composition, bulk density, adsorption capacity, and saturation time are complex. From Figure 19 it can be concluded that higher densities result in quicker saturation, potentially due to a decrease in available surface area. Figure 20 indicates that higher amounts of the original amine-based additive cause higher densities. From Figure 21 it is shown that saturation times decrease with larger amounts of original amine-based additive. The influence on saturation times could be attributed to the density, however, Figure 22 shows no correlation between density and final uptake, suggesting that the correlations in Figure 19-21 could be attributed to the additive's composition and the chemical properties of the additives. It is also possible that the original additive

increases density and that the shorter saturation times may be attributed to both its chemical properties and the resulting higher density. However, repeats are needed, especially for the gravimetric studies.

## 4.5. Moisture uptake

A moisture uptake evaluation ensures that the adsorbents do not adsorb substantial amounts of moisture from the surrounding environment – a phenomenon that can significantly decrease adsorption capacity – and thereby guaranteeing maintained functionality across varying humidities. A gravimetric study was performed where the developed prototypes were exposed to a humidity of 55%. Moisture uptake was measured as  $g_{\text{moisture}}/g_{\text{adsorbent}}$  as indicated in Equation 1 and the results for all prototypes and a reference sample are presented in Figure 23.

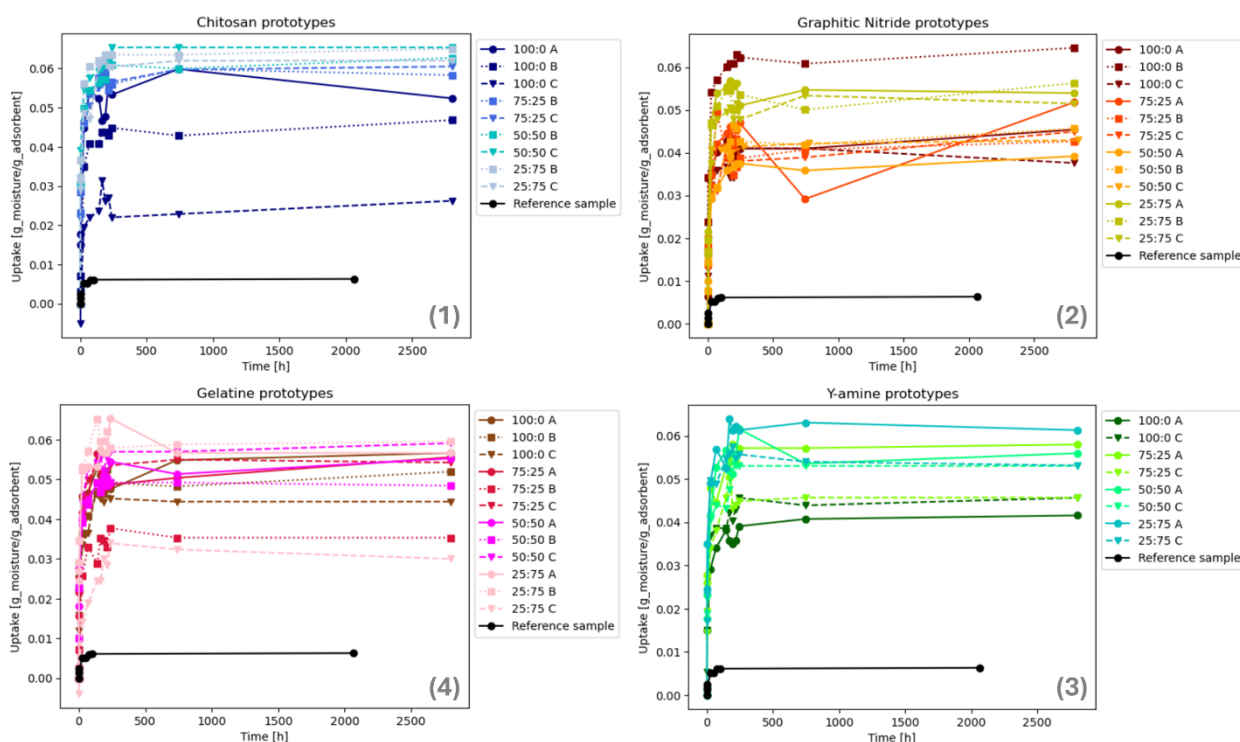


Figure 23. Moisture uptake for prototypes containing chitosan, graphitic nitride, gelatine and Y-amine and the reference sample included for comparison. The prototypes containing chitosan are shown in (1), graphitic nitride in (2), gelatine in (3) and Y-amine in (4) and the point of addition is indicated in the legend as A, B and C. The uptake is measured in weight increase ( $g_{\text{moisture}}/g_{\text{adsorbent}}$ ).

Figure 23 shows consistent plateauing for all prototypes between 0.02 and 0.07  $g_{\text{moisture}}/g_{\text{adsorbent}}$ , a significantly lower uptake compared to their pollution uptake (see Figure 18). As the study was performed over several months, this is assumed to be the maximum moisture uptake, showing that moisture uptake at 55% humidity does not have significant adverse impacts on pollution adsorption. However, it is of interest to note that the reference sample plateaus at a lower level of uptake than the prototypes, indicating less moisture is adsorbed. This can be explained by the variety of interactions available for water in the large chitosan, gelatine, and graphitic nitride molecules. However, the same explanation cannot be done for the Y-amine sample, as the molecules are small. It may be attributed to the higher density of the reference sample that results in less available surface area. In all cases, these uptakes can be deemed low and with little effect on the adsorption of VOCs.

## 4.6. Microbial evaluation

Knowing a material's microbial properties provides valuable information on potential issues with colonization and use for microbial removal. The MIC – the smallest concentration that visibly impairs growth – was determined through a broth dilution assay. One broth dilution was performed to evaluate adsorbents (the reference sample, the negative control, and prototypes with a 100:0 ratio, all in the size range 2.8–1 mm and made using addition point A) and one to assess the adsorbents' individual components. Additionally, a disk diffusion assay was performed to complement the broth dilution on the assessment of the adsorbents' microbial properties. The non-pathogenic, gram-positive bacteria *S. epidermidis* was used in both assays.

### 4.6.1. MIC using broth dilution

This section presents the results from the broth dilution assays and discusses possible explanations to the antibacterial properties exhibited. In the broth dilution assay, 2 ml wells with growth media and a standardized concentration of *S. epidermidis* bacteria were filled with (i) increasing amounts of adsorbent granules (0.0225–0.4 g) and (ii) increasing amounts of the components used to produce the adsorbents. The wells were incubated for 24 hours and the growth was measured using OD, with pure growth media for calibration, to determine the MICs.

#### 4.6.1.1. MIC of adsorbents

The results from all tested adsorbents – prototypes with 100:0 ratio, the reference sample, and the negative control – are presented in Table 4, with Yes or No signifying which wells indicated growth or no growth, respectively. Note that the results from both repeats with the Y-amine prototypes are included. The controls across all broth dilution tests were successful, with growth indicated in the GC and no growth indicated in the SC. However, recall that no adsorbents were produced during sterile conditions and thus they must all be classified as contaminated.

Table 4. Broth dilution assay results of adsorbent prototypes, the negative control, and the reference sample. OD measurements indicating growth are presented as Yes and lack of growth as No.

Adsorbents tested	Adsorbent amounts [g/ml growth media]					
	0.025	0.05	0.1	0.2	0.4	0.8
Negative control	–	No	No	No	No	No
Reference sample	–	No	No	No	No	No
Chitosan	–	No	No	No	No	No
Graphitic Nitride	–	No	No	No	No	No
Gelatine	–	No	No	No	No	No
Y-amine repeat 1	–	Yes	Yes	Yes	Yes	No
Y-amine repeat 2	Yes	Yes	Yes	Yes	Yes	No

As seen in Table 4, all adsorbent, except the Y-amine prototypes, presented no growth at any of the tested concentrations, including the negative control. As recommended by the protocol used, these results are interpreted as the negative control, the reference sample, and the prototypes containing chitosan, graphitic nitride, and gelatine all having a MIC of  $\leq 0.05$  g/ml. The results from the Y-amine prototypes are presented in Figure 27 and further discussed in the Y-amine prototypes section.

The original amine-based additive and chitosan are both known to possess antimicrobial properties and consequently a lack of growth was expected. However, neither graphitic nitride nor gelatine are known to possess any antimicrobial properties, and the negative control contains no amine-based

additives. The lack of growth in the wells containing these granules suggests other components in the adsorbents have antibacterial properties against *S. epidermidis*. This is further investigated in the broth dilution assay with adsorbent components.

#### 4.6.1.2. MIC of adsorbent components

Most adsorbents, including the negative control, unexpectedly presented a lack of growth (see Table 4). Consequently, a second broth dilution assay was motivated, assessing the adsorbent components separately to investigate the source of the antimicrobial properties. Components of the adsorbents deemed as relevant – cellulose fibers, additive A, the carrier particle, and additive B – were tested separately. Notably, the adsorbents consist of a complex matrix that was exposed to a heat treatment, causing chemical changes to the material. However, evaluating the components individually and without heat treatments may still provide some indication of the source of the adsorbent’s inherent antimicrobial properties.

The concentrations tested in this second assay correspond to the concentrations of each component present in the first assay. As the amounts of each component differ in the material, the corresponding concentrations evaluated in the second assay differ. Consequently, the concentration series is indicated as 5 to 1 for all components, with 5 representing the highest and 1 the lowest concentrations, ensuring simplicity and confidentiality. The results for the components tested are summarized in Table 5, with Yes, No, or Inc signifying which wells indicated growth, no growth, or inconclusive results respectively. The results suggest the carrier particle and additive B as the most likely candidates to induce antimicrobial properties, as these presented most wells with no growth. The GC and SC were successful across all broth dilution tests.

Table 5. Broth dilution assay results of separate components, 5 indicates highest amount tested and 1 lowest. Apparent growth indicated as Yes, lack of growth indicated as No, and inconclusive results indicated as Inc.

	<b>Amounts of additive low (1) – high (5)</b>				
<b>Concentrations of components</b>	<b>1</b>	<b>2</b>	<b>3</b>	<b>4</b>	<b>5</b>
Cellulose fibers	Yes	Yes	Yes	Yes	Yes
Additive A	Yes	Yes	Yes	Yes	Inc
Carrier particle	Yes	Yes	No	No	No
Additive B	Inc	No	No	Yes	No

Notably, the cellulose fibers, being a powder, absorbed most of the liquid in the wells, making OD measurements unfeasible. As a substitute, a small amount of liquid (2 µl) was extracted from each well, re-incubated in fresh growth media for 4 hours, and used for OD measurements. Notably, this measurement does not indicate growth in the wells, but presence of live bacteria. Although this shows biocidal activity, potential growth limiting properties will be missed. However, as the cellulose fibers have no records of antimicrobial activities, this risk was deemed as negligible. The results are presented in Table 5, using the same format as previous broth dilution results. As seen in Table 5, live bacteria were found in all concentrations tested.

Additive A, when dissolved, caused visible turbidity, disturbing OD measurements. Consequently, a dilution series of growth media and additive A was made and used as a reference, attempting to distinguish growth from turbidity disturbances. The results, along with the additive A reference measurements, are presented in Figure 24. However, despite the reference, quantifying bacteria using OD in the presence of nano particles, such as additive A, presents unreliable results due to light scattering from the nanoparticles. At higher concentrations of additive A (see Figure 24, concentrations 4–5), the measurements from the broth dilution assay are similar to the additive A reference, causing

inconclusive results. However, the wells containing lower concentrations (see Figure 24, concentrations 1–3) present markedly different measurements. Despite the uncertainty, these apparent differences are interpreted as indications of growth. In the literature reviewed, additive A has no recorded antimicrobial properties, strengthening this interpretation. The summarized results are presented in Table 5, showing additive A is unlikely to induce antimicrobial properties in the

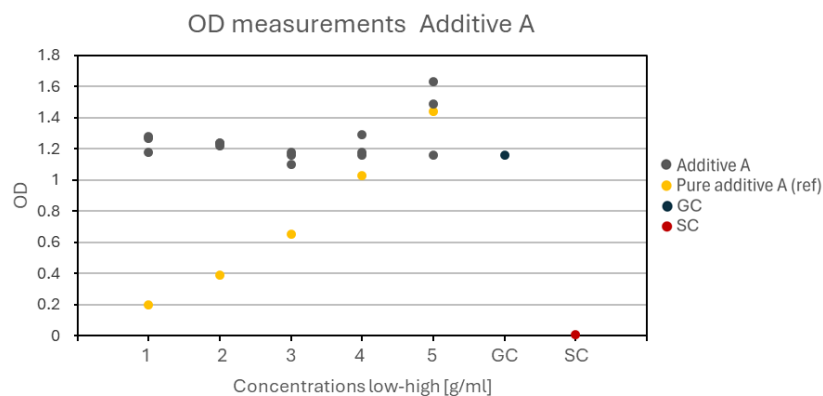


Figure 24. OD measurements from broth dilution assay with additive A, concentrations ranging from lowest (1) to highest (5). A dilution series of purely growth media and the same amounts of additive A is included as a reference sample. The results of the GC and SC are included for comparison.

adsorbents.

The remaining compounds, the carrier particle and additive B, show lack of growth in several concentrations (see Table 5). Hence, they are deemed as the most likely candidates to induce antimicrobial properties in the adsorbents. To further illustrate their influence on growth in the assay, the OD measurements from their concentration series are plotted below in Figure 25 and Figure 26.

Figure 25 presents the OD measurements from the carrier particle. Notably, the compound is nano-sized and, consequently, uncertainties of quantifying bacteria with OD measurements apply, rendering the results unreliable. However, Figure 25 presents a clear decrease in turbidity, starting at concentration 2. Assuming the results are viable, this is, as detailed in the protocol, interpreted as a MIC at concentration 2. Interestingly, the carrier particle does not have any recorded antimicrobial properties in the literature reviewed. However, the compound used is noted as a mixture by the producer, although the precise content is not divulged. Therefore, it is hypothesized that additional content in the mixture includes preservatives with antimicrobial properties. Hence, the mixture with the carrier particle potentially explains the antimicrobial properties seen.

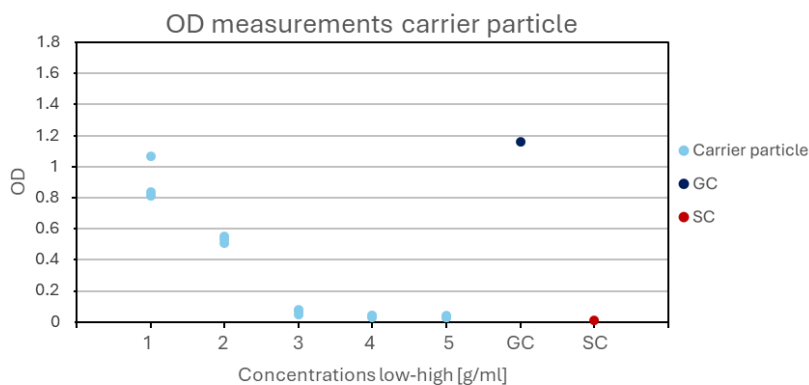


Figure 25. OD measurements from wells containing the carrier particle, concentrations ranging from lowest (1) to highest (5). The results of the GC and SC are included for comparison.

The OD measurements from additive B are presented in Figure 26, showing a lack of growth in all but one well. Concentration 4 (see Figure 26) presents an exception, indicating a small amount of growth. The protocol specifies that such growth, in an isolated well, indicates contamination and recommends

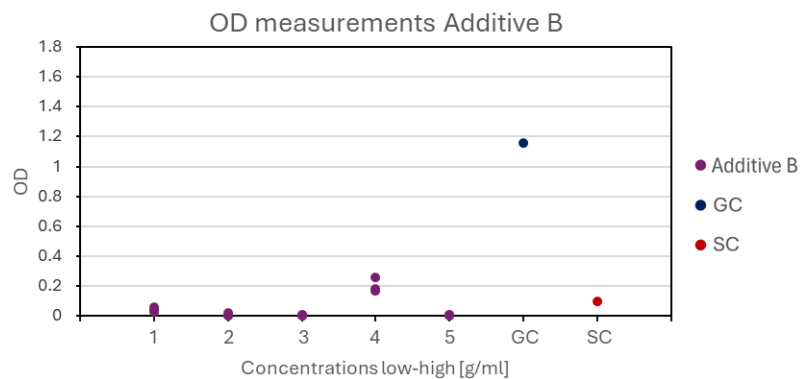


Figure 26. OD measurements from wells containing additive B, concentrations ranging from lowest (1) to highest. The results of the GC and SC are included for comparison.

no concluded MIC and repeating of the test. However, as most wells present no growth, it was surmised that additive B presents antimicrobial properties.

Additive B contains multiple compounds, including three with recorded antimicrobial properties, some of which are cationic. The first compound listed possesses significant antibacterial properties below, but not above, pH 6, the second has antibacterial properties, mainly due to the presence of primary amines, and the third is classified as acutely toxic to bacteria, seemingly regardless of pH [53, 54, 40].

Although the growth media is neutral, the pH in the wells were not measured after adsorbents were added. The pH of the liquid binder (see Figure 11) was measured at pH 10-11, potentially increasing the pH in the wells containing adsorbents. Assuming a pH increase, the antimicrobial properties of the first compound would be rendered obsolete. The second substance attains its antimicrobial properties from primary amines, similar to Y-amine. If its properties behave similar to Y-amine, the antimicrobial activity may have been decreased by a higher pH. Consequently, the presence of the third compounds may serve to explain the antimicrobial properties exhibited.

The results are interpreted as indicating the following MICs for the compounds:

- **Cellulose fibers**– all wells containing cellulose fibers had live bacteria, as recommended by the protocol this is interpreted as the MIC being higher than the concentrations tested.
- **Additive A** – The wells containing additive A presented some issues for OD measurements. However, as the results from the wells consistently presented a higher OD value than the reference sample concentrations, this is interpreted as growth and the MIC is interpreted as being higher than the concentrations evaluated.
- **Carrier particle** – Despite it having no known antimicrobial properties, the carrier particle tested indicates a MIC at concentration 2.
- **Additive B** – Although the test should be repeated, it suggests the MIC is lower than the concentrations evaluated.

The carrier particle mixture and additive B show antimicrobial properties in the broth dilution assay. Although the components do not accurately represent the complex matrix of the adsorbents, their presence is currently the most likely explanation for the adsorbents' inherent antibacterial properties seen in the first broth dilution assay. However, the test should be repeated.

### 4.6.1.3. The Y-amine prototypes

Although most of the adsorbents showed antimicrobial properties, the Y-amine prototypes present an exception, as seen in Table 4. Therefore, the assay was repeated, and the results of both MIC broth dilution assays are summarized in Table 5 and the OD measurements presented in Figure 27, both showing similar results from the two repeats. These results and potential explanations are subsequently discussed.

As presented in Figure 27, the OD measurements from both repeats indicate an increase, then a decrease in growth with increasing concentrations of adsorbents. Only the highest concentration shows no growth. These results are notably unexpected for several reasons: (i) the negative control – with no additives – indicated no growth at any concentrations tested, (ii) the expected result from a MIC test is a decrease in growth with increased concentration of the agent tested, and (iii) Y-amine is a known biocide that is active against gram-positive bacteria. Consequently, the expected result was a lack of growth in all wells or a decrease in growth with increasing amounts of adsorbents, not the pattern seen in Figure 27.

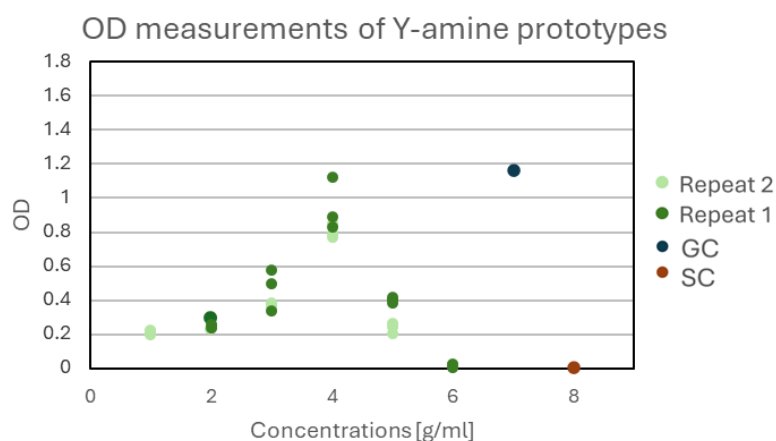


Figure 27. OD measurements from both repeats of the broth dilution assay of granules containing Y-amine. Growth control and sterility control are included as reference sample.

The likely explanation for the unexpected results is a repeated experimental error. Unexpected growth in a well is, according to the protocol used, a sign of contamination and it is already known that the material is contaminated. Susceptibility testing in general is, according to Bayot and Bragg (2024), influenced by a range of factors throughout the entire process and small variations in procedure may have significant effects on the final results. Poor specimen quality, poor standardization of bacterial colonies, individual variations of procedure etcetera can all influence the results significantly [46]. However, it is odd that the contamination only affected the Y-amine prototypes and that the repeats show such similar patterns in the OD measurements.

Y-amine is known to kill bacteria, but at pH above 9 its antimicrobial properties decrease. The pH of growth media is neutral, however the pH in the wells after the addition of the adsorbent granules were not measured. During production, the pH of the liquid binder was measured at around pH 10–11. Due to the basicity of the liquid binder, the addition of adsorbents to the growth media might increase the pH, potentially diminishing the biocidal effects of Y-amine. The concentration of Y-amine may also have been too low to have any substantial biocidal effects.

The biocidal effects of the carrier particle and additive B that disrupt growth in the negative control are still to be accounted for though. As the only difference between the negative control and the Y-amine prototypes is the presence of Y-amine, it seems logical that Y-amine counteracts or neutralizes the antimicrobial agents in the carrier particle and additive B. Amines are known to interact with several of the functional groups present in the antimicrobial agents in additive B, potentially diminishing their

activity [55]. As the antibacterial agent in the carrier particle is unknown, its reactivity with amines cannot be known.

The results from the MIC test with Y-amine prototypes are unexpected. Although some hypotheses have been put forward on the influence of pH and the reactivity of Y-amine, the most likely explanation is the large, inherent variability of susceptibility testing using live bacteria and experimental errors.

## 4.7. Disk diffusion

The disk diffusion assay involved streaking an agar plate with the *S. epidermidis*, placing adsorbent granules on the surface and incubating overnight. Any circular area around the granules showing inhibited growth indicates antimicrobial activity and the size of the circle is measured in diameter (mm). In this section, the results of the disk diffusion are discussed and compared to the results from the broth dilution assay.

The disk diffusion was done in three repeats, an average diameter was calculated for each of the adsorbent granules, as presented in Figure 28. The results indicate that Y-amine has the most significant antimicrobial effect, followed by the original amine-based additive. Chitosan also presented a zone with inhibited growth, but smaller in comparison. The rest of the adsorbent granules presented zones similar to the diameter of the granule itself. This made differentiating any antimicrobial properties from the granules blocking the surface difficult. Therefore, these diameters are indicated as ranges beginning with zero. Despite contradicting the results from the broth dilution, these results align with what was initially expected.

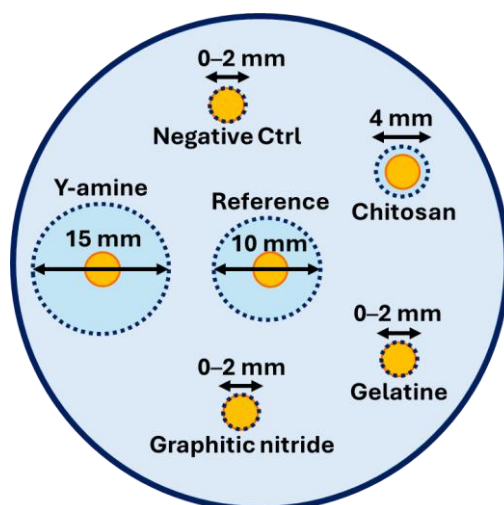


Figure 28. The average diameter of the zones presenting inhibited growth around the granules, based on the three replicates, are presented for all granules evaluated.

The growth around the negative control suggests there is no significant leakage from the adsorbents when they are not soaked in a liquid. Additionally, it suggests that the inhibited growth seen around other adsorbents are primarily due to the amine-based additive present, as this is the only factor in which the adsorbents differ.

The largest zones were observed around the Y-amine granules, which is consistent with the Y-amine being a known biocide. However, with the results from the broth dilution, it indicates the differing conditions in the disk diffusion assay does not result in the diminished antimicrobial properties discussed above. The hypothesis of pH may still apply, as one granule may not be enough to change the pH of the surrounding agar gel. Consequently, the biocidal properties of Y-amine are maintained.

Additionally, the zone may be larger due to Y-amine being a smaller molecule that diffuses into the agar gel to a higher extent than the other additives, consisting of larger molecules.

The second largest zones were seen around the reference sample, indicating both leakage and antibacterial properties of the original composition. Chitosan, also known to exhibit antibacterial activity, presents a visible growth-inhibited zone, but markedly smaller. A plausible explanation is that chitosan is a larger molecule than Y-amine and the original additive and thus diffused to a lesser extent. Y-amine is the smallest compound, followed by the original additive and chitosan, corresponding to the sizes of the zones. A smaller size might facilitate a more rapid and substantial diffusion in the agar gel, increasing the size of the growth-inhibited zone.

Graphitic nitride and gelatine are not known to possess any antimicrobial properties, which is consistent with the results presented in Figure 28. Additionally, they are both larger molecules which hinder diffusion into the agar.

The disk diffusion test indicates that the Y-amine prototypes present the highest antimicrobial activity, followed by the reference sample and chitosan prototypes. The difference in bactericidal activity between the disk diffusion and the broth dilution assays was primarily attributed to the different conditions. In the disk diffusion the adsorbents were not submerged in liquid, resulting in less leakage into the surroundings. The negative control presented no inhibited growth, suggesting only the amine-based additives leaked. As Y-amine and the original amine-based additive are the smallest molecules, they likely present higher diffusion rates, which explain their marked effect on the bacteria on the agar plate. Chitosan also has antibacterial properties, but as its molecular weight is higher it may have only been diffused to a lesser extent. The graphitic nitride and gelatine prototypes presented no growth inhibition, which is consistent with the compounds having no known antibacterial properties. The results of the disk diffusion align with what was expected of the prototypes' antimicrobial properties.

## 5. Conclusions

For gaseous air purification, the most common method is adsorption, using adsorbent materials. The company Adsorbi produces a novel adsorbent with improved pollution removal performance and a smaller environmental footprint compared to the current standard activated carbon. An amine-based additive of fossil origin in the material raises some concern though, and as part of continuous development and sustainability work, Adsorbi is looking for replacements.

In this project, four alternative amine-based additives – chitosan, graphitic nitride, gelatine, and dodecyl dipropylene triamine (henceforth referred to as Y-amine) – were incorporated into Adsorbi's material, separately and in combination with the original additive. As the material production involves a granulation step – a method involving mixing of dry powder with a liquid binder to form granules – the way in which additives are incorporated into the production process is of importance. Thus, prototypes were made with variations on (i) amine-based additive composition and (ii) methods of incorporation. Additive composition is indicated as weight ratios of alternative to original (100:0, 75:25, 50:50, 25:75) and methods of incorporation included mixing into the aqueous liquid binder (A), mixing with dry cellulose fibers (B), and adding during granulation after mixing with a small amount (C). The resulting prototypes were subsequently evaluated and compared to a reference sample (made according to Adsorbi's original composition and procedure) and a negative control (containing no amine-based additives).

The size distributions of the prototypes were skewed towards larger granules compared to the reference sample, likely due to the alternative additives influencing the viscosity and volume of the liquid binder. Prototypes where chitosan and gelatine were incorporated at addition point A and C caused increased viscosity, resulting in larger adsorbent granules. As Y-amine was in liquid phase, the Y-amine prototypes contained an increased volume of liquid binder, resulting in larger adsorbents. The size increase was less apparent in prototypes containing both alternative and original additives, as these formulations had a comparatively smaller impact on the viscosity and volume of the liquid binder. Prototypes with larger ratios of original additive presented size distributions similar to the reference. The graphitic nitride prototypes and all prototypes made using addition point B present size distribution similar to the reference sample, likely due to a lack of influence on the liquid binder.

Functionality was evaluated in terms of pollution and moisture uptake using gravimetric studies. Although the adsorption capacity and kinetics differed, all prototypes showed adsorption of the VOC acetaldehyde. This is primarily attributed to the reactivity of the amine-based additives, mainly to the presence of primary amines but also to other functional groups such as hydroxyl groups. The various adsorption kinetics are attributed to the varying reactivity of the active groups, with higher reactivity resulting in quicker adsorption. The presence of primary amines in the additives seems to result in the fastest adsorption rates – with the Y-amine prototypes as the primary example of rapid adsorption and readily available primary amines – while less reactive functional groups such as hydroxyl groups seem to prolong adsorption, giving slower rates and longer saturation times. However, the results were varied, and repeats are needed. The moisture uptake study suggests all prototypes adsorb more moisture than the reference sample, however the amounts are still substantially lower than the amount of VOC adsorbed and are deemed to be negligible.

Higher densities were seen to correlate with shorter saturation times, possibly due to the decreased available surface area in denser materials. Higher densities also correlated with larger amounts of the original amine-based additive, suggesting this additive has a significant influence on the bulk density. Additionally, larger amounts of the original amine-based additive also correlate with shorter saturation times, suggesting rapid reactions with this additive as a plausible explanation. It is hypothesized that the original additive increases density and that the shorter saturation times can be attributed to both its chemical properties and the resulting higher density.

The disk diffusion assay indicated no antibacterial properties in the negative control or the prototypes containing 100:0 gelatine and graphitic nitride. Some antibacterial properties were observed in the chitosan prototypes, likely due to the leaching of chitosan which has antibacterial properties. The small size of the circle is attributed to chitosan being a large molecule, which limits the extent of its diffusion into the agar gel. The most apparent antibacterial properties were seen in the Y-amine prototypes, followed by the reference sample. This is attributed to leaching of Y-amine and the original additive, both of which have antibacterial properties. The larger circles are also attributed to both having a smaller molecular weight, which allows for more extensive diffusion.

The broth dilution assay diverges from the disk diffusion results and indicates antibacterial properties across all samples (except the Y-amine prototypes), giving an assessed MIC of < 0.05 g/ml for the negative control, the reference sample, and the prototypes containing chitosan, graphitic nitride, and gelatine. The second broth dilution, evaluating separate components, suggested these antibacterial properties may be attributed to the presence of preservatives in the carrier particle and an antibacterial component present in additive B. In the disk diffusion assay, the granules were not submerged in liquid and therefore these components likely did not leach but remained within the material, thus explaining why they only influenced the bacterial growth in the broth dilution assay.

The Y-amine prototypes presented diverging results in the broth dilution, with growth in all but the highest concentrations tested (0.8 g/ml). As all other adsorbents tested presented antibacterial properties and Y-amine is a known disinfectant, these results were unexpected. It was theorized that a higher pH may have diminished the antibacterial properties of Y-amine and that chemical reactions between Y-amine and the antibacterial agents from the carrier particle and additive B may have decreased the antibacterial properties of the latter two. However, a more likely explanation is experimental error such as the contaminated material and it may serve as an example of the inherent variability of susceptibility testing.

Future studies should look at what chemical reactions occurred between acetaldehyde and the surface of the adsorbents and what the internal structure of the adsorbent granules is in terms of pore size distribution to validate or contradict the hypothesis relating pollution uptake to chemisorption and material density. Repeats of the gravimetric studies are required for the results to be reliable. Additionally, a pollution uptake study of the negative control adsorbents would provide an interesting comparison to how much functionality the amine-based additive adds to the material. For microbial evaluation, repeats are needed and further research on potential interactions between Y-amine and other components of the adsorbents. To rule out contamination, prototypes should be produced with sterile conditions, if possible.

## 6. Bibliography

- [1] J. L. Harris, "Air pollution," *Research Starters*, Salem Press Encyclopedia of Science, 2023.
- [2] WHO, "WHO global air quality guidelines. Particulate matter (PM<sub>2.5</sub> and PM<sub>10</sub>), ozone, nitrogen dioxide, sulfur dioxide and carbon monoxide," World Health Organization (WHO), 2021.
- [3] UNDP, "What is the Right to a Healthy Environment? Information Note," Office of the High Commissioner for Human Rights (OHCHR), United Nations Environmental Programme (UNEP), United Nations Development Programme (UNDP), 2023.
- [4] G. Liu, M. Xiao, X. Zhang, C. Gal, X. Chen, L. Liu, S. Pan, J. Wu, L. Tang and D. Clements-Croome, "A review of air filtration technologies for sustainable and healthy building ventilation," *Sustainable Cities and Society*, vol. 32, p. 375–396, July 2017.
- [5] R. Ganjoo, Sharma, A. K. Kumar and M. M. Arê mou Daouda, "Chapter 1: Activated Carbon: Fundamentals, Classification, and Properties," in *Activated Carbon: Progress and Applications*, C. Verma and M. A. Quraishi, Eds., Royal Society of Chemistry, 2023, p. 1–22.
- [6] T. M. Mata, A. A. Martins, C. S. C. Calheiros, F. Villanueva, N. P. Alonso-Cuevilla, M. Foneseca Gabriel and G. Ventura Silva, "Indoor Air Quality: A Review of Cleaning Technologies," *Environments*, p. 118, 7 september 2022.
- [7] A. Vilén, "Environmental impact of activated carbon production from various materials," Aalto University, Helsinki, 2021.
- [8] WHO, "Air Quality Guidelines for Europe – second addition," World Health Organisation Regional office for Europe, Copenhagen, 2000.
- [9] WHO, "WHO guidelines for indoor air quality: selected pollutants," WHO Regional office for Europe, Copenhagen, 2010.
- [10] C. Seigneur, "Gaseous Pollutants," in *Air Pollution: Concepts, Theory, and Applications*, Cambridge University Press, 2019, p. 146–189.
- [11] M. Scheithauer, "Concentration of Solvents in Various Industrial Environments," in *Handbook of Solvents, Volume 2 – Use, Health, and Environment (3rd Edition)*, ChemTec Publishing, 2019.
- [12] Z. Shayegan, M. Bahri and F. Haghghat, "A review on an emerging solution to improve indoor air quality: Application of passive removal materials," *Building and Environment*, vol. 219, 2022.
- [13] A. Hussein, "Flow Assurance," in *Essentials of Flow Assurance Solids in Oil and Gas Operations – Understanding Fundamentals, Characterization, Prediction, Environmental Safety, and Management*, 2022.
- [14] B. Balasubramaniam, Prateek, S. Ranjan, M. Saraf, P. Kar, S. P. Singh, V. K. Thakur, A. Singh and R. K. Gupta, "Antibacterial and Antiviral Functional Materials: Chemistry and Biological Activity toward Tackling COVID-19-like Pandemics," *ACS Pharmacol Transl Sci.*, vol. 4, no. 1, p. 8–54, 29 December 2020.

- [15] F. Rouquerol, J. Rouquerol, K. S. Sing, G. Maurin and P. Llewellyn, "Introduction," in *Adsorption by Powders and Porous Solids: Principles, Methodology and Applications*, Elsevier Science & Technology, 2013, p. 1–22.
- [16] L. Wang, C. Shi, L. Pan, X. Zhang and J.-J. Zou, "Rational design, synthesis, adsorption principles and applications of metal oxide adsorbents: a review," *Nanoscale*, vol. 12, p. 4790–4815, 2020.
- [17] IUPAC, "Definitions, Terminology and Symbols in Colloid and Surface Chemistry," in *Manual of symbols and terminology for physicochemical quantities and units*, 1971.
- [18] F. He, J. Zhang, A. Liu and G. Zhu, "Influence of Humidity on Adsorption Performance of Activated Carbon," 2023.
- [19] M. Davarpanah, K. Rahmani, S. Kamravaei, Z. Hashisho, D. Crompton and A. E. Andersen, "Modeling the effect of humidity and temperature on VOC removal efficiency in a multistage fluidized bed adsorber," *Chemical Engineering Journal*, vol. 431, no. Part 2, 2022.
- [20] T. Dutta, T. Kim, K. Vellingiri, D. C. Tsang, J. Shon, K.-H. Kim and S. Kumar, "Recycling and regeneration of carbonaceous and porous materials through thermal or solvent treatment," *Chemical Engineering Journal*, vol. 364, p. 514–529, 2019.
- [21] H. Jiang, M. Muneeshwaran, X. Liu, K. An, X. Zhao, S. Ozcan, T. Aytug and K. Li, "A review of antimicrobial implications for improving indoor air quality," *Journal of Materials Science*, vol. 59, p. 13725–13755, 22 July 2024.
- [22] E.-R. Kenawy, S. D. Worley and R. Broughton, "The chemistry and applications of antimicrobial polymer: A state-of-the-art review," *Biomacromolecules*, vol. 8, no. 5, 2007.
- [23] G. McDonnell and D. Russell, "Antiseptics and Disinfectants: Activity, Action, and Resistance," *Clinical Microbiology Reviews*, vol. 12, no. 1, p. 147–179, January 1999.
- [24] C. L. McKenzie, F. D. Guerra, J. Dhulekar, F. Alexis and D. C. Whitehead, "Target-Specific Capture of Environmentally Relevant Gaseous Aldehydes and Carboxylic Acids with Functional Nanoparticles," *Chemistry*, p. 14834–14842, 1 September 2015.
- [25] M. Loudon and J. Parise, "The Chemistry of Amines," in *Organic Chemistry*, 6 ed., New York, W.H. Freeman and Company, 2016, p. 1183–1224.
- [26] W. Reusch, "Amines," in *Virtual Textbook of Organic Chemistry*, 2013.
- [27] F. Brotzel, C. Ying Cheung and H. Mayr, "Nucleophilicities of Primary and Secondary Amines in Water," *The journal of Organic Chemistry*, vol. 72, no. 10, p. 3679–3688, 6 April 2007.
- [28] F. Brotzel, "Nucleophilicities of Amines, Amino Acids and Pyridines [Doctoral thesis]," Ludwig-Maximilians-Universität, München, 2008.
- [29] J. Ashenurst, "Nucleophilicity of Amines," Master Organic Chemistry, 2022.
- [30] I. Aranaz, A. Alcántara, M. Concepción Civera, C. Arias, B. Elorza, A. Heras Caballero and N. Acosta, "Chitosan: An Overview of Its Properties and Applications," *Polymers*, vol. 13, 24 September 2021.

- [31] E. Szymańska and K. Winnicka, "Stability of Chitosan—A Challenge for Pharmaceutical and Biomedical Applications," *Mar Drugs*, vol. 13, no. 4, p. 1819–1846, 01 April 2015.
- [32] Biosynth, "YC58325 Chitosan – water soluble," 2024. [Online]. Available: <https://www.biosynth.com/p/YC58325/9012-76-4-chitosan-water-soluble>.
- [33] A. Alaghmandfard and K. Ghandi, "A comprehensive Review of Graphitic Carbon Nitride (g-C<sub>3</sub>N<sub>4</sub>)-Metal Oxide-Based Nanocomposites: Potential for Photocatalysis and Sensing," *Nanomaterials*, vol. 12, no. 2, 2022.
- [34] W.-J. Ong, L.-L. Tan, Y. Hau Ng, S.-T. Yong and S.-P. Chai, "Graphitic Carbon Nitride (g-C<sub>3</sub>N<sub>4</sub>)-Based Photocatalysts for Artificial Photosynthesis and Environmental Remediation: Are We a Step Closer To Achieving Sustainability?," *Chemical Reviews*, vol. 116, no. 12, p. 7159–7329, 2016.
- [35] J. Zhu, P. Xiao, H. Li and S. A. C. Carabineiro, "Graphitic Carbon Nitride: Synthesis, Properties, and Applications in Catalysis," *Applied Materials and Interfaces*, vol. 6, no. 19, p. 16449–16465, 8 October 2014.
- [36] Z. Wei, L. Kong, Q. Wang, J. Xu and L. Li, "P- $\pi$  conjugated hydroxyl grafted carbon nitride with enhanced carriers generation and transfer for boosting H<sub>2</sub> evolution," *Optical Materials*, vol. 138, 2023.
- [37] F. Milano, A. Masi, M. Madaghiele, A. Sannino, L. Salvatore and N. Gallo, "Structure and Properties of Gelatin," *Scholarly Community Encyclopedia*, 2023.
- [38] T. R. Senadheera, D. Dave and F. Shahidi, "Collagen," *Scholarly Community Encyclopedia*, 2020.
- [39] Kremer Pigmente, "Gelatine Restoration 1," 2024. [Online]. Available: <https://www.kremer-pigmente.com/en/shop/mediums-binders-glues/63038-gelatine-restoration-1.html>. [Accessed 2024].
- [40] Sigma-Aldrich, 2024.
- [41] R. Borgmann-Strahsen, "Triameen® Y12D – High Performance, Broad Spectrum Biocide for Disinfection and Preservation," *sofw journal Home & Personal Care Ingredients & Formulations*, vol. 145, 19 December 2019.
- [42] Nouryon, "Cleaning applications – Europe, the Middle East and Africa edition," 2024.
- [43] S. Shanmugan, "Granulation techniques and technologies: recent progress," *Bioimpacts*, vol. 5, no. 1, p. 55–63, 2015.
- [44] V. De Simone, A. Dalmoro, M. d'Amore and A. A. Barba, "Inside the Phenomenological Aspects of Wet Granulation: Role of Process Parameters," in *Granularity in Materials Science*, G. Kyzas and A. Mitropoulos, Eds., IntechOpen, 2018, p. 63–84.
- [45] E. Gregersen, "Gravimetric analysis," *Encyclopedia Britannica*, 2022.
- [46] M. L. Bayot and B. N. Bragg, "National Center for Biotechnology Information," *National Library of Medicine*, 2024.

- [47] J. S. Prusty, "Antifungal discovery from plant sources," in *Phytoconstituents and Antifungals - Developments in Applied Microbiology and Biotechnology*, 2022, p. 5–33.
- [48] W. MacFarlane and L. Samaranayake, "Use of the microbiology laboratory," in *Clinical Oral Microbiology*, 1989, p. 187–203.
- [49] "Staphylococcus epidermidis Biological Agent Reference Sheet (BARS)," Cornwell University, 2023.
- [50] I. Wiegand, K. Hilpert and R. E. Hancock, "Agar and broth dilution methods to determine the minimal inhibitory concentration (MIC) of antimicrobial substances," 2007.
- [51] H. Pan, Y. Zhang, G.-X. He, N. Katagori and H. Chen, "A comparison of conventional methods for the quantification of bacterial cells after exposure to metal oxide nanoparticles," *BMC Microbial*, vol. 14, no. 222, 2014.
- [52] J. Hudzicki, "Kirby-Bauer Disk Diffusion Susceptibility Test Protocol," American Society for Microbiology, 2009.
- [53] PubChem, 2021.
- [54] "Nippon Shokuhin Kogyo Gakkaishi," 1994.
- [55] "Scientific Reports," 2021.
- [56] F. Rezaei and C. W. Jones, "Stability of Supported Amine Adsorbents to SO<sub>2</sub> and NO<sub>x</sub> in Postcombustion CO<sub>2</sub> Capture. Single-Component Adsorption," *Industrial & Engineering Chemistry Research*, 23 July 2013.
- [57] N. A. Fine and G. T. Rochelle, "Absorption of Nitrogen Oxides in Aqueous Amines," *Energy Procedia*, vol. 63, p. 830–847, 2014.
- [58] B. Fostås, A. Gangstad, B. Nenseter, S. Pedersen, M. Sjøvoll and A. L. Sørensen, "Effects of NO<sub>x</sub> in the Flue Gas Degredation of MEA," *Energy Procedia*, vol. 4, p. 1566–1573, 1 April 2011.
- [59] R. Agarwal and N. Yadav, "Pharmaceutical Processing – A Review on Wet Granulation Technology," *International Journal of Pharmaceutical Frontier Research*, vol. 1, no. 1, p. 65–83, 2011.

# Appendix A: Adjusted protocol for MIC using broth dilution and for agar diffusion

This protocol was made based on the protocol *Agar and broth dilution methods to determine the minimal inhibitory concentration (MIC) of antimicrobial substances* by Irith Wiegand, Kai Hilpert and Robert E.W Hancock and the protocol *Kirby-Bauer Disk Diffusion Susceptibility Test Protocol* by Jan Hudzicki, using the bacteria *S. epidermidis*.

## **Prior preparations**

Thaw bacterial culture, streak agar plates, and incubate at 37 °C overnight and then store in refrigerator.

## **Day 1 – preparations**

### Growth medium and agar plates

Make 1 l growth medium. Suspend 21 g of MH broth in 1 l distilled water, stir and heat to dissolve. Check for specific instructions on MH broth bottle.

Split medium, add agar to half (17 g agar per liter gives 8.5 g per half liter), heat and stir to dissolve.

Autoclave all medium, wait to cool, 3–4 hours.

Let the agar cool to 50–60 °C. Pour 15 agar plates, 25 ml in each. Let cool in room temp. Dry plates in incubator or laminar air flow for 30 min. Put in plastic bags, store in fridge bottom up.

Store cooled media at room temperature.

## **Day 2 – granule samples and streaking of agar plates**

### Broth macrodilution

Take 3–5 colonies from plate with bacteria with loop, add to 3–4 ml medium, vortex, incubate on shaker for 4 hours.

Measure turbidity, using pure media as control. Dilute with fresh media to OD 0.55–0.75, giving  $10^9$  cfu/ml.

Take 20  $\mu$ l of the bacterial media and dilute with 19.98 ml media (giving 20.00 ml total).

Label well plates on bottom as indicated below in Figure 1A. The letters indicate what additive is present: Ref for original amine-based additive, C for Chitosan, GN for graphitic nitride and Y for Y-amine. The negative control (Ctrl) are granules made with no additive. The numbers indicate concentration or amount, 1 being the lowest amount and 5 being the highest. The three repeats are labeled a, b, and c. The repeat with Y-amine granules is done identically with the addition of one lower concentration, the well plates and their labeling are shown in Figure 2A.

Amount of samples used: 0.4; 0.2; 0.1; 0.05; 0.025 g granules. Add granules to wells as indicated below in Figure 1A. Add 1 ml diluted bacterial media and 1 ml media to all wells (this gives  $5 \times 10^5$  cfu/ml as final concentration), pipette up and down to mix. Make sure bacterial media is well vortexed.

Add 1 ml diluted bacterial media and 1 ml media to GC. Add 2 ml media to SC.

Make three repeats and label as a, b, and c. Incubate overnight (16–20 h).

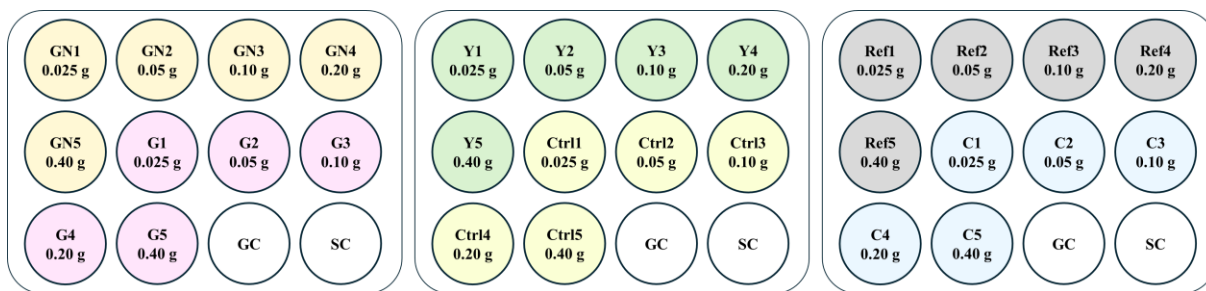


Figure 1A. The well plates. The letters indicate present additives: Ref for reference sample, C for Chitosan, GN for graphitic nitride, Y for Y-amine, and Ctrl for negative control. Numbers indicate concentration or amount, 1 being the lowest amount and 5 being the highest. The three repeats are labeled a, b, and c.

Repeats of Y, including one extra lower concentration than before.

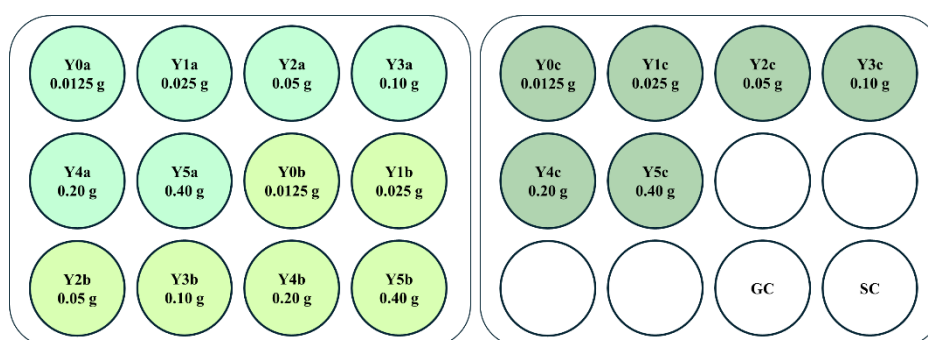


Figure 2A. Well plated for the repeated test with Y-amine additives. Numbers indicate concentration or amount, 0 being the new lowest and 5 being the highest. The three repeats are labeled a, b, and c.

### Agar diffusion

Label disks on bottom.

Use loop to transfer colonies from plate to 2 ml media. Vortex, adjust turbidity to McFarlan 0.5 standard of  $1-2 \times 10^8$  cfu/ml with more organisms or media.

Dip cotton swab in bacterial media, remove excess liquid to avoid drip. Streak the swab over the entire surface of the agar plate, rotate  $60^\circ$  and repeat two times.

Let dry, then add granules evenly spaced on plate on labels. Put 1 drop of growth media on each granule to wet them and stick them to surface.

Incubate 16–18 hours.

### **Day 3 – analysis**

Measure turbidity from all wells, pure media as control.

Look at growth on agar plates: measure the growth free zone diameter with ruler, round up to the nearest millimeter.

## Appendix B: Adjusted protocol for MIC test on separate components

This protocol was adjusted from the protocol in Appendix A, originally based on the protocol *Agar and broth dilution methods to determine the minimal inhibitory concentration (MIC) of antimicrobial substances* by Irith Wiegand, Kai Hilpert and Robert E.W Hancock. The bacteria used was gram positive *S. epidermidis*.

The experiment was set up so that the amounts of all separate components in all wells in the first MIC test (MIC 1, with granules) would be the same as the amounts assessed in the second MIC test (MIC 2, with components separately). Since the components are present to different extents and the amounts in the negative control granules are measured in dry weight, some calculations needed to be done.

- For each well (1, 2, 3, 4, 5) it was calculated how much of the granules consisted of each component (in dry weight). This was done based on the known amounts added in the preparation of the granules.
- The calculated dry weight was converted into wet weight based on indicated water contents.
- The wet weights (corresponding to all wells in MIC 1) were added to MIC 2.

The amount added to the wells was therefore different for each component and is shown in Table 1B, the amounts used are shown in Table 2B. For some components in liquid form, a dilution series was made as in figure 1B.

*Table 1B. The amount of negative control granules (dry weight, g) tested in each well in MIC 1. Below, the amount of each separate component the granules contain (converted to wet weight).*

<b>Amount of Neg.Ctrl granules MIC 1 (g)</b>	<b>0.4</b>	<b>0.2</b>	<b>0.1</b>	<b>0.05</b>	<b>0.025</b>
<b>Cellulose fibers (g)</b>	0.180126	0.090063	0.045031	0.022516	0.011258
<b>Additive A (g)</b>	0.042221	0.021110	0.010555	0.005278	0.002639
<b>Carrier particle (g)</b>	0.139613	0.069807	0.034903	0.017452	0.008726
<b>Additive B (g)</b>	0.152030	0.076015	0.038008	0.019004	0.009502

The values in Table 1B were rounded up to create a dilution series similar to the one in MIC 2. The amounts of each component tested are presented in Table 2B.

*Table 2B. The amount of each separate component added to the wells in MIC 2.*

	<b>Amounts used in MIC 2</b>				
<b>Cellulose fibers (g)</b>	0.2000	0.1000	0.0500	0.0250	0.0125
<b>Additive A (g)</b>	0.0400	0.0200	0.0100	0.0050	0.0025
<b>Carrier particle (g)</b>	0.1500	0.0750	0.0375	0.0188	0.0094
<b>Additive B (g)</b>	0.1500	0.0750	0.0375	0.0188	0.0094

### Day 1 – samples

#### Broth macrodilution

Take 3–5 colonies from plate with loop, add to 3–4 ml medium, vortex, incubate on shaker for 4 hours.

Measure turbidity of bacterial media, pure media as control. Dilute with fresh media to OD 0.55–0.75, giving 10<sup>9</sup> cfu/ml. Take 20 µl of the bacterial media and dilute with 19.98 ml media.

Label well plates on bottom as shown in figure 1B.

Amounts of compounds used and dilution series are indicated in Table 2B. Dissolve liquid compounds in 8 ml media as indicated and then make dilution series, as shown in Figure 2B. Add dry components directly to wells as indicated in Figure 1B.

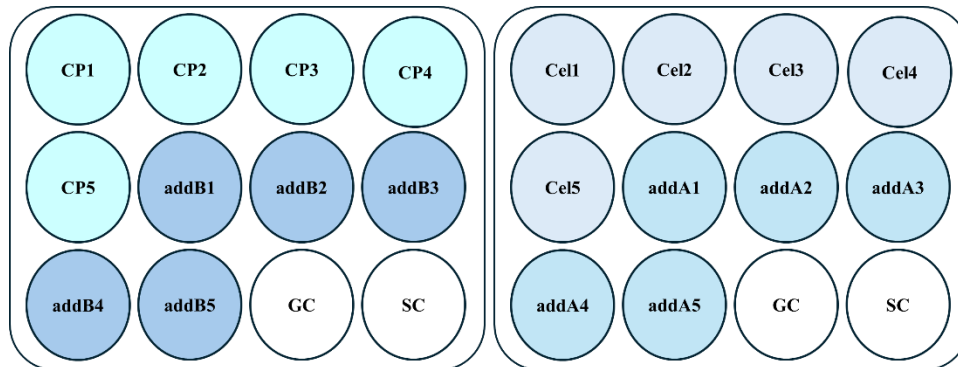


Figure 1B. The well plates with separate components. The letters indicate components: CP for carrier particle, addA for additive A, Cel for cellulose fibers, and addB for additive B. Numbers indicate concentration or amount, 1 being the lowest amount and 5 the highest.

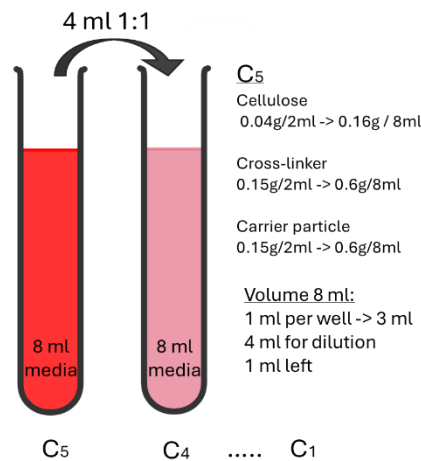


Figure 2B. Dilution series for liquid components.

Make sure bacterial media is well vortexed. Add 1 ml media to dry components and GC and add 2 ml pure media to SC. Add 1 ml media from dilution series to wells with liquid components. Add 1 ml diluted bacterial media to all wells except SC (this gives  $5 \times 10^5$  cfu/ml as final concentration).

Make three repeats and label as a, b, and c. Incubate overnight (16–20 h).

## Day 2 – analysis

Measure turbidity with OD, pure media as control.

OBS, some exceptions were necessary:

- The dry, loose cellulose made the liquid very thick and turbid, which made OD measurements difficult. It was decided to extract some liquid and grow it for 4 hours in pure culture media. The turbidity of these was then measured to show wither or not there was growth.
- Dissolved additive A became turbid and the effect of this was clearly visible. Therefor the turbidity of only additive A and media (in a dilution series with the same concentrations as in the wells) was measured as comparison, while pure media was still used to calibrate for measurements of the samples.

DEPARTMENT OF CHEMISTRY AND CHEMICAL ENGINEERING  
CHALMERS UNIVERSITY OF TECHNOLOGY

Gothenburg, Sweden 2025  
[www.chalmers.se](http://www.chalmers.se)



**CHALMERS**  
UNIVERSITY OF TECHNOLOGY